State-of-the-art review on vertical mixing in the Baltic Sea and consequences for eutrophication

Jan Hinrich Reissmann, Hans Burchard, Rainer Feistel, Eberhard Hagen, Hans Ulrich Lass, Volker Mohrholz, Günther Nausch, Lars Umlauf , Gunda Wieczorek

Leibniz Institute for Baltic Sea Research (IOW)
Seestraße 15
D-18119 Rostock-Warnemünde
Germany

jan.reissmann@io-warnemuende.de

Abstract

The vertical mixing in the transition area from the North Sea to the Baltic Sea is dominated by entrainment processes of the inflowing saline water within near bottom layers. The hot spots of these processes are located at the Darss Sill and the Bornholm Channel in the western Baltic Sea. In the central Baltic Sea temporal changes and associated transports are dominated by the horizontal advection of saline water in deep layers below the permanent halocline. This is accompanied by the turbulent vertical transport through the halocline into the surface layers. The related vertical salt transport into the entire surface mixed layer is estimated by various methods to be around values slightly above 30 kg/(m² a). During so-called stagnation periods the corresponding residence time of the deep water in the Eastern Gotland Basin drastically increases roughly by a factor of five. Therefore vertical mixing through the halocline seems to be drastically reduced when inflows are lacking. The potential processes of diapycnal mixing are discussed to the present knowledge. The turbulent motion resulting from breaking internal waves seems to be capable of turbulent transports through the halocline corresponding to the estimates of the salt transport into the surface mixed layer. The actual knowledge about boundary mixing due to internal waves in the Baltic Sea is found to be poor. Mesoscale eddies are evaluated to be able to contribute to the vertical mixing, but it is not known if they really do and which of the possible direct and indirect mixing mechanisms is most effective. Near bottom currents induced by inflow events are found to be likely to enhance vertical mixing. Coastal upwelling certainly contributes to the vertical transport, but the depth of its origin and the volume transport are hard to determine for large-scale quantifications. The short spatiotemporal scale of turbulent transports through the halocline resulting in a weakening of the halocline during summer and the mixing of the entire surface layer down to the halocline in winter are combined to a consistent description of the vertical salt transport. The longer residence time of the deep water during stagnation periods is hypothesised to be attributed to the lack of energy imported by the inflows and directly or indirectly feeding the diapycnal mixing processes. The discussion about consequences of vertical mixing processes crossing the seasonal thermocline and affecting the embedded ecosystem arrives at the conclusion that the vertical transport of nutrients such as the phosphate is quantitatively not sufficiently understood and needs further interdisciplinary research activities.

1. Introduction - General aspects of vertical mixing

Turbulent mixing plays a major role for the dynamics of marine ecosystems. For the surface mixed layer of the open ocean and shelf sea waters this has been illustrated first in the classical publication of Sverdrup (1953) where he showed that spring phytoplankton blooms are initiated when the surface mixed layer depth becomes smaller than a critical depth. This idea has been later refined by the concept of critical turbulence (Huisman et al. 1999) where the depth of the mixing layer (zone of active vertical mixing), in contrast to the mixed layer, is considered instead. Vertical mixing is also responsible for the maintenance of deep chlorophyll maxima, zones of relatively high phytoplankton abundance fuelled by upward turbulent nutrient fluxes within the thermocline below nutrient depleted surface water (Sharples et al. 2001).

However, in the Baltic Sea, a European semi-enclosed marginal sea (see Fig. 2), turbulent mixing plays a much more complex role for the dynamics of the marine ecosystem. Due to its positive freshwater budget non-linearly coupled with episodic events of salt water inflows through the narrow and shallow straits connecting the Baltic Sea with the saline North Sea, the central Baltic Sea is permanently stratified with a halocline located about 60 m below the surface. On the other hand, the eutrophic Baltic Sea produces large amounts of organic matter sinking into the stratified deeper water where it mineralises and thus lowers the oxygen concentration in the water. Major Baltic Inflows (MBIs, see Matthäus and Franck 1992) occurring on the decadal time scale are the main process which ventilates these depleted deeper water. During the stagnation periods between two MBIs the near-bottom water of the deeper basins typically becomes anoxic with the consequence that large amounts of phosphate are released from the sediments. By means of complex and not fully understood vertical transport mechanisms this phosphate reaches the surface water of the Baltic Sea in winter, inducing there a nitrogen to phosphorus ratio significantly lower than the physiological Redfield ratio of 16. Once the spring phytoplankton blooms have depleted the near-surface nitrate, nitrogen fixating cyanobacteria take advantage of the residual excess phosphate, such that in warm and calm summers massive cyanobacteria blooms are characteristic for the Baltic Sea.

In many senses the processes leading to the upward transport of phosphate are non-trivial. In-situ turbulence measurements in the stratified water below the halocline of the Baltic Sea result in vertical turbulent transport with eddy diffusivities of the order of 10^{-5} m^2s^{-1}, whereas vertical eddy coefficients around 10^{-4} m^2s^{-1} are obtained by simple salt budget estimates. Thus other mixing processes than internal mixing must take place in the Baltic Sea, the identification and quantification of which is a major open question in Baltic Sea research.

Stigebrandt (2003) has sketched a conceptual model for the vertical circulation in the central Baltic Sea. In Fig. 1 this overview is refined by listing all known relevant vertical mixing and transport processes in the Baltic Sea.

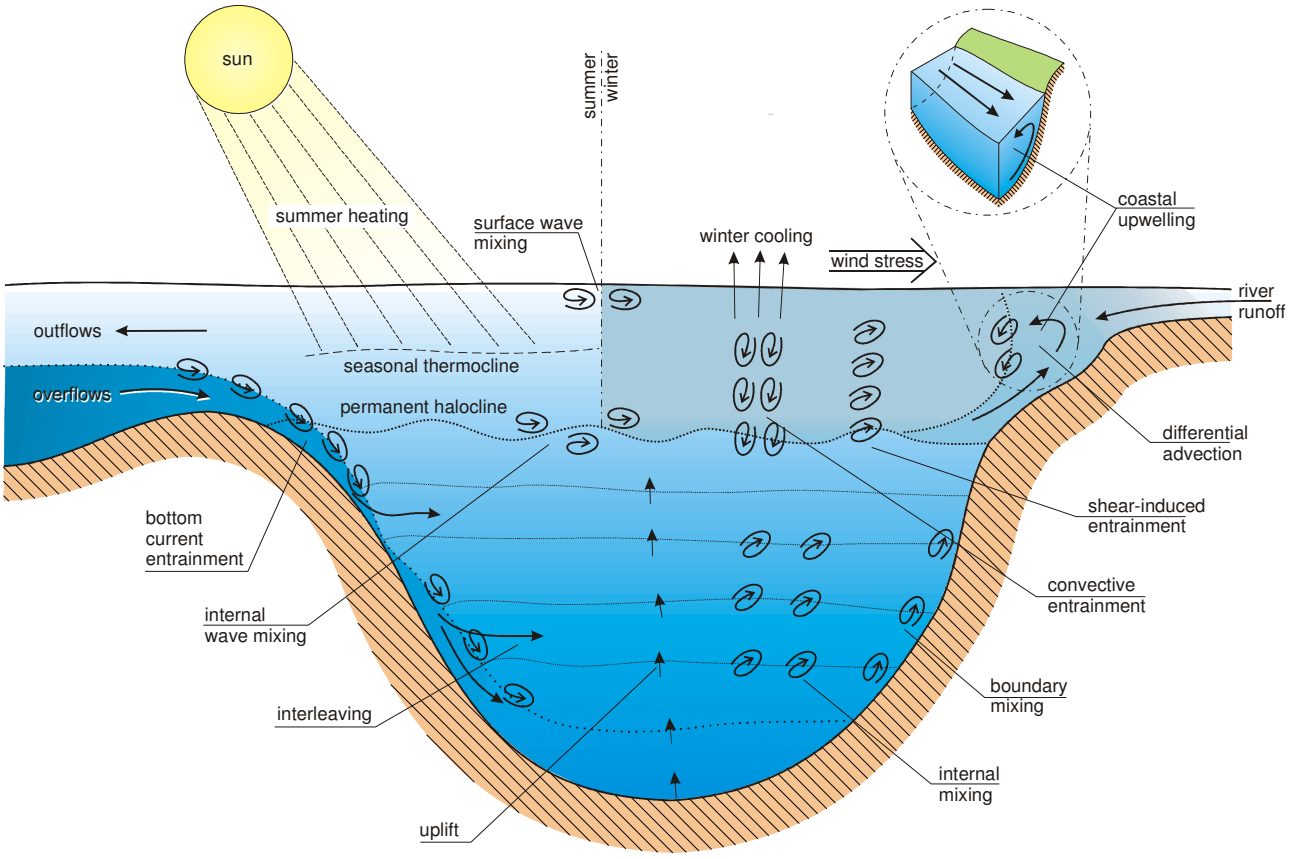

Fig. 1: Scheme of vertical mixing and transport processes in the Baltic Sea.

Episodic overflows over the Belt Sea sills transport saline water into the entrance areas of the Baltic Sea where they form dense bottom currents, see Subsection 4.1. Those are subject to entrainment of less saline ambient water lowering their salinity and thus their density, see Subsection 4.2. Once the density of the bottom currents equals the density of the ambient water (due to entrainment and deeper propagation) they interleave with the ambient water masses and ventilate them. Because of volume conservation the deep inflows generate a compensating uplift of the water column in the central Baltic Sea, see Subsection 3.3. Vertical turbulent transport is enhanced by internal mixing due to inertial waves and internal wave breaking, see Subsection 5.1, as well as by mesoscale Baltic Sea Eddies (the so-called Beddies), see Subsection 5.3. The latter may also contribute to boundary mixing when they propagate towards the sloping sea bed. Other potential boundary mixing effects are internal wave breaking at the sloping sea bed or shear-induced convection, see Subsection 5.2, or near-bottom currents induced by inflow events, see Subsection 5.4. Coastal upwelling has the potential of transporting sub-halocline water towards the surface and irreversibly mixing them into less saline surface water due to differential advection, see Subsection 5.5. During winter surface cooling will establish statically unstable stratification leading to convective entrainment of surface water into the halocline. Similarly, the surface wind stress causes shear-induced entrainment into the halocline. During summer the halocline is protected against entrainment from above by a seasonal thermocline below which however internal wave mixing erodes the halocline, see the discussion in Subsections 2.2 and 3.2. Finally, surface waves generate near-surface turbulence and modify the surface mixed layer in a complex way. Breaking surface waves inject turbulence into the surface mixed layer and have thus a strong impact on the near-surface dynamics, see, e.g., the field data by Terray et al. (1996) and the model-data comparisons by Craig (1996) and Stips et al. (2005). The interaction between wave-induced Stokes drift and mean shear generates pairs of

counterrotating vortices aligned with the wind direction, the so-called Langmuir Circulation (LC). LC is strongly modified by turbulence and typically homogenizes the surface mixed layer, see, e.g., the Large Eddy Simulation study by McWilliams et al. (1997) and the field data by Thorpe et al. (2003) and Gemmrich and Farmer (2004). Since the mixing due the presence of surface waves is characteristic to all wind affected surfaces of natural waters, it will not be discussed in this review in further detail. Because of the character of the Baltic Sea as an almost enclosed marginal sea, tidal mixing however does not play a significant role in the Baltic Sea.

The manuscript is organised as follows: after this brief introduction, the bathymetry and hydrography of the Baltic Sea is presented in Section 2 with special emphasis on inflow events in Subsection 2.1 and the surface mixed layer dynamics in Subsection 2.2. In Section 3 the vertical salt transport through the halocline is estimated by means of various methods, which are water and salt balances in Subsection 3.1, the quantification of pycnocline erosion in Subsection 3.2, the quantification of uplifts by inflows in Subsection 3.3 and the construction of an analytical diapycnal response function in Subsection 3.4. In Section 4 pathways of dense inflows in the western Baltic Sea are reconstructed (Subsection 4.1) and entrainment estimates are made for these inflows (Subsection 4.2). In Section 5 the potential mechanisms for vertical mixing in the Baltic Sea are discussed in detail as already listed above. The ecosystem perspective is presented in Section 6, mainly showing the responses of marine ecosystem parameters to inflow events. A final discussion of Baltic Sea vertical mixing in Section 7 concludes this state-of-the-art review.

It should be noted that the unit g/kg for the salinity is used here. The numerical value of absolute salinity in grams of salt per kilogram of seawater deviates from Practical Salinity (psu) by about 0.5% (Jackett et al. 2006), which is an irrelevant uncertainty for the estimates made in this paper. For the calculation of the mass transport of salt, values of absolute salinity rather than Practical Salinity are required.

2. Bathymetry and hydrography of the Baltic Sea

The Baltic Sea is a landlocked sea. The water exchange with the open ocean only takes place through the North Sea. The Baltic Sea is divided into different deep basins connected by narrow sills and channels, see Fig. 2. The exchange transition area is the Kattegat. It is connected to the south-western Baltic Sea mainly by two straights, the Øresund and the Great Belt followed by the Fehmarn Belt. Before entering the Arkona Basin (AB), the first of a chain of deep basins, the inflowing water has to pass the only 18 m deep Darss Sill or the 7 m deep Drogden Sill. The AB has a maximum depth of about 45 m and is connected to the Bornholm Basin (BB) by the Bornholm Channel. The BB is almost round with a diameter of about 80 km and has a maximum depth of approximately 100 m. The adjacent Słupsk Furrow (SF) is a channel-like basin with an extension of nearly 80 km in the east-west direction and a depth of about 90 m at maximum, separated from the Bornholm Basin by the only 60 m deep Słupsk Sill. Southeastward of the SF the Gdańsk Basin is located with a maximum depth of about 110 m. In the northeast direction the SF is connected to the Eastern Gotland Basin (EGB). The EGB is the largest and the central basin of the Baltic Sea. It is enclosed by the 150 m isobath and has a maximum depth of about 250 m. In the east of the EGB the Gulf of Riga is located. Northern of the EGB the Farö Deep continues the chain-like alignment of the basins. The Landsort Deep in the Western Gotland Basin marks the deepest location of the Baltic Sea with a depth of about 490 m. In the northeast, the Gulf of Finland with east-west extension constitutes the easternmost part of the Baltic Sea. In the north, northward of the Åland Sea, the Baltic Sea is bounded by the Gulf of Bothnia with north-south extension consisting of the Bothnian Sea in the south and the Bay of Bothnia in the north.

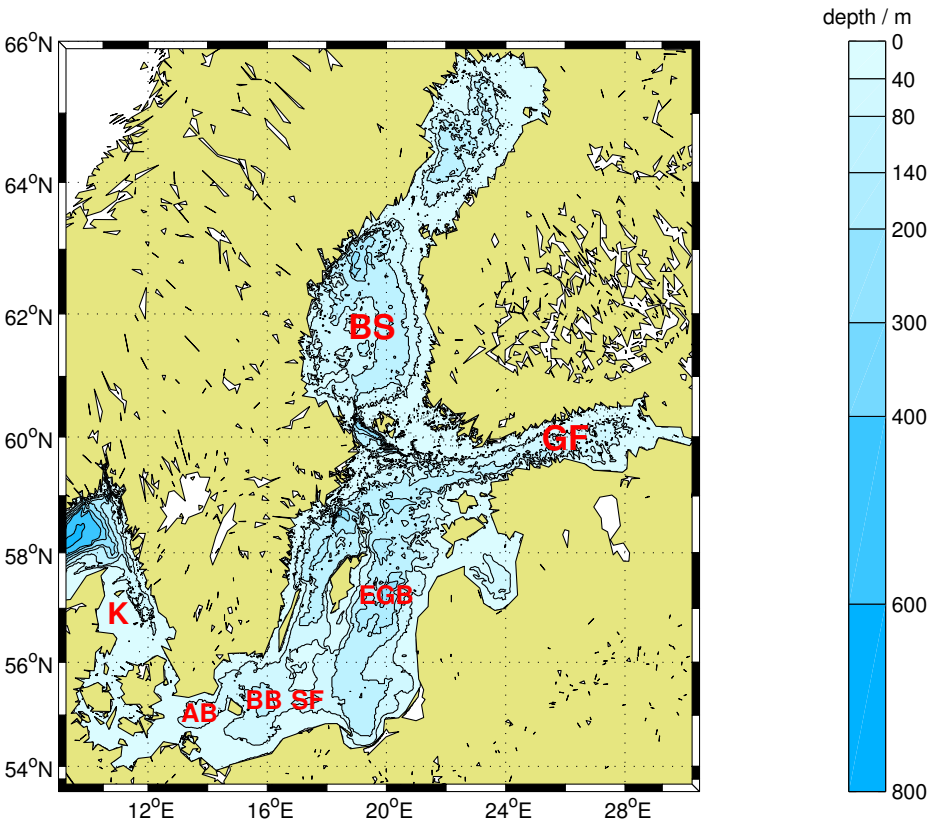

Fig. 2: Topographic map of the Baltic Sea, indicated regions are the Kattegat (K), the Arkona Basin (AB), the Bornholm Basin (BB), the Słupsk Furrow (SF), the Eastern Gotland Basin (EGB), the Gulf of Finland (GF), and the Bothnian Sea (BS). Some additional details of the western Baltic Sea are displayed in Fig. 5.

Saline inflows from the North Sea produce a lateral surface salinity gradient throughout the whole Baltic Sea with high salinities of about 25 psu in the transition area of the Kattegat and low salinities around 5 psu in the Gulf of Bothnia. Compared to the open ocean and the North Sea the salinity in the Baltic Sea is generally low due to large amounts of fresh water provided by river discharges with an annual river run-off of about 436 km³ resulting from the huge drainage area in conjunction with the humid climate. In addition, the annual water budget amounts to 224 km³ precipitation, 184 km³ evaporation, and 947 km³ surface water outflow given by Brogmus (1952) and HELCOM (1993) and is compensated by an appropriate inflow of nearly 500 km³ saline water from the North Sea. Generally, the water exchange between the Baltic Sea and the North Sea is greatly restricted by the connecting narrow and shallow belts and sounds.

A permanent halocline separates the surface water from the deep water in the basins. The halocline in the AB is found in about 35 m to 40 m depth. In the EGB it is significantly deeper at 70 m to 90 m depth (Stigebrandt 1987a, Elken 1996). This prominent halocline is found throughout the southern and central Baltic Sea. During the summer a seasonal thermocline develops at depths between 10 and 30 m (Matthäus 1984). The thermocline disappears in winter due to cooling and mixing of the surface water by wind and convection. However, these processes do not affect the deep water which is isolated from the surface water by the halocline. When passing the sills, 50% of the deep water in the AB is replaced by inflowing saline water. During strong inflow events volumes exceeding 100 km³ of mixed "old" and "new" Arkona Deep Water replace the "old" Arkona Deep Water (Omstedt and Axell 1998). Because of its high density the inflowing saline water spreads along the bottom and is subject to further entrainment of brackish surface water on its way along the chain of deep basins (Kõuts and Omstedt 1993).

During stagnation periods without inflows of highly saline and oxygenated water from the North Sea, the oxygen in the Baltic deep water becomes depleted and hydrogen sulfide may occur. The thermohaline properties in the deep layers are mainly determined by advection. Vertical mixing occurs only by diffusion and turbulent exchange (Stigebrandt et al. 2002).

2.1. Inflow of high-salinity seawater from the North Sea into the Baltic Sea

Owing to an open connection to the North Sea and the Atlantic Ocean, the Kattegat contains seawater of high salinities with typically 17 psu at the surface and exceeding 30 psu in the deep layers. In contrast, the inner Baltic Sea has a fresh water excess causing regular surface salinities up to 10 psu with strong vertical and lateral gradients. The resulting climatological density differences in the Belt Sea drive a permanent near-bottom inflow of saltier and a near-surface outflow of more brackish water, severely hampered by the narrow and shallow Danish straits, their tidal oscillations and the permanently changing wind conditions in the westwind belt.

Only under specific meteorological circumstances, when either very strong or very calm conditions prevail for typically 20 days or longer, and the water column in the Belt Sea is either strongly mixed or strictly stratified, significant amounts of very salty water can penetrate into the internal Baltic Sea. Once it has reached the Baltic Sea it can propagate eastward across the sills and basins, substituting stagnating water masses there and refilling the Baltic Sea salt budget. Such occasional inflow events occur very irregularly, from repeated events within a single year to stagnation periods lasting for a decade. The significant impact of such events on the physical, chemical, and biological status of the Baltic Sea has intensively been investigated in the past 50 years. A recent review is given by Matthäus (2006). Nevertheless, the way these inflows depend on the global climatic change, and the complex non-linear cascades of processes they trigger are only partly understood yet.

So-called barotropic inflows are characterised by the following features (Wyrtki 1954, Franck et al. 1987, Matthäus and Franck 1992, Fischer and Matthäus 1996, Feistel et al. 2003b):

- They are driven by barotropic pressure gradients, especially sea level differences.
- They appear during persistent westerly gales (mostly in autumn, winter, spring).
- They import salt (typically 2 Gt) into the Baltic Sea along with the water volume import (typically 200 km^3)
- They import oxygen-saturated water (typically 1 Mt of O_2) if they happen in winter or spring.
- They pass through the Sound and the Belts.

In contrast, so-called baroclinic inflows have these properties (Knudsen 1900, Thiel 1938, Hela 1944, Wüst et al. 1957, Welander 1974, Jacobsen 1980, Matthäus et al. 1983, Feistel et al. 2003c, 2004, Mohrholz et al. 2006):

- They are driven by baroclinic pressure gradients, especially horizontal salinity differences.
- They appear during persistently calm wind conditions (usually in late summer).
- They import salt into the Baltic Sea along with water volume export.
- They import oxygen-deficient water, but ventilate the deep Baltic basins by entrainment.
- They pass only through the Great Belt/Darss Sill gateway.

Winter and spring inflows of either type give rise to higher salinities, low temperatures and increased oxygen levels in the deep basins. Summer and autumn inflows increase salinities and raise temperatures but carry only very little oxygen.

As a prerequisite for a barotropic inflow of saline deep water into the EGB a strong easterly wind lasting for several weeks is needed to lower the sea level of the Baltic Proper to less than 70 cm above normal (Matthäus and Franck 1992), although sea level differences between the Kattegat and the Baltic Sea fluctuate due to variations in the wind field during major events. Afterwards a strong wind from the west pushes saline North Sea water through the belts and sounds into the southwest Baltic Sea. The westerly wind has to last for about 10-12 days to push enough water across the Darss Sill, which will mix with the "old" deep water in the AB. Only if this "new" deep water has a higher density than the "old" deep water in the subsequent basin, it would be able to replace the deep water in that adjacent basin, steered by internal pressure gradients. These conditions usually occur in late autumn, winter, or early spring when the saline water of the Kattegat is well ventilated due to strong mixing and cooled as well as the haline stratification is destroyed for a number of days.

Matthäus and Franck (1992) found that the total volume transports through the belts and sounds must exceed 10 km^3/d to replace the deep water in the Baltic Proper completely. In general, such major inflow events happen on a timescale of about 3-5 years. The volume capacity of the deep Baltic basins in connection with the mixing of the deep water with the intermediate water controls the residence time of the deep water in the basins. For illustration, a volume of approximately 40 km^3 fills the deepest layers of the central basin of the Baltic Sea, the EGB, between 190 m and 245 m depth (Hagen 2004).

During and after inflow events large lateral pressure and salinity gradients between the central EGB with low pressure and its rim with high pressure cause the saline water at the rim to follow the bottom topography and circulate cyclonically within the basin (Lehmann and Hinrichsen 2000). Stagnation periods without strong inflow events can last for several years and also result in an increase of nitrate and phosphate below the halocline. Only major inflows of highly oxygenated and saline water are capable to renew the "old" deep water.

In conclusion, inflow events are likely to be the key to the most important vertical transport mechanisms in the central Baltic Sea, since they are the only mechanism of the “Baltic Deep Convection” and in this way driving the “Baltic Conveyor Belt”. The estimated residence time of the Baltic deep water in the order of 20 years suggests that inflows and vertical transport are controlling the properties of the Baltic Sea on the time scale of decades (Meier and Kauker 2003, Feistel et al. 2006a, Meier et al. 2006).

2.2. Surface mixed layer dynamics

The bulk sea surface salinity in the Baltic Proper is determined by the freshwater fluxes into the surface layer, i.e. the net freshwater flux through the surface resulting from precipitation and evaporation, melting and freezing, as well as the lateral freshwater fluxes due to river run-off, and the rate of upward turbulent salt flux through the uppermost pycnocline. The latter is defined by the seasonal thermocline in summer and the permanent halocline in winter.

The summer and the winter halocline differ essentially, see also Section 3.2: During summer the thermocline protects the halocline against erosion by surface mixed layer turbulence. Therefore the halocline is relatively weak in summer as a result of turbulent mixing. In contrast, the absence of the thermocline in winter allows the surface mixed layer to reach down to the halocline, which is abraded by the associated turbulent mixing. In this way the halocline is restored and the vertical salinity gradients in the halocline reach their maximum again.

Here we are going to refine the picture of the seasonal near-surface cycle by numerical simulations with a high-resolution one-dimensional model. Such models are applicable in situations where vertical processes are dominant compared to horizontal processes. This is the case for the Baltic Proper on the seasonal time scale, cf. Section 3.1. The water column model applied here is the General Ocean Turbulence Model (Umlauf et al. 2005, www.gotm.net) which has successfully reproduced observations of near-surface mixing processes, see e.g. Burchard and Bolding (2001), Burchard et al. (2002). The setup which is used here has been extracted from a decadal simulation recently carried out for the Baltic Proper, see Burchard et al. (2006). Here we present simulation results for the years 1989 and 1990, after the model has been spun up during the whole year 1988. The geographical position for the model simulation is at 20° E, 57.3° N in the centre of the Eastern Gotland Basin at a water depth of about 250 m. Here the upper 100 m of the water column are simulated. The initial conditions for this position have been interpolated from observations. The meteorological forcing has been extracted from the ERA15 reanalysis data set (http://www.ecmwf.int/research/era/ERA-15/). Prognostic equations are numerically approximated for momentum, potential temperature, salinity, and two turbulent properties, namely the turbulent kinetic energy k and its dissipation rate ε. An algebraic closure by Chen et al. (2002) has been used for the second moments. The turbulence integral length scale is limited by the Ozmidov scale $L_O = (\varepsilon/N^3)^{1/2}$ in the case of stable stratification. For details of the turbulence closure model see Burchard et al. (2006). The estimate of 3 m/a for the vertical uplift at the 10 psu isohaline resulting from inflows has been used as the vertical advection velocity at 60 m below the surface, cf. Section 3.3. This vertical velocity was set to zero at the surface and at 100 m depth for continuity reasons. From these two depths it was linearly interpolated to 60 m depth. With this setup a net surface freshwater flux of 1.26 m/a (partially accounting for unresolved lateral freshwater fluxes) was sufficient to balance the vertical salt flux into the surface mixed layer in such a way that the annual surface mixed layer salt budget was closed. The model resolution was 0.5 m in the vertical and 10 min in time. These choices ensured that all numerical schemes were converging and the simulation results were not significantly affected by numerical artefacts.

The results of this simulation for potential temperature, salinity, eddy diffusivity, and squared Brunt-Väisälä frequency are shown in Fig. 3. It should be noted that the graphics are composed of snapshots at midnight. The temperature shows a clear annual cycle with a summer thermocline at about 20 m depth, which builds up in mid April and is eroded down to 60 m in late December. During maximum surface warming the surface mixed layer depth is less than 10 m. The annual cycle of salinity is much weaker. It has a surface amplitude of about 0.3 psu. This is a 50 % underestimation compared to the salinity amplitude given in Table 1. This disagreement may result from the seasonal variability in the freshwater flux which has been neglected in this simulation. During winter the surface mixed layer extends downwards into the main halocline, which leads to an erosion process with upward salt flux and increasing surface salinities during the winter season. Once a thermocline is established in spring the halocline is protected from surface mixing. However, internal mixing processes (cf. in particular Section 5.1), which are here parameterised by means of a minimum *TKE* value and the length scale limited by the Ozmidov scale, weaken the gradients in the halocline during the summer season. These process descriptions are strongly supported by the simulation results for the eddy diffusivity and the squared Brunt-Väisälä frequency. Directly below the surface mixed layer the squared Brunt-Väisälä frequency shows values of more than 0.001 s^{-2}, specifically in the thermocline during summer and in the halocline during winter. The weakening of the summer halocline can be seen clearly. Near-surface stratification is mostly unstable, since all results are from midnight snapshots ("night convection"). Exceptions are the winter months, during which the temperature probably has fallen below the maximum density temperature, in particular during the winter 1988/1989. As a result further cooling at the surface stabilises the water column. Eddy diffusivity reaches values of up to 0.1 m^2/s during winter cooling. Interestingly, values of 2-3 $\times$ 10^{-6} m^2/s are simulated in the halocline, which is consistent with the observations discussed in Section 5.1.

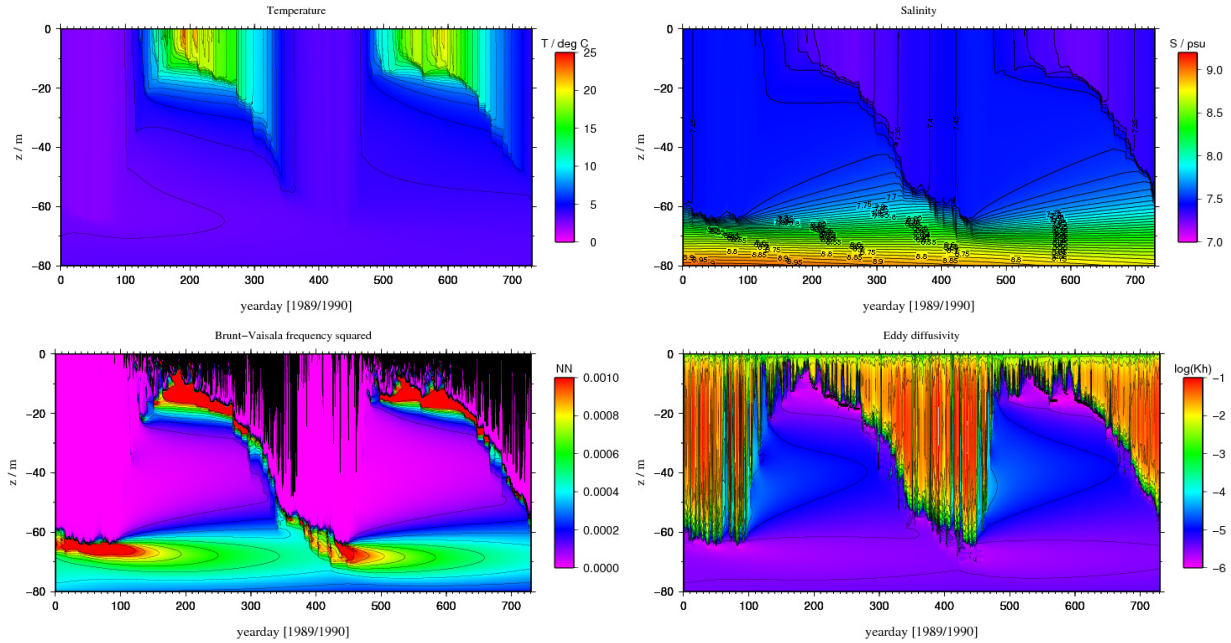

Fig. 3: Simulation results for potential temperature (upper left, in °C), salinity (upper right, in psu), squared Brunt-Väisälä frequency (lower left, in s^{-2}), and eddy diffusivity (lower right, in m^2/s). Shown are results for the years 1989 and 1990 for the upper 80 m. For the squared Brunt-Väisälä frequency all values larger than 0.001 s^{-2} are shown in red, all negative values are shown in black.

Comparisons between these simulation results and observations of temperature and salinity (not shown here) show that the simulated mixed layer depths are generally too shallow, which may be a result of missing horizontal processes. However, this simulation qualitatively reproduces the relevant processes in the surface mixed layer of the Baltic Proper. Detailed observational studies of these dynamics including turbulence measurements would be required in order to better quantify near surface mixing, which has a strong impact on the succession of plankton dynamics.

3. Vertical salt transport through the permanent halocline

This section has the focus on the salt balance in the central Baltic Sea and the associated vertical transport of salt to provide an easy measure and an estimate of the order of magnitude of any upward tracer transport through the permanent halocline which is connected to this by the corresponding volume transport. The estimates are made by various entirely different approaches to form a consistent picture. Some of them are independent of the detailed mixing processes, but some others are already connected to certain transport mechanisms, mainly the erosion of the pycnocline by deep convection in winter.

3.1. Bulk estimates from water and salt balance

Since the only source of sea salt in the Baltic Sea is the input from the Kattegat/North Sea, in form of irregular injections into layers beneath the permanent pycnocline, and its only sink is the near-surface outflow of brackish water into the Kattegat, the surface salinity above the pycnocline is a robust integral measure of the net upward transport through the pycnocline. The related bulk parameters are known for more than a century (Knudsen 1900) and have since then been discussed

by various scientists (Fonselius 1962, Jacobsen 1980, Matthäus and Schinke 1999, Rodhe and Winsor 2002, Fonselius and Valderrama 2003, Meier and Kauker 2003, Stigebrandt and Gustafsson 2003, Meier et al. 2006).

The climatologic surface salinity 1900-2005 of the Baltic Sea is available from e.g. the BALTIC atlas (Feistel 2006, Feistel et al. 2008). The permanent entrainment of salt from lower layers into the surface water forms the well-known stable NE-SW salinity gradient during the surface water renewal period of about 30 years (Meier and Kauker 2003, Meier et al. 2006, Feistel et al. 2006a). The excess freshwater input of about 500 km³/a causes a comparable export of brackish water (Knudsen 1900, Matthäus 2006) with a salinity of about 8 g/kg. Thus the Baltic Sea exports about 4 Gt of salt per year, and imports on average the same amount (Feistel and Feistel 2006). Divided by the sea surface area of almost 400,000 km², a rough estimate of the mean apparent vertical salt transport is 10 kg/(m² a). With regard to the smaller surface area of the pycnocline at about 60 m depth of 130,000 km², the true mean diapycnal transport rate at this depth is in fact higher by the same factor, namely a salt flow of about $J = 30$ kg/(m² a). This mass of salt originates from the Kattegat, imported with a mean inflow rate of another 500 km³/a, balanced by the same outflow volume with lower salinity. The seasonal signal of this exchange flow is observed up to the Bornholm Basin (Matthäus 1978).

The climatologic salinity distribution in the surface water is suggesting further useful information about the lowest-order dynamical processes in the Baltic Sea. Accepting the argument that salt is only transported upward from the deep to the surface water, the salinity of a particular parcel in the surface layer can only increase in time, if regions not too close to the river mouths are considered and evaporation and precipitation are balanced. Under these assumptions, salinity is a measure of the surface water age, and the lateral salinity gradient reflects the climatologic advection trajectories. The water from river Neva needs about 30 years to cross the Baltic Sea over a distance of about 1500 km (Meier et al. 2006, Feistel et al. 2006a), corresponding to an average advection speed of 50 km/a = 4 km/month = 0.2 cm/s. For the typical BALTIC grid cells with dimensions of about 100 × 50 km, the related residence time of surface water is 1-2 years. This estimate justifies the dynamical consideration of a particular 1° × 1° water column in terms of a one-dimensional vertical model on the monthly or seasonal time scale, thereby ignoring the influence of lateral advection. If, alternatively, surface advection velocities in the Baltic Sea were signifcantly higher than estimated here and, say, forming a fast gyre circulation on the basin scale, the observed lateral salinity gradient would not persist in a stable manner.

In the deep water, however, permanent current velocities in the order of 3 cm/s = 80 km/month = 1000 km/a are prevailing near the bottom (Hagen and Feistel 2004). Thus, seasonal changes in the deep water of an 1° × 1° water column are likely to be influenced by advective exchange processes between adjacent cells. Even these velocities are still exceeded significantly during occasional inflow processes. The leading front of a typical inflow event like 1997 or 2003 travels the distance of 800 km from the Danish Straits to the Gotland Basin within 3-4 months, i.e. with an average speed of roughly 200 km/month = 10 cm/s (Hagen and Feistel 2001, Feistel et al 2003b).

Summarising the estimates made before, temporal changes on the monthly scale encountered in a selected water column of the size 1° × 1° are likely attributed to horizontal advection in the near-bottom water but rather to vertical exchange in the surface water. This working hypothesis is borne in mind in the following when we shall discuss certain observations and possible explanations thereof.

3.2. Erosion of the pycnocline

As an example for the seasonal dynamics of the halocline, the time series measured by SMHI 2005 at the Gotland Deep may serve, as shown in Table 1. The year 2005 was a year of very weak inflow activity, with only decaying remnants of the inflow events observed in 2002 and 2003 (Nausch et al. 2006, Feistel et al. 2006a), as discernible from the minor salinity decrease in the bottom line of Table 1. The levels below 100 m seem unaffected by the seasonal cycle. The pycnocline, if defined by the strongest vertical gradient, is weak during the existence of the summer thermocline (May – September) and is strong in winter (January – February). The steepness is correlated with the homogeneity of the surface layer, i.e. the winter convection, but also with the surface salinity, which rises in fall/winter and falls in spring/summer.

A likely explanation of this observation can be that in summer the pycnocline becomes weakened under the protection of the thermocline, while the winter convection erodes its uppermost part and distributes the salt enclosed over the whole surface layer, restoring the steep density leap at its lower boundary.

Table 1: Time series 2005 of salinity from the Gotland Deep measured by SMHI. The halocline, defined here by the strongest vertical gradient, is marked in bold. The virtually homogeneous surface layer is shown in italic. The steepest halocline of 2.12 (g/kg) / 10 m is observed in January, together with the deepest extension of the mixed layer, down to the halocline.

Quantity: Salinity Year: 2005 Station: BY 15 Lat: 57°20' Lon: 20°03'

Depth	Jan20	Feb25	Apr07	Apr28	May19	Jun16	Jul14	Aug11	Sep01	Sep29	Oct27	Nov16	Dec12
0m	-	*7.43*	*7.39*	*7.31*	*7.19*	*7.17*	*6.93*	*6.82*	*6.84*	*6.97*	*6.93*	*7.06*	*7.13*
5m	*7.42*	*7.43*	*7.39*	*7.31*	*7.19*	*7.17*	7.05	*6.82*	*6.85*	*6.96*	*6.93*	*7.06*	*7.13*
10m	*7.41*	*7.43*	*7.39*	*7.31*	*7.18*	*7.16*	7.14	*6.83*	*6.84*	*6.96*	*6.93*	*7.06*	*7.13*
15m	*7.41*	*7.43*	*7.39*	*7.32*	*7.19*	*7.16*	7.15	6.88	6.88	6.95	*6.93*	*7.06*	*7.13*
20m	*7.41*	*7.43*	*7.39*	7.36	7.22	7.18	7.13	6.84	7.08	7.08	*6.93*	*7.06*	*7.13*
30m	*7.42*	7.45	*7.39*	7.37	7.36	7.31	7.26	7.07	7.20	7.38	*6.94*	7.10	*7.13*
40m	*7.41*	7.47	*7.39*	7.43	7.41	7.39	7.36	7.22	7.35	7.48	7.43	7.11	*7.14*
50m	*7.42*	7.47	7.41	7.51	7.53	7.49	7.46	7.34	7.44	7.57	7.53	7.13	7.17
60m	***7.42***	**7.46**	**7.50**	**7.64**	**7.73**	**7.63**	7.59	7.68	7.55	7.67	7.63	7.24	7.55
70m	**9.54**	**9.32**	**9.05**	**8.77**	**8.82**	**8.78**	**8.44**	**8.71**	**8.20**	**8.08**	**7.92**	**7.80**	8.24
80m	10.36	10.37	9.73	9.80	9.81	9.85	**9.73**	**9.96**	**9.68**	**9.56**	**8.36**	**9.49**	**8.99**
90m	10.64	10.86	10.66	10.56	10.40	10.51	10.39	10.47	10.43	10.26	9.72	10.23	**10.23**
100m	10.90	11.16	11.03	10.98	10.74	11.05	10.96	11.06	10.94	10.67	10.35	10.86	10.58
125m	11.84	11.75	11.68	11.78	11.52	11.91	11.86	11.90	12.01	11.77	11.48	11.85	11.46
150m	12.34	12.23	12.21	12.25	12.19	12.28	12.33	12.31	12.30	12.29	12.23	12.37	12.17
175m	12.47	12.49	12.44	12.45	12.47	12.46	12.53	12.49	12.48	12.45	12.33	12.48	12.45
200m	12.63	12.49	12.59	12.59	12.61	12.60	12.63	12.58	12.61	12.59	12.51	12.59	12.55
225m	12.77	12.61	12.69	12.70	12.73	12.69	12.73	12.66	12.70	12.69	12.61	12.66	12.56
240m	12.80	12.71	12.76	12.74	12.76	12.70	12.74	12.70	12.73	12.73	12.68	12.69	12.68

Between the minimum surface salinity of 6.82 in August 2005 and the maximum of 7.43 in February we find a difference of 0.61 g/kg. The corresponding difference between minimum and maximum of the mean seasonal cycle is 0.52 g/kg (Matthäus 1978). Integrated over a surface layer of $H = 60$ m thickness, this entrainment amounts to a salt flow of $\Delta S \times \rho \times H = 37\,\mathrm{kg/m^2}$, eroded from the halocline over the year 2005, or 31 kg/(m² a) in the long-term mean, which meet very well the bulk estimate in Subsection 3.1.

3.3. Uplift by inflows

The strongest perturbations on timescales between hours and years are Major Baltic Inflows (MBI) from the Kattegat. During such an event lasting 10-20 days, typically additional 200 km³ of water flow into the Baltic Sea, importing about 2 Gt of salt (Fischer and Matthäus 1996, Feistel et al 2003c, Feistel et al. 2006a, Matthäus 2006), corresponding to an average salinity of 10 g/kg. The near-bottom salinity in the Arkona Sea during an inflow event is 20 g/kg or higher, i.e. only about 100 km³ of the inflow volume are injected into the deep water below the pycnocline. Independent of future mixing processes on its way to the central basins, this volume elevates the pycnocline with its surface area of 130000 km^2 on average by 80 cm. This is a small number compared to the typical lowering of the halocline in winter by some 10 m in the Gotland Basin. If this uplifted layer, assuming its typical salinity as S = 10 g/kg, is eroded during the vertical convection in the following winter(s), 1 Gt of salt becomes entrained and mixed into the surface layer with its total volume of about 15000 km^3, thus increasing its salinity on average by less than 0.1 g/kg. In reality, this process is likely more constrained to the pathway of the inflowing tongue, rather than being spread homogeneously over the whole Baltic Sea area.

Within the deep basins the uplift of ambient water masses by the newly arriving one is much more pronounced than it is observed at the pycnocline. During the inflow of September 1997, for example, estimated 56 km^3 of the inflow water with a salinity of about 12 g/kg arrived at the Eastern Gotland Basin, entirely substituting the residing water volume of 38 km^3 beneath 150 m depth there, and pushing it into the adjacent basins further north and west (Hagen and Feistel 2001). The original inflow volume was estimated to 140 km^3 (Hagen and Feistel 2001), its salt import to 1.2 Gt (Matthäus 2006).

The pycnocline uplift during the MBI 2003 as well as its seasonal erosion is very well seen from the distribution of hydrogen sulfide as a tracer in the ambient deep water in Fig. 32. The oxygen-rich inflow near the bottom (green, beginning in April/May 2003) causes an elevation of the stagnant water (yellow) below the pycnocline from 100 m to 70 m depth, i.e. by almost 30 m. Subsequent erosion, in particular between February and April, gradually suppresses the excited vertical oscillation of the pycnocline.

The salt budget of the entire Baltic Sea is about 120 Gt (Winsor et al. 2001, Rodhe and Winsor 2002), which rises by about 1-5% in the course of a strong MBI event, but shrinks by 4% regularly every year due to the outflow to the Kattegat (Feistel and Feistel 2006). In order to substitute the mean annual surface salt loss of 4 Gt/a by an equivalent supply from the deep water, the required apparent mean vertical advection speed at the S = 10 g/kg isohaline would be on average $w = 4\,\mathrm{Gt}/\left(1\mathrm{a}\times 10\,\mathrm{g/kg}\times\rho\times 130{,}000\mathrm{km}^2\right)$, i.e. $w = 3\,\mathrm{m/a} = 10\,\mathrm{mm/d} = 0.1\,\mu\mathrm{m/s}$.

3.4. Diapycnal response function

The temporal development of the salinity at the surface (above 20 m) and in the deep water (at 200 m) between 1968 and 2005 at the Gotland Deep is shown in Fig. 4. In the upper series, inflow events are visible by the salinity leaps, followed by a slow decay. This decay is particularly apparent in the long stagnation period from 1978 to 1993. In the lower series, the readings scatter stronger, but reflect the deep-water record with a delay of about 10 years, smaller amplitude, and low-pass filtered. From the simple linear 2-box vertical exchange model,

$$\frac{\partial S}{\partial t} = D\times\left[S_\mathrm{B}(t) - S\right] \qquad (1)$$

describing the "answer" $S(t)$ of the surface salinity to the "signal" $S_B(t)$ of the bottom salinity (Feistel et al. 2006a), a linear response function can be derived by solving the differential Eq. 1, as

$$S(t) = D\int_0^\infty \exp(-\tau/T_\mathrm{R})\, S_B(t-\tau)\mathrm{d}\tau\,. \qquad (2)$$

The memory, $T_\mathrm{R} = 13a$, and the deep-water residence time, $1/D = 21\mathrm{a}$, can be estimated from mean salinity difference and the signal delay between the two depth levels as shown in Fig. 4 (Feistel et al. 2006a). The related residence time of the surface water appears to be 33 years. These values agree very well with estimates derived earlier by several workers from entirely different arguments (Meier and Kauker 2003, Meier et al. 2006).

None the less, the model according to Eq. 2 is an extreme simplification of the real complexity of vertical exchange. It is derived from the temporal behaviour at merely a single location, but its inherent time constants correspond to basin-scale processes of the whole Baltic Sea, which comprise dynamically so different regions as the Belt Sea or the Bothnian Bay. Another deficiency of the model is the fact that it predicts an exponential decay of the bottom salinity during stagnation periods, i.e. without salt inflow $\Phi_S(t) = 0$, from the complementary balance relation to Eq. 1

$$\frac{\partial S_\mathrm{B}}{\partial t} = \Phi_S(t) - D\times S_\mathrm{B}\,. \qquad (3)$$

As Fig. 4 clearly shows, the curve at 200 m between 1983 and 1993 is concave rather than convex, i.e. the salt loss is accelerating rather than slowing down. A possible explanation is that the salt depletion in the deep water reduces the density gradient at the pycnocline, thus permitting the winter convection to gradually deepen its erosion of the "lid" (Feistel et al. 2006b). Such a self-accelerated decay ends in a total destruction of the halocline already after a finite period of time, in contrast to an exponential law, which takes infinitely long to let the stratification disappear.

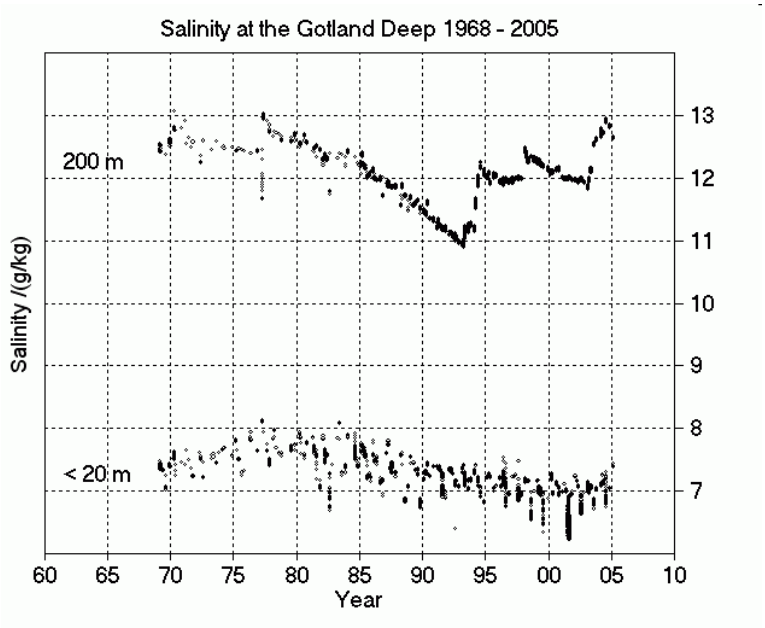

Fig. 4: Salinity at the surface (above 20 m) and in the deep water (at 200 m) between 1968 and 2005 at the Gotland Deep.

The mean vertical transport rate D, corresponding to a deep-water residence time of 21 years, includes the occasional uplift processes of deep water by inflow events as shown in Fig. 4. In the absence of the latter ones, as observed during the long stagnation period, the typical salinity decrease at 200 m is about 1.5 g/kg from 1983 to 1993, or slightly more than 1% per year, which corresponds to a residence time of almost a century. These two very different residence times suggest that deep water uplift during inflow events and the subsequent erosion of the pycnocline is by far the dominating vertical transport mechanism in the Baltic Sea (Feistel et al. 2006a).

The related transport rate across the pycnocline into the surface layer of about 60 m thickness can correspondingly be computed from Eq. 1 as a salt flow of

$$J = D \times S_B \times \rho \times 60\,\mathrm{m} = 34\,\mathrm{kg/(m^2\,a)}, \qquad (4)$$

in excellent agreement with the estimates derived in Subsections 3.1 and 3.2 from rather different models. During the Great Stagnation Period 1983-93 without major inflows, this value appeared reduced by a factor of 5 due to the longer residence time of about $1/D = 100$ a used in Eq. 4, so that probably 80% of the long-term vertical salt transport originates from occasional inflow processes and the subsequent elevation and erosion of the halocline, and only less than 10 kg/(m² a) are due to other mechanisms.

A similar estimate was made earlier by Ozmidov (1994a), who supposed a deep-water volume of 200 km³ with salinity 20 g/kg, possessing a (guessed) residence time of 10 years beneath the thermohalocline with a surface area of 80,000 km², and obtained a vertical salt flow of $J = 5$ kg/(m² a). Alternatively, derived from a diffusion equation approach to the vertical salinity profile measured in the Eastern Gotland Basin in April 1993, the vertical salt transport estimated by Ozmidov (1994a) is about $J = 1$ kg/(m² a), i.e. even smaller. Evidently, the vertical salt transport of $20\,\mathrm{g/kg} \times 200\,\mathrm{km^3}/10\,\mathrm{a} = 0.4\,\mathrm{Gt/a}$ estimated by Ozmidov (1994a) can explain only 10% of the observed salt export of 4 Gt/a by the brackish Baltic Current.

We finally note that the vertical salt flow of $J = 34$ kg/(m² a) amounts to a related potential power density of $p = g \times J = 11\,\mu\mathrm{W/m^3}$, corresponding to the potential energy stored in the uplifted mass of dissolved salt in excess to the ambient mass of water.

4. Mixing in straits

In contrast to the previous section this section has a strong regional focus on the entrance area of the Baltic Sea addressing the mixing and dilution of inflowing saline bottom water on its way through channels and over sills to the central parts of the Baltic Sea and the associated processes. The amount of dense water arriving in the deep basins of the Baltic Sea depends on the net amount of dense water flowing over Darss Sill and Drogden Sill into the Arkona Sea, cf. Fig. 5, and on the rate of entrainment of brackish water into the inflow water along the pathway of the dense water towards the Baltic Proper.

Considering the inflow along a chain of subsequent sills and basins, starting from the Kattegat, through the Belt Sea into the Arkona Sea, through the Bornholm Channel into the Bornholm Sea and furthermore through the Słupsk Furrow into the Eastern Gotland Basin, Kõuts and Omstedt (1993) estimated the amount of volume flow increase due to entrainment for each of these regions. Analysing salinity and temperature observations during two decades, they came up with 79 % for the Belt Sea, 53 % for the Arkona Sea and 28 % for the Słupsk Furrow. For the Bornholm Channel and the Bornholm Sea no mixing was identified.

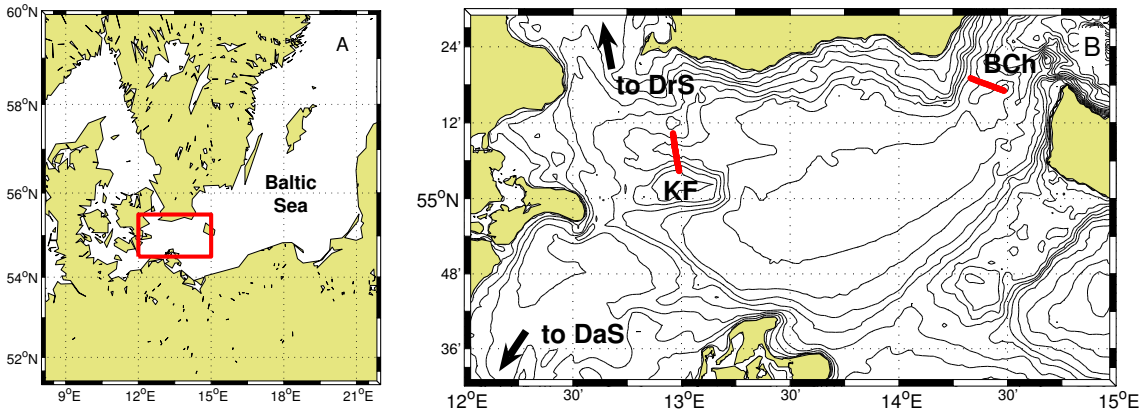

Fig. 5: Detailed map of the western Baltic Sea covering the Arkona Basin as indicated on the left side (map A). The arrows in map B on the right side indicate the direction to the Darss Sill (DaS) and Drogden Sill (DrS). Indicated in red are the transects north of Kriegers Flak (KF) and across the Bornholm Channel (BCh), shown in Figs. 7 and 8, respectively. The bathymetry is drawn in contours with a spacing of 5 m.

4.1. Dense water pathways

In order to obtain a more detailed picture of the regional and temporal distribution of entrainment and a deeper understanding of the underlying processes, the pathways of dense inflowing water along the major chain of subsequent straits and basins need to be identified. Because of the episodic nature of these inflows and the general undersampling problem, this is actually not an easy task. The classical picture is that the dense bottom currents adjust to a major balance between Coriolis force and pressure gradient, whereas bottom and interfacial friction is of secondary importance (Liljebladt and Stigebrand 1996). This has the consequence that water spilling over the Darss and Drogden Sills are basically spiralling cyclonically along the rims of the Arkona Basin (Fig. 5), dragged by some small frictional effects into the core of the Arkona Basin (Lass and Mohrholz 2003). These feed episodically into an up to 15 m thick bottom pool of dense water resting in the relatively plain eastern part of the Arkona Sea (Stigebrandt 1987b), generating a Kelvin-wave type of cyclonic circulation pattern (Lass and Mohrholz 2003). This pool has a residence time of 1 to 3 months, see Lass et al. (2005), and is reduced in volume by permanent leakage through the Bornholm Channel (Walin 1981).

This view of cyclonically spiralling dense bottom currents into the Arkona Sea has recently been challenged by means of numerical modelling (Burchard et al. 2005, Lass et al. 2005, Burchard et al. 2007) and field observations (Sellschopp et al. 2006, Umlauf et al. 2006). Burchard et al. (2005) carried out a simple numerical lock exchange experiment for the Arkona Sea, using a three-dimensional hydrostatic model (GETM, General Estuarine Transport Model, see Burchard and Bolding 2002). The Arkona Sea was initially filled with brackish water of homogeneous salinity of 8 psu. The model was then forced with elevated water levels and high salinity of 25 psu in the Sound, leading to a strong overflow over Drogden Sill. On its southward propagation the plume turned eastwards and passed along the northward slope of Kriegers Flak, cf. Fig. 5. Only a small fraction of the plume followed the expected pathway west of Kriegers Flak, thus contradicting the earlier assumptions of basically geostrophically balanced inflows. The separated dense bottom currents joined south-eastern of Kriegers Flak and meandered into the eastern part of the Arkona Sea. This was independently confirmed by another idealised numerical model study carried out by

Lass et al. (2005), based on the modular ocean model (MOM-3, Pacanowski and Griffies 1999) applied to a numerical model of the North Sea and Baltic Sea. There an inflow event was forced by sea surface elevation gradients and westerly winds, resulting first into an inflow through the Sound with similar dynamics as obtained by Burchard et al. (2005). About 5 days after Drogden Sill is passed by saline water a saline overflow occurs at Darss Sill, which subsequently runs down a submarine terrace, flowing cyclonically along the southern rim of the Arkona Basin, and stratifying over the denser plume from the Sound. Parts of these rather complex dynamics have been confirmed by Sellschopp et al. (2006) who observed an inflow event through the Sound in Jan./Feb. 2004. They found that most of the dense water flowing over Drogden Sill did afterwards pass through the channel north of Kriegers Flak. Burchard et al. (2007) set up a realistic numerical model for the western Baltic Sea covering the period of observations carried out by Sellschopp et al. (2006). They could obtain good agreement between the observed and simulated salinities at the positions of the Drogden Sill, Darss Sill and Arkona Sea moored stations, see Fig. 6, and between the observed and simulated salinities and currents north of Kriegers Flak. With such a validated numerical model various analyses of derived properties which cannot be directly quantified by observations can be carried out as discussed in the next subsection.

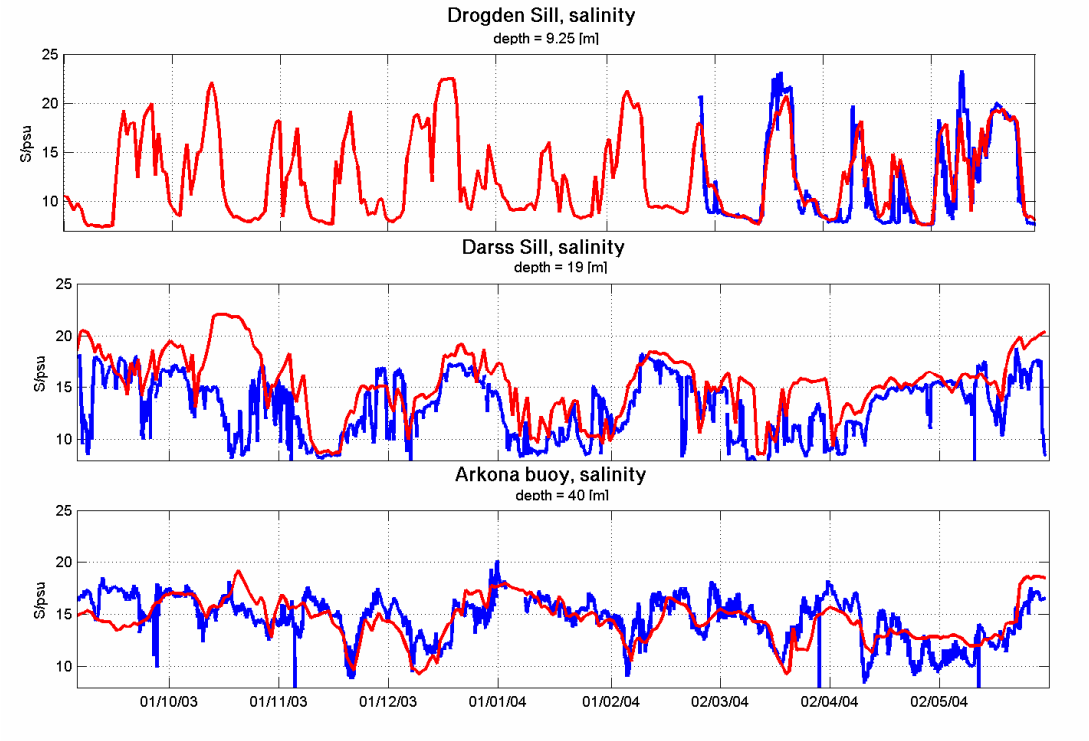

Fig. 6: Time series of simulated (red) and observed (blue) near-bottom salinities at three positions in the Baltic Sea. Upper panel: Drogden Sill, middle panel: Darss Sill, lower panel: Arkona Sea. Note that the station at Drogden Sill did not observe any salinity data until March 2004.

These observations could be further confirmed by Umlauf et al. (2006) who observed a strong inflow over Drogden Sill via the channel north of Kriegers Flak in November 2005 with improved instrumentation at high spatial resolution. During several transects they found a distinct cross-sectional structure of the dense bottom current with a strong pycnocline leaning towards Kriegers Flak, with the dense core moved by the cross-channel Ekman transport towards the northern slopes of the channel, a characteristic transverse circulation, and a complex pattern of high and low mixing, see Fig. 7. This pattern is repeated across the Bornholm Channel, see Fig. 8. For the Słupsk Sill this characteristic transverse structure of dense overflows into the Baltic Sea has also been

observed by Paka et al. (1998) and Paka et al. (2006). They attributed the dislocation of the dense core to the north and the vertically erected isopycnals near the bed of the southern slope to the mechanism of arrested Ekman layers (Garrett et al. 1993), balancing the southward near-bed Coriolis acceleration by the transverse density gradient. The possible impacts of these dynamic features on entrainment are discussed in the next subsection.

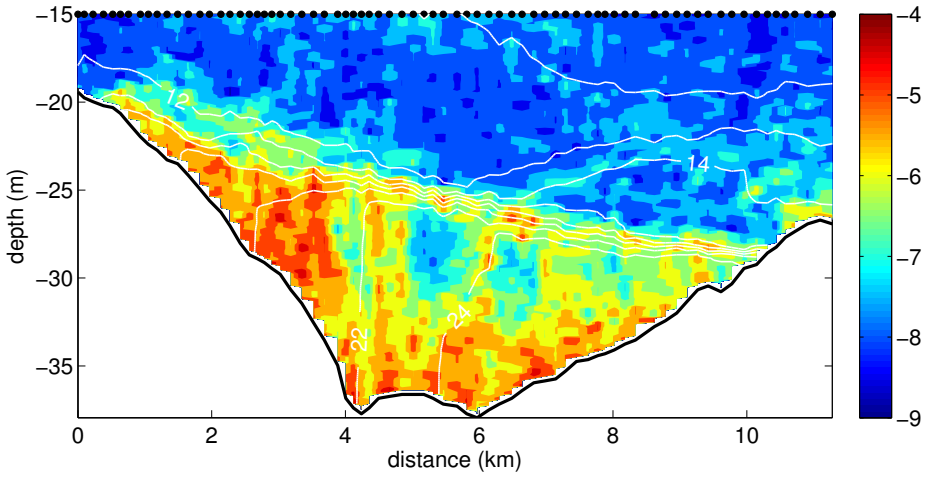

Fig. 7: Meridional transect across the channel north of Kriegers Flak, as indicated in Fig. 5, on November 17, 2005 between 8:00 h and 10:45 h UTC, south is to the left and north is to the right. Shown are contours of salinity in psu, drawn as intervals of 2 psu. The colour scale indicates the decadal logarithm of the viscous dissipation in W/kg, which is a measure of the turbulence intensity and an indication of mixing. The data are obtained by means of a free-falling microstructure profiler. The position of each cast is indicated by a bullet. The upper 15 m of the transect are not shown.

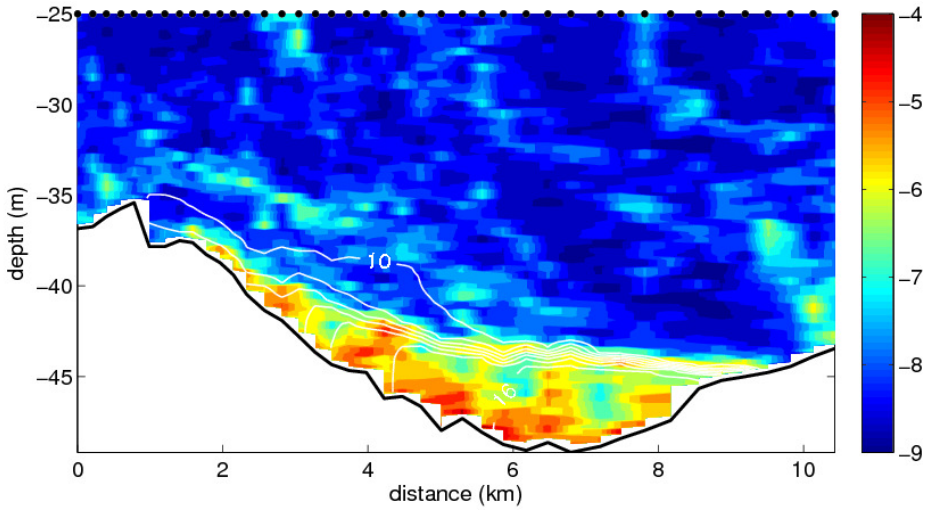

Fig. 8: Transect across the north-western part of the Bornholm Channel, as indicated in Fig. 5, on November 19, 2005 between 10:20 h and 12:30 h UTC, south-east is to the left and north-west is to the right. Shown are contours of salinity in psu, drawn as intervals of 1 psu. The colour scale indicates the decadal logarithm of the viscous dissipation in W/kg, which is a measure of the turbulence intensity and an indication of mixing. The data are obtained by means of a free-falling microstructure profiler. The position of each cast is indicated by a bullet. The upper 25 m of the transect are not shown.

The outflow from the Bornholm Sea over the Słupsk Sill into the Słupsk Furrow shows a high variability as well. Meier et al. (2006) list three different overflow regimes, (i) simple overflow when isopycnals in the Bornholm Sea are higher than the sill depth, (ii) overflow with strong shift of the dense bottom current core towards the southern slopes of the sill, and (iii) eddy-like episodic exchange across the sill. Each of these overflow regimes may be subject to various mixing and entrainment processes which are not yet well investigated.

4.2. Entrainment

The data analysis of Kõuts and Omstedt (1993) located the regions of increased mixing of inflows into the Baltic Sea, but did not discuss the processes causing the mixing. In a more detailed and process-oriented investigation Lass and Mohrholz (2003) identified three major mixing mechanisms, (i) wind mixing in the vicinity of sills, (ii) differential advection in the head region of the dense bottom currents, and (iii) shear-induced entrainment of ambient water into dense bottom currents. However, the wind related mixing can only be effective at relatively shallow depths, such as the Darss and Drogden sills, whereas in the deeper Bornholm Channel and Słupsk Furrow the dense bottom currents are mostly protected against wind mixing by an overlaying stratified layer. The differential advection mechanism which increases mixing by shearing denser water over less dense water in the presence of density increasing in flow direction has been suggested earlier by van Aaken (1986).

The entrainment across the pycnocline on top of the dense bottom current due to interfacial shear has been investigated in much detail since several decades (Turner 1986, Baines 2001, Cenedese et al. 2004). This generally results in a dependence of the entrainment parameter $E = W_E/U$ (with the entrainment velocity W_E representing the rising velocity of the pycnocline and the mean downslope velocity U) on the Froude number $F_r = U/(g'H)^{1/2}$ (with the reduced gravity g' and plume thickness H), which is of the form

$$E = c\, F_r^{\,a}$$

with the positive non-dimensional parameters a and c. The entrainment formulation derived by Stigebrandt (1987a), based on the Kato-Phillips entrainment formula (Kato and Phillips 1969) and calibration of a horizontally integrated numerical model, parameterises this as

$$E = 2\, C_d\, R_f\, F_r^{\,2}$$

using the notation of Arneborg et al. (2007), with the bed friction coefficient C_d and the bulk flux Richardson number R_f, which is the ratio of the buoyancy flux and the shear production of turbulence. Stigebrandt (1987a) applied this with constant values of $C_d = 0.0035$ and $R_f = 0.035$. By validating the turbulence model GOTM (General Ocean turbulence Model, see Umlauf and Burchard, 2005) with time series observations of current, salinity, and turbulence dissipation rate in a dense bottom current north of Kriegers Flak Arneborg et al. (2007) refined the entrainment formula by considering the effect of the Ekman number $K=(C_dU)/(fH)$ (with the Coriolis parameter f) and the Froude number F_r on the bulk flux Richardson number R_f:

$$E = a\, C_d\, K^{\,b}\, F_r^{\,c} \qquad (5)$$

with $a = 0.084$, $b = 0.6$ and $c = 2.65$.

Based on mass conservation Sellschopp et al. (2006) estimated the entrainment velocity between Drogden Sill and the region north of Kriegers Flak to w_E=3×10^{-6} m/s. Inserting the observed values of C_d=0.0037, U = 0.5 m/s, f = 1.2×10^{-4} s^{-1}, H = 10 m and g' = 0.089 m/s^2 into the formulation Eq. 5 by Arneborg et al. (2007), which gives a Froude number of F_r = 0.53 and an Ekman number of K = 1.54, the entrainment velocity is w_E = 3.75×10^{-5} m/s, about one order of magnitude higher than the estimate derived from a larger scale spatial average mass conservation consideration. This demonstrates how highly variable in time and space entrainment may be, see also Fig. 9.

One complication is the complex transverse structure of dense bottom currents as shown by Umlauf et al. (2007), see Fig. 7. The dissipation rate, representing the mixing intensity, shows four clearly distinct regions. There are strongly elevated levels of dissipation rate in the bottom boundary layer of the dense bottom current, at the left side where vertical isohalines are advected towards the center of the channel by the Ekman transport associated with the strong bottom turbulence, and in the sharp pycnocline itself where the local shear has a maximum. In contrast to that, a region of low dissipation rate is visible in the core of the dense bottom current.

Observations from the Bornholm Channel in November 2005 clearly show a similar pattern, see Fig. 8. From this we conclude that substantial mixing and subsequent entrainment must also be present at the Bornholm Channel. For the Słupsk Sill substantial mixing can be inferred from detailed hydrographic surveys, see Piechura and Beszczynska-Möller (2004) and Paka et al. (2006).

Because of the high spatial and temporal variability of entrainment processes and the small value of the entrainment velocity, mixing in straits is substantially undersampled. A successful method to still obtain quantitative estimates of mixing in straits over long periods, is the application of high-resolution numerical models for these regions. Arneborg et al. (2007) have already demonstrated this for the position north of Kriegers Flak with a one-dimensional example. It is essential that these models are able to reproduce the basic processes associated with mixing and the few observations which are available. Using the same turbulence module as Arneborg et al. (2007), Burchard et al. (2007) have set up the GETM model for the western Baltic Sea and Kattegat region for the period September 2003 – May 2004. They could reproduce time series observations at the Darss and Drogden sill stations and in the Arkona Sea as already shown in Fig. 6. The vertically integrated, time averaged turbulent vertical salt flux has been calculated utilising this validated model, see Fig. 9. Areas of strong mixing can be clearly identified in the pathways of dense bottom currents through the Sound towards north of Kriegers Flak and through Darss Sill as well as over the submarine terrace east of it. Moreover, the strongest salt fluxes are observed across the Bornholm Channel. Effective mixing rates calculated by the model may however be artificially increased due to numerical diffusion (e.g. Lee et al. 2002) such that some attention is necessary when analysing mixing rates from numerical models.

The strong mixing observed in the Bornholm Channel is in disagreement with the findings of Kõuts and Omstedt (1993), who concluded that mixing in the Bornholm Channel is irrelevant. How can this be explained? A closer look at the dissipation rates in Fig. 7 shows that increased dissipation is present in the region of the halocline, located above the quiet core of the plume with minimum dissipation rates. Thus the entrainment cannot be mediated through bottom friction, but can be fully explained by interfacial instabilities. Although the mixing effect of this entrainment is substantial, the dynamic effect on the dense bottom current due to the entrainment stress may be small. Thus the fact that the dense bottom current is basically in geostrophic balance (Kõuts and Omstedt 1993) does not contradict to the fact that entrainment is large. Actually, Sellschopp et al. (2006) could show that the shape of the density profiles north of Kriegers Flak can be largely explained by the thermal wind equation, even though the same data imply strong entrainment at this position at the same time (Arneborg et al. 2007).

Mixing in the Słupsk Furrow has been estimated to be substantial by Kõuts and Omstedt (1993). Although direct observations of entrainment activities in this region have not been carried out, this high entrainment is indicated by the fact that the Słupsk Furrow near-bottom areas are almost always well ventilated with oxygen while the water masses are mostly poor in oxygen at the same depths in the Bornholm Sea (Feistel et al. 2006a). This can be explained by oxygen-rich surface water being entrained into the oxygen depleted dense bottom currents during the passage over the Słupsk Sill.

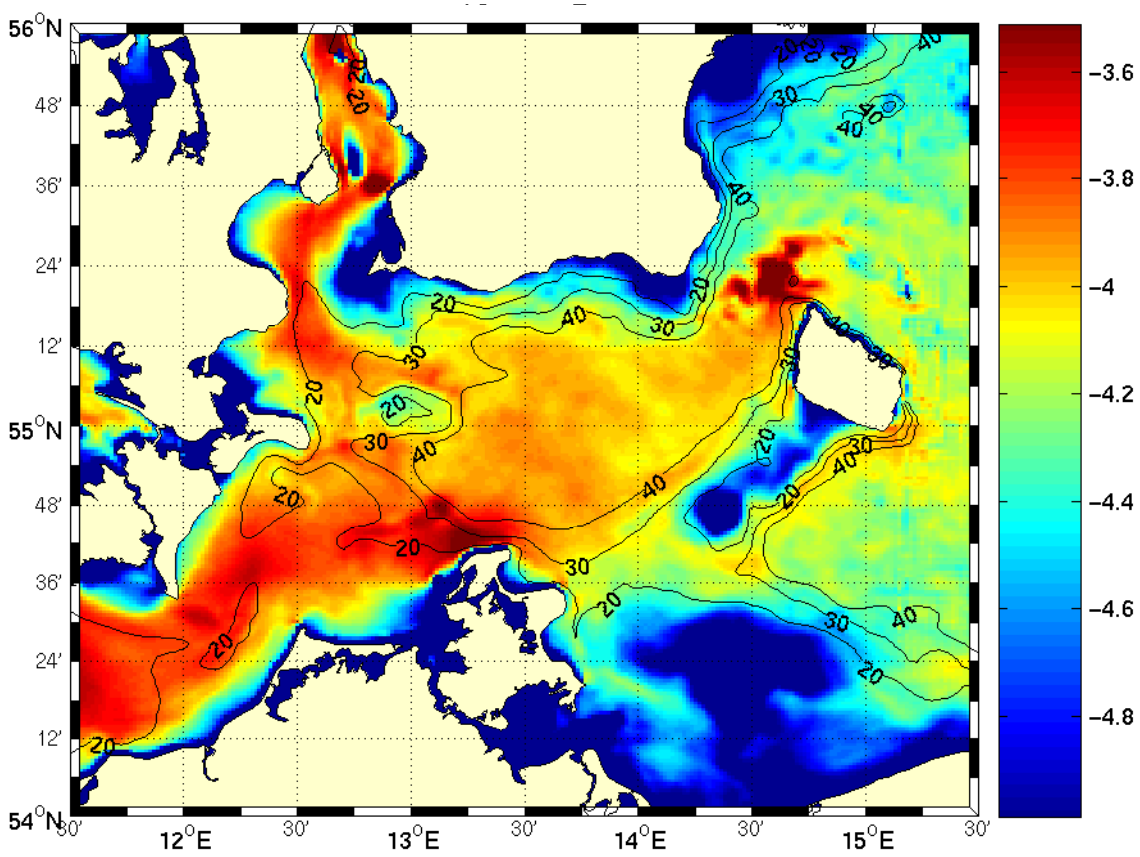

Fig. 9: Decadal logartithm of simulated vertically integrated, time averaged turbulent vertical salt flux in (m^2 psu)/s in the Arkona Sea area for the period September 2003 – May 2004. Isobaths are indicated as contours.

The natural mixing processes in the western Baltic Sea may actually be modified by massive off-shore constructions such as bridges and wind farms. During the planning phase of the Great Belt Link and the Sound Bridge a zero-blocking solution has been postulated, meaning that the bridge constructions must have no influence on the volume flux through the Sound and Great Belt (Hansen and Møller 1990). Stigebrandt (1992) estimated that a flow reduction by only 0.6 % would result for the Sound bridge with almost no measurable effect for the Baltic Sea hydrography. Møller et al. (1997) carried out laboratory experiments with obstacles dragged through stratified water and found no significant mixing effect. However, recent observations of currents, stratification, and turbulence upstream and downstream from the western part of the Great Belt Bridge carried out by Lass et al. (2006) revealed significant effects of the bridge piles on the vertical flow structure. They observed von Karman straits in the wake of the bridge piles with the potential to generate internal waves. These may propagate away from the constructions and release their energy into diapycnal mixing remotely, compare Subsection 5.1. In recent years extensive off-shore wind farms have been

planned in the western Baltic Sea. Many of them are located near the coast at shallow depths, where dense bottom currents do not occur, but it is the intention to locate some of these projected wind farms in overflow areas such as around Kriegers Flak. Their foundations may also act as obstacles for dense bottom currents with the effect of increased entrainment. However, bulk estimates of the mixing effects of these existing or projected constructions and their potential impacts on the ecosystem of the Baltic Sea have not been carried out so far.

5. Potential mechanisms of vertical mixing

After the erosion of the pycnocline by deep convection in winter seems to be identified as the main vertical transport mechanism from the permanent halocline into the entire mixed layer in the central Baltic Sea in Section 3, this section is devoted to some other vertical mixing mechanisms which are assumed to be relevant in the Baltic Sea. According to Section 3, they may gain in importance temporarily during stagnation periods or on timescales shorter than one year. Furthermore, they may have regionally or in depth levels other than the halocline significant impact. The knowledge about the mechanisms discussed in this section is quiet different. It ranges from quiet well known to completely unexplored for the Baltic Sea. In addition, it has to be mentioned that they are not necessarily independent from each other or may respond to the same forcing conditions.

5.1. Mixing due to inertial waves and internal wave breaking

Dissipation of wave energy to turbulent motion and mixing

Lass et al. (2003) have shown that there exists a well defined internal turbulence regime in the Baltic Sea which is embedded between the surface layer and the bottom layer turbulence regime. Turbulence below the surface mixed layer is quite independent of the actual wind forcing at the sea surface and occurs in intermittent patches due to pelagic and benthic disintegration of internal waves that are sub-grid phenomena in most models. The general view has been that non-linear interaction of internal waves cascades energy to small scales where it subsequently supports turbulence in the ocean interior. This can be quantified in different ways depending on the assumptions made about the wave field and about the nature of the interactions. The Garrett-Munk model of the internal wave field (Garrett and Munk 1975) has been used for most discussions of open ocean conditions. Predictions of the energy contributed by the internal wave field to turbulence and ultimately lost to dissipation in the course of mixing the fluid were reviewed by Gregg (1989).

There are areas in the ocean and in marginal seas where the internal wave field deviates from the Garrett-Munk model. The internal wave field in the Baltic Sea deviates in several aspects from that of the ocean. Firstly, internal tides are lacking in the Baltic Proper due to the virtual absence of barotropic tides. Secondly, there are no permanent geostrophic currents in the Baltic Sea whose temporal variations are associated with the radiation of inertial waves due to the adjustment to the varying geostrophic balance (Gill 1982). The dominant process of the generation of internal waves in an enclosed sea is expected to be the radiation of barotropic inertial waves generated at the coasts in order to maintain the zero flux boundary condition in the presence of fluctuating Ekman transports in the surface layer of the open sea. Barotropic inertial waves passing stratified water on a sloping bottom generate baroclinic inertial waves. This may explain why baroclinic inertial motions are so energetic in the Baltic Sea (e.g. Gustafsson and Kullenberg 1936 and Kielmann, Krauss, and Keunicke 1973). Although the shape of the internal wave spectrum in the Eastern Gotland Basin is similar to that of the Garrett-Munk spectrum in the frequency space, Lass et al. (2003) found that the internal waves below the halocline were characterised by a dominance of

waves with upward phase propagation. This implies that the spectrum of internal waves in the Baltic Sea can not be modelled by the Garrett-Munk spectrum. Polzin et al. (1995) were able to find a scaling of the dissipation rate of turbulent kinetic energy in terms of the frequency distribution of energy within the deep-ocean internal wave field for wave fields that differed from the Garrett-Munk model.

Wave-wave interaction parameterisation assumes that the energy flux is directed from the large energy containing waves via weak non-linear interaction toward the small scale waves, which become unstable and finally break into turbulent motion. The rate ε of dissipation of turbulent kinetic energy depends on the energy flux through the spectrum of the internal waves and depends on its parameters. The parameterisation of Henyey et al. (1986), Gregg (1989), and Polzin et al. (1995), which is based on the wave-wave interaction mechanism, predicts $\varepsilon \propto N^2$ with the Brunt-Väisälä frequency N and has been successfully compared to dissipation measurements in the open ocean (Polzin et al. 1995).

Gargett and Holloway (1984), using WKB scaling of the internal wave velocities, have shown that the dependence of the dissipation rate depends on properties of the internal wave spectrum. In case of narrow band internal waves the averaged kinetic energy production term and hence the dissipation rate in the stratified ocean is $\varepsilon \propto N$. In the broad band case (GM-spectrum) it is $\varepsilon \propto N^{1.5}$. In the ocean thermocline averaged dissipation rates are reported to vary systematically with N between $\varepsilon \propto N$ and $\varepsilon \propto N^2$ (e.g. Gregg 1987 and also Polzin et al. 1995). MacKinnon and Gregg (2003, 2005) found an $\varepsilon \propto N$ scaling for data collected over the continental slope. The parameterisation $\varepsilon \propto N$ was also successfully used by Stigebrandt (1987a) in a vertical-circulation model for the deep water of the Baltic Sea. Lass et al. (2003) verified this parameterisation by direct dissipation measurements in the Eastern Gotland Basin and found evidence that the proportionality factor is the sum of the kinetic and potential internal wave energy, i.e.

$$\varepsilon = \alpha(E_{kin} + E_{pot})N \qquad (6)$$

with α=0.001.

This result suggests that the dissipation of kinetic energy in the stratified layers may vary in space and time as the total energy of the internal wave field varies in the Baltic Sea.

Vertical mixing in the interior

Estimates of the vertical turbulent diffusivity in the Baltic Sea have been performed mainly with three different methods.

Beneath the halocline the Baltic Sea acts like a filling-box system maintained by horizontal advection from inflowing sea water, upwelling along the rims of the basins, and vertical diffusion through the halocline. Using information about the temporal changes of salinity and the advection of the bottom water into the deep basins, estimates of the long-term averaged vertical diffusivities have been made for the deep water of the Baltic Sea by several authors (e.g. Shaffer 1979, Stigebrandt 1987a, Matthäus 1990, and Axell 1998). However, vertical diffusivities estimated by these methods represent the effects of both turbulent vertical mixing and upwelling.

For numerical models the vertical turbulent diffusivity k_v is parameterised in terms of the Brunt-Väisälä frequency N by

$$k_v = \frac{a}{N}. \qquad (7)$$

It was tuned by varying the constant a until the observed and modelled variations of the stratification were in maximal agreement. Stigebrandt (1987a) obtained in his horizontally integrated model a=2x10^{-7} m²/s². In this type of model the upwelling at the rims of the basins is not resolved.

A refined one-dimensional numerical ocean model of the southern Baltic Sea was used by Axell (2002) to investigate suitable parameterisations of unresolved turbulence and compared it with available observations. The turbulence model is a k-ε model that includes extra source terms of turbulent kinetic energy production by unresolved breaking internal waves and Langmuir circulations. The energy for deepwater mixing in the Baltic Sea was provided by the wind. A range of values for the power of N^n in the proportionality relation to k_v was tested in hundreds of 10-year simulations of the southern Baltic Sea. It was concluded that n = 1.0 +/- 0.3 and that a mean energy flux density to the internal wave field of about (0.9 +/- 0.3) × 10^{-3} W/m^2 is needed to explain the observed salinity field. Finally, it was also shown that Langmuir circulations are important to be included when modelling the oceanic boundary layer. Using a fully 3-dim circulation model of the Baltic Sea, which resolves coastal upwelling, Meier (2001) obtained a somewhat smaller constant of a=1×10^{-7} m²/s².

Direct estimates of diapycnal exchange coefficients have been made by Kullenberg (1977) from dispersion measurements of injected dye tracer in the thermo- and halocline of the Arkona Basin and the Bornholm Basin in the Baltic Sea.

The turbulent diapycnal exchange coefficient in stratified water can be estimated according to Osborn (1980) assuming a balance between the production of turbulent kinetic energy, the buoyancy flux, and the dissipation of turbulent kinetic energy

$$k_v = \Gamma \frac{\varepsilon}{N^2} \qquad (8)$$

where $\Gamma = 0.2$.

Dissipation measurements in the Eastern Gotland Basin were performed by Lass et al. (2003) during winter stratification in April 1999 and during summer stratification in September 2000. Dissipation profiles were measured about every 10 minutes over a time interval of about 9 days. This provided a data set allowing for the estimation of quite reliable averaged dissipation profiles in spite of the huge intermittency of dissipation in stratified water, see Fig. 10. The dissipation decreases from the surface to a depth of about 50 m. Maximum dissipation is observed in the halocline while it decreases below the halocline to an absolute minimum in the deep water until it increases again in a bottom boundary layer with a thickness of about 10 m.

There are significant differences between the dissipation profiles measured in winter and summer stratification below the surface mixed layer.

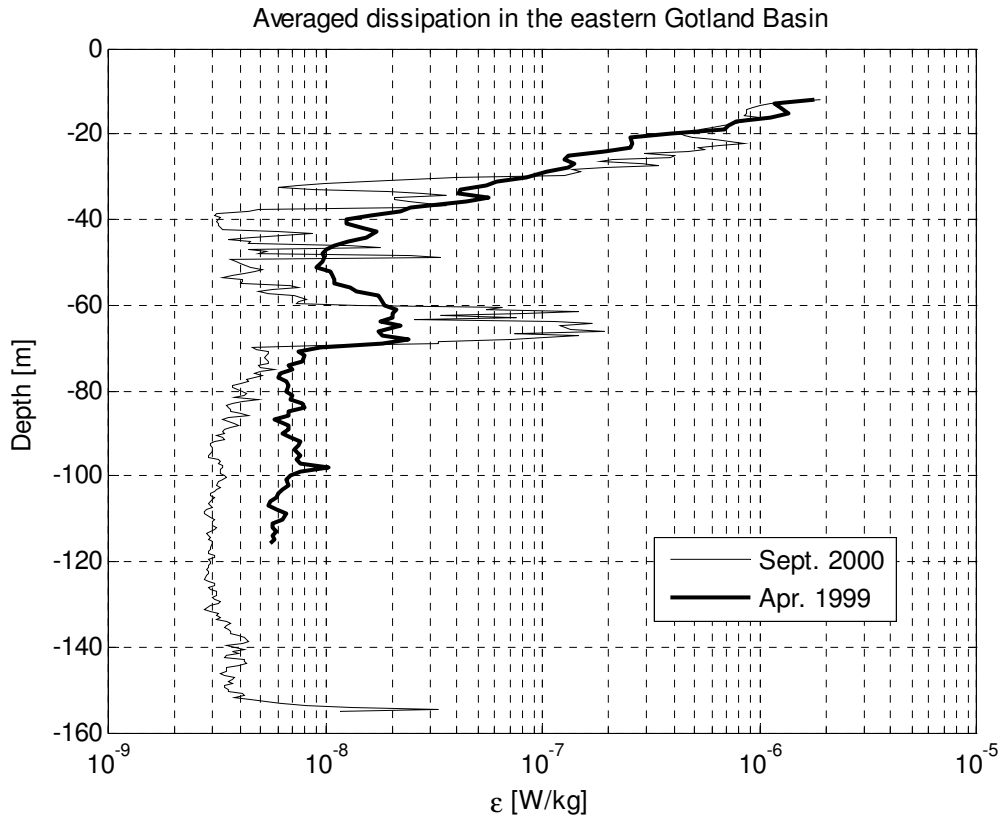

Fig. 10: Averaged dissipation of turbulent kinetic energy measured in the Eastern Gotland Basin in April 1999 and September 2000.

During summer stratification the thermocline is located at about 20 m depth and the dissipation decreases in the core of the intermediate winter water in the depth range between 40 m and 60 m to a minimum level, which is usually observed in the stratified layers well below the halocline. In winter the dissipation is much stronger at the bottom of the brackish winter water since it belongs to the surface mixed layer in winter. The dissipation in the halocline is larger by one order of magnitude during summer stratification compared to winter stratification. Since the Brunt-Väisälä frequency in the halocline does not change by more than 20% during the seasons of the year, the total energy of the internal waves must be higher by about a factor of 10 according to Eq. 6. In summer the dissipation in the bottom water below the halocline is by 50% lower than the dissipation during the winter stratification except for the bottom boundary layer, where the dissipation increases again by a factor of 10 compared to the minimum dissipation in the centre of the bottom water body. The annual variations of the Brunt-Väisälä frequency below the halocline are quite low in the Eastern Gotland Basin. This suggests that the total energy of the internal waves below the halocline is significantly lower during the summer than during the winter stratification.

Diapycnal mixing in the turbulent regime below the surface layer was estimated by a relation according to Osborn (1980) which is based on the balance between the shear turbulent production, the work on buoyancy forces, and the dissipation rate assuming a constant Richardsson flux number, see Fig. 11.

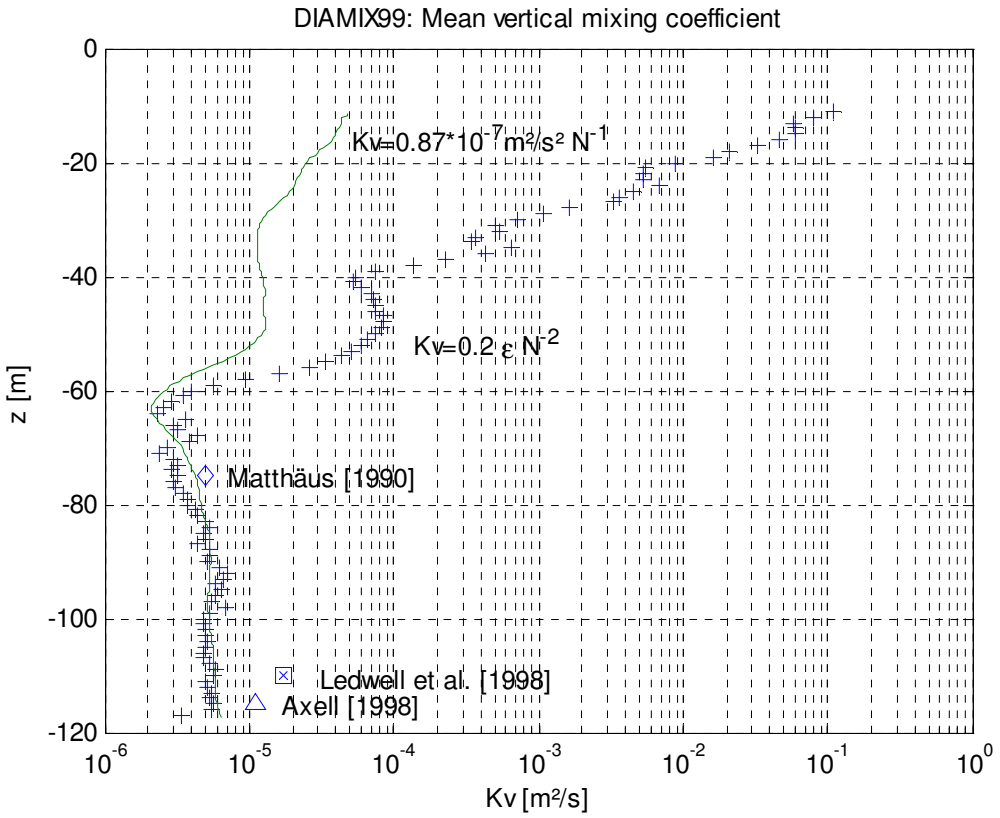

Fig. 11: Averaged diapycnal mixing coefficients according to Eqs. 7 and 8. Vertical exchange coefficients estimated by means of the bulk method for the Baltic Sea by Matthäus (1990) at 75 m depth and by Axell (1998) at 115 m depth as well as by means of dye tracer dispersion at about 300 m depth in the ocean thermocline by Ledwell et al. (1998).

The halocline turned out to be an isolating layer with respect to diapycnal mixing. The minimum diapycnal mixing coefficient of 2×10^{-6} m²/s was observed at this depth. Below the halocline the diapycnal mixing increases gradually to 6×10^{-6} m²/s and exhibits a local maximum of about 8×10^{-6} m²/s. Diapycnal diffusivity at the depth of the halocline was estimated by means of the salt budget method for the Eastern Gotland Basin by Matthäus (1990) and by Axell (1998). Matthäus (1990) obtained a value of 5×10^{-6} m²/s at 75 m depth while Axell (1998) reported $k_v = 11\times10^{-6}$ m²/s at 115 m depth during spring time. The values from Matthäus (1990) and Axell (1998) are both larger by a factor 1.7 to 1.8 than the estimates of Lass et al. (2003) in the corresponding depth. Comparing the "directly measured" dissipation-based diapycnal exchange coefficients with those estimated by the bulk method, one has to take into account that the bulk method supplies long term averages which include the vertical transport by diapycnal mixing as well as by upwelling in the Baltic Sea. This is due to the short time scale of upwelling events and the fact that the upwelled water is partly mixed with the surface water due to the Ekman offshore transport. Therefore the bulk method should provide larger values. Our diffusivity estimates based on dissipation measurements agree well with the average value given by Kullenberg (1977) obtained from dispersion of dye tracers released in the thermocline and halocline of the Arkona and Bornholm Basin in the Baltic Sea. This suggests that the diapycnal exchange coefficients estimated for the halocline of the Eastern Gotland Basin hold for large areas of the Baltic Sea.

Another comparison of directly and indirectly estimated turbulent diffusivities is possible by the assumption that the mean vertical salt flow through the halocline must balance the export of salt from the Baltic Sea. In Subsection 3.1 the required vertical salt transport through the halocline is estimated to $J_s = 30$ kg/(m² a) $= 9.5\times10^{-7}$ kg/(m² s). Assuming that this salt transport is maintained

by a vertical turbulent exchange coefficient Kv with a characteristic vertical salinity gradient in the halocline of the Eastern Gotland Basin of $\Delta S / \Delta z = 5\text{psu} / 10\text{m}$ we obtain $k_v = 2 \times 10^{-6}$ m²/s. This suggests that a large fraction of the vertical salt transport through the halocline may be maintained by turbulent diapycnal mixing resulting from breaking internal waves. However, some additional vertical transport by other processes such as entrainment resulting from vertical convection or upwelling at the rim of the basin is expected.

5.2. Boundary mixing due to internal waves

Boundary mixing in lakes and the ocean

A frequently observed feature of stratified water bodies is a well-mixed bottom boundary layer (hereafter abbreviated as BBL) existing right above the sediment surface. The height of this well-mixed layer varies between a few meters in lakes and reservoirs (e.g. Gloor et al. 2000, Hondzo and Haider 2004, Lemckert et al. 2004) up to several tens of meters in the ocean (e.g. Caldwell 1978, Lentz and Trowbridge 1991, Moum et al. 2004). The turbulent kinetic energy required to generate and maintain such mixed layers is usually assumed to be produced by bottom friction of basin- or large-scale currents (Fricker and Nepf 2000, Wüest et al. 2000), shoaling and critical reflection of high-frequency internal waves (Thorpe 1997, Imberger 1998), or the interaction of large-scale currents with rough topography (Rudnick et al. 2003). Fully non-linear and non-hydrostatic numerical models have been able to reproduce the mechanisms of energy transfer from the primary internal wave to higher modes (Vlasenko and Hutter 2002b, Vlasenko and Alpers 2005), as well as the processes of shoaling and breaking of internal waves on a slope, and the subsequent generation of turbulent BBLs (Vlasenko and Hutter 2002a).

Direct observations of enhanced mixing in the presence of boundaries were reported in numerous studies in lakes and the ocean (e.g. MacIntyre et al. 1999, Ledwell et al. 2000, Garrett 2003, Wüest and Lorke 2003b). Turbulence in BBLs is an interesting scientific topic in itself, but it has received particular attention due to the fact that the presence of turbulent BBLs has important implications for the global flux paths of salinity, heat, and matter in closed and stratified basins, the most obvious being the potential to greatly increase basin-scale vertical mixing (Imberger 1998; Müller and Garrett 2004). Indeed, enhanced basin-scale vertical transport due to turbulent BBLs has been confirmed by tracer experiments in lakes (Goudsmit et al. 1997), fjords (Stigebrandt 1979), and ocean basins (Ledwell and Bratkovich 1995, Ledwell and Hickey 1995). Apart from being an important contribution to the effective basin-scale vertical transport, the presence of a well-mixed BBL is also known to give rise to secondary circulation patterns that may considerably affect the whole system, e.g. by effectively reducing the bottom friction (Weatherly and Martin 1978, Trowbridge and Lentz 1991, McCready et al. 1994).

A different mechanism capable of generating buoyancy-driven (convective) mixing in BBL on slopes was proposed by Lorke et al. (2002) and Wüest and Lorke (2003a). This mechanism is associated with up-slope currents on slopes in stratified basins, produced by long inertial-internal waves, internal seiches, and internal tides. The decrease of the cross-slope current velocity towards the sediment surface (‘law of the wall’, Wüest and Lorke 2003b) leads to a differential transport of water masses in the cross-shelf direction. This mechanism can result in a net transport of dense water on top of light water, and hence to shear-induced convective mixing. Evidence for the occurrence of convectively-driven mixing in BBLs in the ocean was presented by numerical simulations of Slinn and Levine (2003), as well as in recent observations on the continental shelf by Moum et al. (2004).

Boundary mixing studies in the Baltic Sea

Compared to the ocean and many fjords, the Baltic Sea is a particular example of a stratified basin with very weak tidal forcing. In the virtual absence of barotropic tidal pressure gradients, internal tides can therefore be excluded as relevant energy sources for diapycnal mixing in the BBL. This fact makes boundary mixing in the Baltic Sea energetically more similar to lakes (Lorke et al. 2002, Umlauf and Lemmin 2005) and fjords with weak tidal forcing (e.g. Arneborg and Liljebladh 2001a, b), where long internal waves and internal seiches adopt the role of the internal tides in the open ocean. The spectrum of internal waves available for energizing the BBL in the Baltic Sea include short internal waves, inertial-internal waves, and coastally trapped long internal waves.

Investigations of internal wave effects on BBL turbulence are challenging because a large number of parameters has to be controlled. First, turbulence and mixing have to be measured either directly, e.g. with the help of microstructure measurements, or by considering the integrated effects of mixing using a budget method for temperature, salinity, or a tracer. Second, the internal wave field has to be appropriately resolved, e.g. using acoustic velocity profilers or high-resolution moored CTD-chains. To our knowledge, no study has been published satisfying all these criteria. Nevertheless, a number of less complete investigations of BBLs has been reported, and will be briefly summarized in the following.

The field measurements conducted during the DIAMIX project (see Stigebrandt et al. 2002) in the Eastern Gotland Basin come closest to the requirements mentioned above. A detailed study of internal wave motion and their relation to mixing in the water column from the first DIAMIX cruise in winter 1999 has been published by Lass et al. (2003), see also Subsection 5.1. Even though during these measurements all parameters were available for a detailed study of turbulence and internal wave motions, the microstructure measurements stopped well above the BBL such that no conclusions can be drawn about its turbulent structure. During the second set of experiments, however, undertaken during the DIAMIX cruise in summer 2000, microstructure measurements resolving the BBL on the slope of the basin (Fig. 12) were obtained (Stigebrandt et al. 2002). The measurements showed clear evidence for the existence of enhanced turbulence in the BBL, but so far these data have not been analyzed in depth, and hence no definite conclusions can be drawn about the physical mechanisms generating turbulence in the BBL.

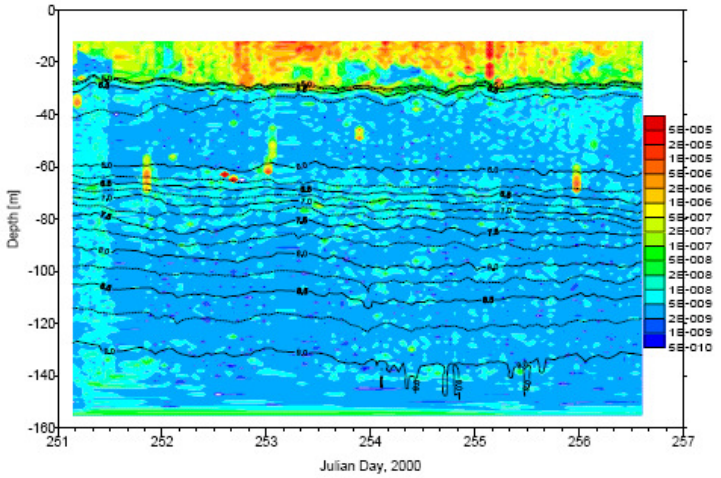

Fig. 12: Logarithm of the dissipation rate (in W kg^{-1}) and density anomaly (in kg m^{-3}) from microstructure measurements conducted in September 2000 on the slope south-east of Gotland. Note the enhanced dissipation rate near the bottom.

Another short paper directly focusing on the effect of breaking internal waves on the stratification at the slopes of the Eastern Gotland Basin has been published by Ozmidov (1994b). This author presented a number of CTD transects across the eastern slope of the basin, demonstrating quite clearly the presence of reduced density gradients in the lowest 10-20 m of the halocline adjacent to the sediment. A model expression for the vertical diffusivity derived by Ozmidov (1983) was shown to be consistent with the observed reduction of the density gradient. However, even though Ozmidov (1994b) briefly mentioned the deployment of a microstructure profiler during the campaign, no turbulence measurements and no direct evidence for the action of internal waves has been reported, and the paper remains inconclusive in that respect.

Breaking internal waves are not the only source of turbulence in the BBL. Coastally trapped long internal waves and internal seiches are an important contribution to the spectrum of motions in the Baltic Sea, and their occurrence has been reported in numerous contexts (e.g. Walin 1972a, b, Pizarro and Shaffer 1998). Their velocity fields periodically move stratified water up and down the slopes, thereby causing friction and strain in the BBL. Both effects may cause turbulence in the BBL as observed in the connection with internal seiching in lakes (see discussing above and Lorke et al. 2002). A direct observation of this effect for the Baltic Sea is lacking, however, some support for the importance of the shear-induced convection process in the Baltic Sea comes from a research cruise in the Arkona Basin (western Baltic Sea) conducted in February 2005 with R/V Alkor. During this cruise the Arkona Basin with a maximum depth of approximately 45 m was filled with a pool of saline water of 19 psu up to a depth of approximately 35 m. The upper part of the water column was well mixed at 8 psu, and thermal stratification was dynamically negligible.

During strong upwelling-favorable winds on the early morning of 18 February 2005 a cross-slope transect of 75 microstructure profiles of temperature, conductivity, and velocity shear was obtained north of the island of Rügen, see Fig. 13.

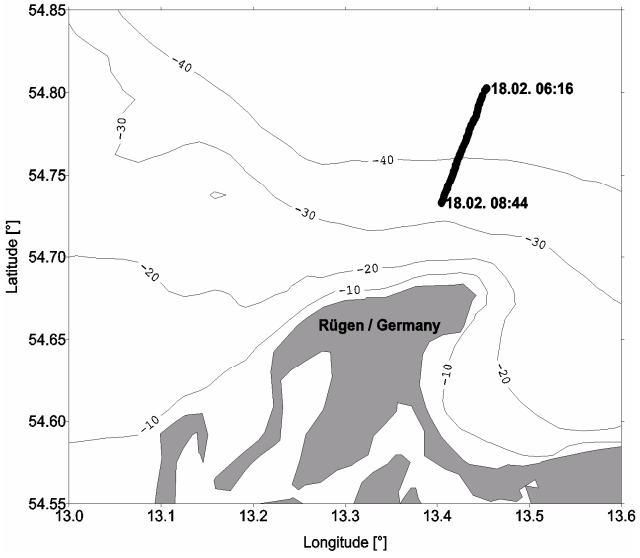

Fig. 13: Topography (in meters) and trace of the up-slope transect during a strong up-welling event in February 2005. 75 microstructure profiles (temperature, salinity, velocity shear) were taken between the indicated start and end times.

The left panel in Fig. 14 shows pronounced upwelling of saline water in a 3-10 m thick BBL, in which a reduction of the vertical density gradient is obvious as the coast is approached. Closest to the coast, the stratification in the BBL is only marginally stable or unstable, and microstructure measurements indicate enhanced dissipation rates (Fig. 14). This suggests that shear-induced convection may play an important role in this type of upwelling boundary layers, similar to the situation described by Moum et al. (2004) for a BBL on the continental shelf during relaxation from coastal upwelling.

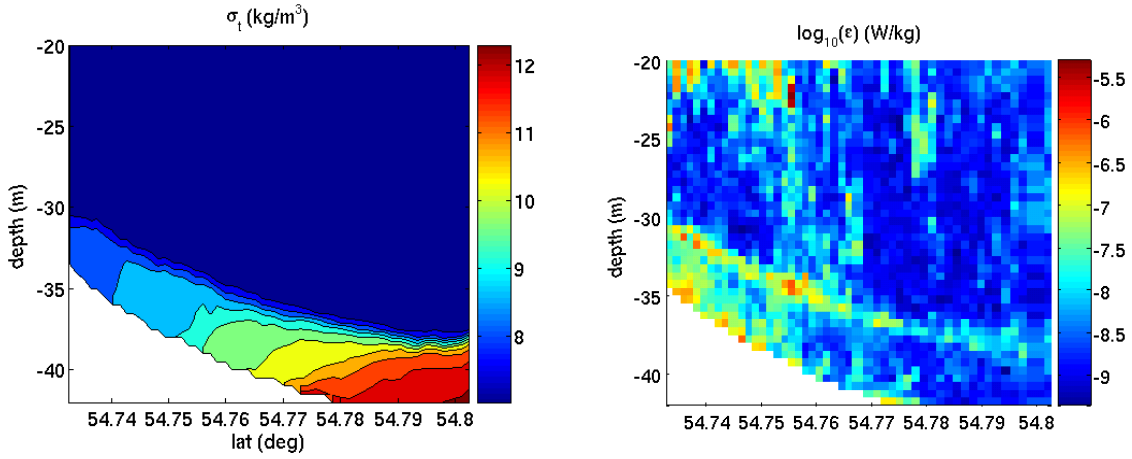

Fig. 14: Density anomaly (left panel) and dissipation rate observed along the transect marked in Fig. 13.

Finally, Stips et al. (1998) reported a detailed study of stratification and mixing in the BBL of the Arkona Basin in the western Baltic Sea. They estimated the dissipation rate from repeated shear microstructure profiles along with high-precision CTD data. The near bottom current structure was simultaneously measured with conventional current meters at fixed depths. A well-mixed, turbulent BBL was observed, a few meters thick with strong fluctuations in thickness due to the effect of horizontal advection. The paper was inconclusive regarding the physical mechanisms controlling turbulence in the BBL, and the effect of internal waves has not been a focus of the study.

5.3. Vertical mixing by mesoscale eddies

Mechanisms of vertical mixing by mesoscale eddies

Vortices with a horizontal scale in the order of the baroclinic Rossby radius are commonly referred to as mesoscale eddies. Mesoscale eddies are found in nearly every region of the world ocean. They carry energy and momentum and can contain significantly different water properties compared to their surrounding. Therefore they have the ability to transport and to influence mixing (Robinson 1983).

Mesoscale eddies are also present in the Baltic Sea. The Baltic Sea Eddies are called Beddies here. They are assumed to contribute to the vertical mixing, in particular to the diapycnal mixing in the permanent halocline, mainly by two mechanisms. One of them is the vertical displacement of water and isopycnals within the Beddies causing their rotation by geostrophic adjustment. In fact, this is rather a displacement than an ongoing transport. It shows up as a lifting or lowering of the isopycnals inside the Beddies. The other one is connected to the decay of the Beddies. During the decay process their kinetic and potential energy becomes available for mixing processes no matter

if they slowly fade away by dissipation or if they are destroyed more in a collapse caused by a collision with the basin rim, for example. Unfortunately, neither the lifetime of the Beddies due to pure dissipation nor their real lifetime is known. However, assuming a lifetime of the Beddies longer than 4 month resulting from pure dissipation in relation to a horizontal basin scale of several 100 km and a drift velocity of some 1 cm/s, such a collapse due to a collision seems to be more likely as the favored decay mechanism of the Beddies than their dissipation. The energy release in such a collapse would show up at least as the mixing of the water contained by the Beddy with the surrounding water masses. Moreover, some of the energy is assumed to be radiated in the form of internal waves. Therefore it may contribute to the vertical mixing by means of the internal wave field, compare Subsection 5.1.

In addition to these more or less direct mechanisms to impact the diapycnal mixing, there is some indication that the internal waves interact with the Beddies (Talipova et al. 1998). This is consequently leading to the widely open question about their indirect impact on the vertical mixing by means of such interactions, e.g. their effect as scattering body for internal waves or the generation of critical layers for the internal wave field resulting in enhanced internal wave breaking.

Observations of mesoscale eddies in the Baltic Sea

Beddies were observed in most regions of the Baltic Sea during diverse field measurements (Aitsam and Elken 1982, Aitsam et al. 1984, Elken et al. 1988, Sturm et al. 1988, Elken 1996, Zhurbas and Paka 1997, Zhurbas and Paka 1999, Stigebrandt et al. 2002, Lass and Mohrholz 2003). All these investigations report on single outstanding features in hydrographic data fields which are considered as mesoscale eddies. They are found in various depths from the surface to the bottom and some cover the whole water column, but most of them are observed in the region of the permanent halocline showing no surface signature. For their diameters values between 10 km and 20 km are given. Their thickness ranges between a few meters and the entire water depth. For the Beddies located inside the halocline vertical extensions in the order of magnitude of the halocline thickness itself are found, which is around 20 m depending on the considered region. The Beddies drift with velocities of a few 1 cm/s. They spin with maximum rotational speeds between 20 cm/s and 30 cm/s. The Beddies seem to be almost in geostrophic balance.

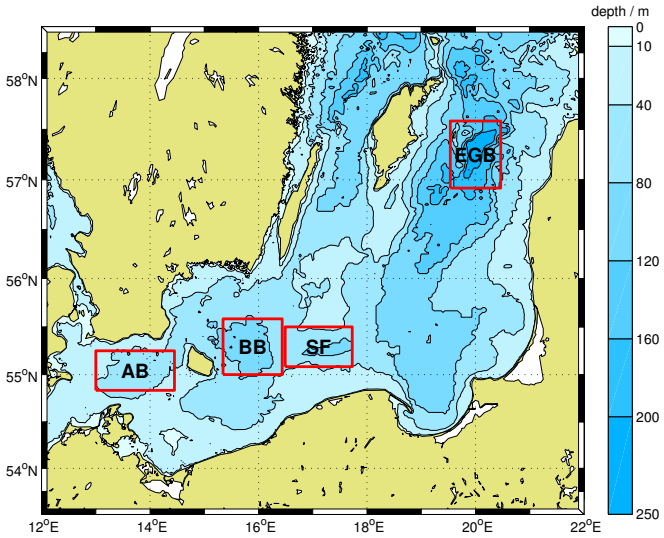

Fig. 15: The four areas covered by hydrographic surveys for the investigation of Beddy fields: Arkona Basin (AB), Bornholm Basin (BB), Słupsk Furrow (SF), and the Eastern Gotland Basin (EGB), see Reissmann (1999) for detailed information about the bathymetry in the four regions.

In contrast to the investigations of single Beddies mentioned before, all Beddies contained in a certain ocean volume at one time are described by their integral properties in another approach using an objective pattern recognition algorithm to automatically detect the Beddies as anomalies in three-dimensional hydrographic data fields (Reißmann 2002, Reißmann 2005). These eddy resolving data fields cover the Arkona Basin (AB), the Bornholm Basin (BB), the Słupsk Furrow (SF), and the Eastern Gotland Basin (EGB) as marked in Fig. 15 during both summer and winter stratification situations, i.e., with and without the thermocline in summer. Overall, the resulting integral properties are in good agreement with the observations of single Beddies. In particular, their spatial scales are reflected well by the corresponding mean values over all Beddies in each data field. However, drift velocities and rotational speeds of the Beddies were not provided by this approach due to the limited capability of the used data fields. Nevertheless, some valuable information about other properties of the Beddy fields is gained for the estimation of their possible impact on the vertical mixing. One of the most important is the number of Beddies coexisting in each region. It varies from about 15 in the AB, BB, and SF up to 30 in the EGB. Most of the Beddies are found in or above the regional main pycnocline. But this is certainly a consequence of the smaller volume available for the Beddies at the bottom due to the basin shape in each region and does not mean that there are no Beddies below the main pycnocline. The horizontal distribution of the Beddies in each of the four basins is consistent with the assumption to be uniform. Perhaps the most striking finding is that all Beddies in each region occupy a constant fraction of about 12 % of the investigated basin volume, see Fig. 16. Taking into account the respective number of Beddies this corresponds to mean volumes of the Beddies ranging from about 1.5 km^3 in the AB over values widely spread around 2 km^3 in the BB and SF to more than 3 km^3 in the EGB. This increase of the mean volume is accompanied by an increase of the mean thickness of the Beddies from around 13 m in the AB up to 23 m in the EGB while their mean horizontal cross-sectional area varies only little within the range corresponding to radii between 4 km and 5 km for the four different regions. So, the increasing mean volume of the Beddies can be linked to the increase of their mean thickness. This in turn may be linked to the generally increasing water depth from the AB to the EGB, but under the assumption that a large number of Beddies is located within the halocline it also can be linked to an analogous increase of the halocline thickness. The resulting consistent picture with the observations of the vertical distribution of the Beddies is appealing and therefore gives some independent evidence for a favored occurrence of Beddies in the halocline.

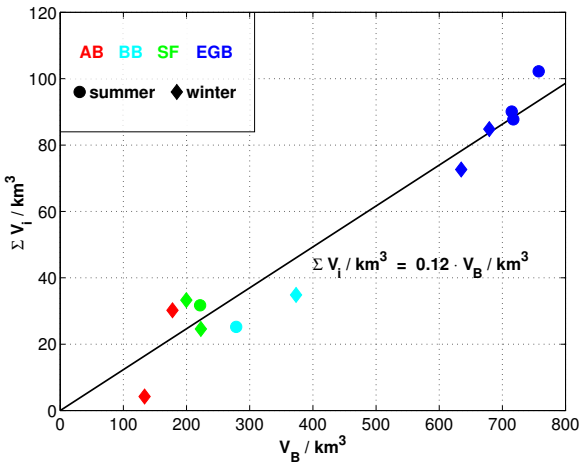

Fig. 16: The total volume ΣV_i occupied by all Beddies in each data field with respect to the total volume V_B of the corresponding investigated water body for 12 data fields from the AB, the BB, the SF, and the EGB. There are no significant seasonal differences due to the different stratification situations. The volume fraction occupied by the Beddies is almost constant and amounts about 12 % as indicated by the depicted straight line resulting from a linear least squares fit.

The mean density of available potential energy of the Beddies is lower than the energy density needed to destroy the stratification in the corresponding halocline for all observed data fields. However, the kinetic energy of the Beddies is not considered in this estimation. Moreover, in most of the data fields there are at least a few Beddies found with available potential energy densities larger than that mixing energy density. The sum of only their available potential energy is already sufficient to destroy the stratification in a relevant fraction of the corresponding halocline of more than 20 % in about the half of the observed data fields. These data fields are originating from the AB and the BB during winter stratification situations and the SF irrespective of the stratification situation. In the EGB this fraction is negligible for all observed data fields. In this way some evidence is given about the regions and the season in which an enhanced vertical mixing by Beddies can be expected preferably. Nevertheless, the mixing capability of the Beddies is presumably underestimated by taking into account only their available potential energy and, consequently, ignoring their kinetic energy, even if not all of their energy would be consumed by mixing processes. Finally, the total available potential energy of all Beddies in each data field seems to be higher during winter than during summer stratification situations. A correlation of the total available potential energy of the Beddies to the external forcing in terms of the wind stress curl could not be proved by Reißmann (2002).

Estimates of the vertical salt transport by Beddies

The simplest approach to evaluate the possible impact of the Beddies on the vertical mixing is to estimate the vertical transport of salt which is feasible by the Beddies. Considering only those Beddies which are located in the permanent halocline, this provides a characteristic measure of the diapycnal mixing which can be easily compared to the corresponding bulk estimates of the vertical transport. For this purpose, typical salinities of 13 g/kg, 12 g/kg, 11 g/kg, and 9 g/kg are presumed within the halocline in the AB, BB, SF, and EGB, respectively (Reißmann 2002, Reissmann 2006). The respective thickness of the halocline in the four regions is chosen to 9 m, 10 m, 9 m, and 11 m using a second derivation criterion according to Reissmann (2006) instead of the half maximum gradient criterion used in Reißmann (2002) which leads to a significantly increasing halocline thickness from the AB to the EGB. Although most Beddies are found in or above the regional main pycnoline and therefore a somewhat higher volume fraction occupied by the Beddies could be expected in the halocline, the constant volume fraction of 12 % is used here referring to Reißmann (2005), because the maxima in the vertical distribution of the Beddies are not dominating. On the contrary, having in mind the effect of the basin-like bathymetry in the four regions on their vertical distribution, the Beddies even may be regarded as rather evenly distributed in space. Finally, the lifetime of the Beddies is assumed to be 4 month, because a destruction of the Beddies due to a collision with the basin rim is most likely after this time span at the latest as estimated above. Assuming that the entire salt carried by the Beddies is transferred upward through the halocline, the given presumptions result in diapycnal transport rates of 42 kg/(m² a), 43 kg/(m² a), 36 kg/(m² a), and 36 kg/(m² a) in the AB, BB, SF, and EGB, respectively. So, they are slightly higher in the basins of the western Baltic Sea, but, overall, they are in the same order of magnitude as the bulk estimates in the contribution about the vertical advection due to the uplift of isopycnals during inflow events. This is at least indicating that the Beddies have the potential capability to contribute significantly to the vertical transport. This conclusion still holds if it is assumed that only half of the salt carried by each Beddy is transported through the halocline for geometrical reasons and/or only half of the Beddies contribute to the transport because half of them may originate from the surface layer, for intance. All these reductions of the diapycnal transport rates may be compensated, for example, by a conceivable shorter lifetime of the Beddies and/or by taking into account the energy release of the Beddies in their decay which nearly would double the mixed volume fraction of the halocline in most cases.

The vertical mixing due to the collapse of Beddies as a result of their collision with the basin rim, obviously, is focused to the region of the basin rim. In particular, for the vertical transport through the halocline this refers to the area around the 30 m, 55 m, 45 m, 70 m isobaths for the AB, the BB, the SF, and the EGB, respectively, according to Reissmann (2006). In contrast, any other mixing process induced by Beddies can be assumed to be nearly homogeneously distributed in space on scales larger than the Beddies themselves.

According to the present knowledge the mixing events induced by Beddies can be assumed to occur uniformly in time. There is neither an indication for a seasonality nor a dependence on the meteorological forcing in terms of the wind stress curl over the Baltic Sea found for the occurrence of Beddies (Reißmann 2002). However, their occurrence may depend on inflow events to the Baltic Sea and its basins. Moreover, the mixing intensity induced by the Beddies may vary in time, in particular, a seasonality of the mixing intensity due to the different properties of the halocline in summer and in winter is conceivable, for example.

5.4. Boundary mixing due to near-bottom currents induced by inflow events

The Eastern Gotland Basin (EGB) represents the largest volume of deep water in the Baltic Proper and the observed thermohaline mixing should be typical for all deep basins of the Baltic Sea. The ultimate question is: Can deep boundary mixing be sufficiently effective to explain basin-averaged vertical diffusion and which role plays the vertical shear of deep rim currents observed beneath the perennial pycnocline by Hagen and Feistel (2004)?

For the open deep ocean Munk (1966) made an estimate of the diffusion coefficient $k_v \sim 10^{-4}$ m²/s to describe turbulent mixing across isopycnal surfaces. Twenty years later the measurements of Moum and Osborn (1986) and Gregg (1987) suggested that k_v is one magnitude smaller. Beside this open question, Phillips et al. (1986) argued that internal mixing over a sloping boundary should spread isopycnals up and down the slope and that resulting buoyancy forces drive a flow, which converges at the pycnocline causing an outflow toward the basin's interior. After further ten years Toole et al. (1994) reported enhanced mixing near steeply-sloping boundaries. Estimated diffusion rates significantly exceeded earlier proposed values. Thus a widely distributed range of k_v values can be detected in the literature, but only very few of them point to what is happening in the Baltic Sea. Concerning its shallow western areas, Stips et al. (1998) concluded from measurements of turbulent dissipation rates that no simple parameterisation seems applicable, because an overall logarithmic near-bottom layer could not be verified. The applied dissipation model relates the diffusivity k_v to the squared stability frequency N^2 and the dissipation rate ε according to Eq. 8 with the efficiency factor $0.1<\Gamma<0.3$, cf. Lilly et al. (1974) for the atmosphere and Osborn (1980) for the ocean. From measurements of ε, which were carried out in the EGB during summer environmental conditions by Stigebrandt et al. (2002), it became evident that the perennial halocline/pycnocline provides an internal source layer for enhanced dissipation rates between 60 and 100 m depth. However, there also was some observational evidence for an increasing ε towards the basin's steep slope, roughly by one order of magnitude. The first aspect may be explained by the breaking of internal waves travelling within the wave guide of the pycnocline, while the second one could be explained by regionally reduced Richardson gradient numbers $R_i = N^2/(\Delta v/\Delta z)^2$. The R_i describes the ratio between stratification and the squared vertical shear of the horizontal current v along the vertical co-ordinate z. Since the pioneering work of Munk and Anderson (1948), vertical mixing due to the exchange of momentum is considered to be inverse proportional to the R_i. Thus one may expect a certain degree of mixing of thermohaline water properties in near-bottom layers originating from significantly reduced values of the R_i through topographically steered deep rim currents.

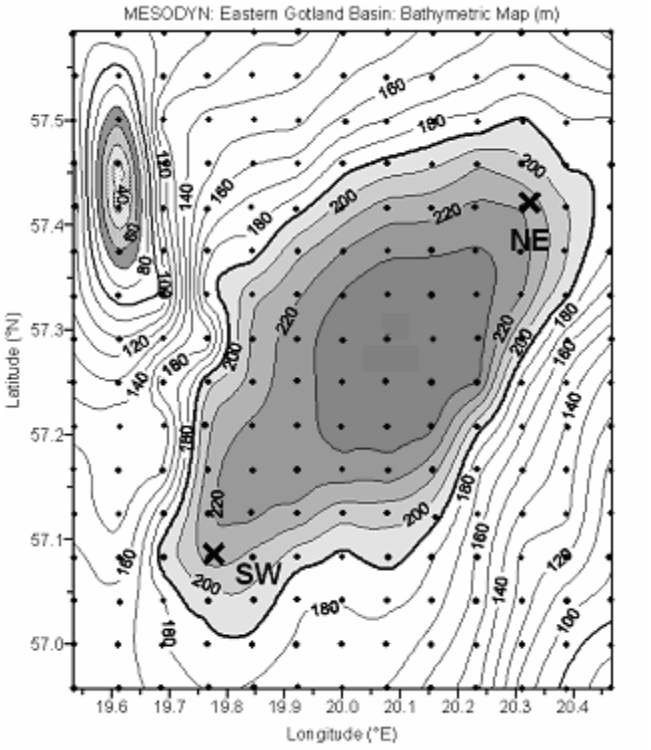

Fig. 17: Hydrographic station grid (dots) with the spacing of 2.5 n.m. over given bathymetric contours (m) carried out before (September 1997) and after the deep water inflow (April 1998) to study released mesoscale dynamics (MESODYN) in the Eastern Gotland Basin. The positions of two subsurface moorings are denoted north-east (NE) and south-west (SW) (crosses). Each moored string was equipped with recording current meters at 170 m (1 h sampling interval) and recording thermometers at 140 and 155 m depth (0.5 h sampling interval), cf. Hagen and Feistel (2001).

Concerning the renewal of deep water in the EGB and associated mixing processes, an effective inflow of relatively warm but dense water in the winter 1997 – 1998 was reported by Hagen and Feistel (2001). During this period of time two subsurface moorings recorded currents and temperature at 170 m depth, while auxiliary thermometers were deployed at the 140 and 155 m horizons, see Fig. 17. The echo-sounded depth was 220 m at both positions. Because of the closed deep bathymetric contours the current measurements suggested a persistent cyclonic circulation of about 0.03 m/s, which occupied the entire deep EGB all over the year. During this inflow event the circulation accelerated by a factor of about two. Superimposed fluctuations with lateral and vertical meanders of the deep rim current modified the vertical current shear to produce corresponding quasi-periods in enhanced daily variances of the local thermal field, see Fig. 18. Such daily changes in the temperature variance can be attributed to enhanced mixing caused, for instance, by breaking internal waves on shorter temporal scales (Gregg 1989). This must be mirrored in corresponding fluctuations of the so-called 'eddy kinetic energy' per unit mass $EKE = (\sigma^2_u + \sigma^2_v)/2$. Here this quantity results from daily variances (σ^2) of the zonal ($u > 0$, eastward) and meridional current component ($v > 0$, northward). On the other hand, the low frequent variability of the currents is described by changes of the 'mean kinetic energy' per unit mass $MKE = (u^2+v^2)/2$.

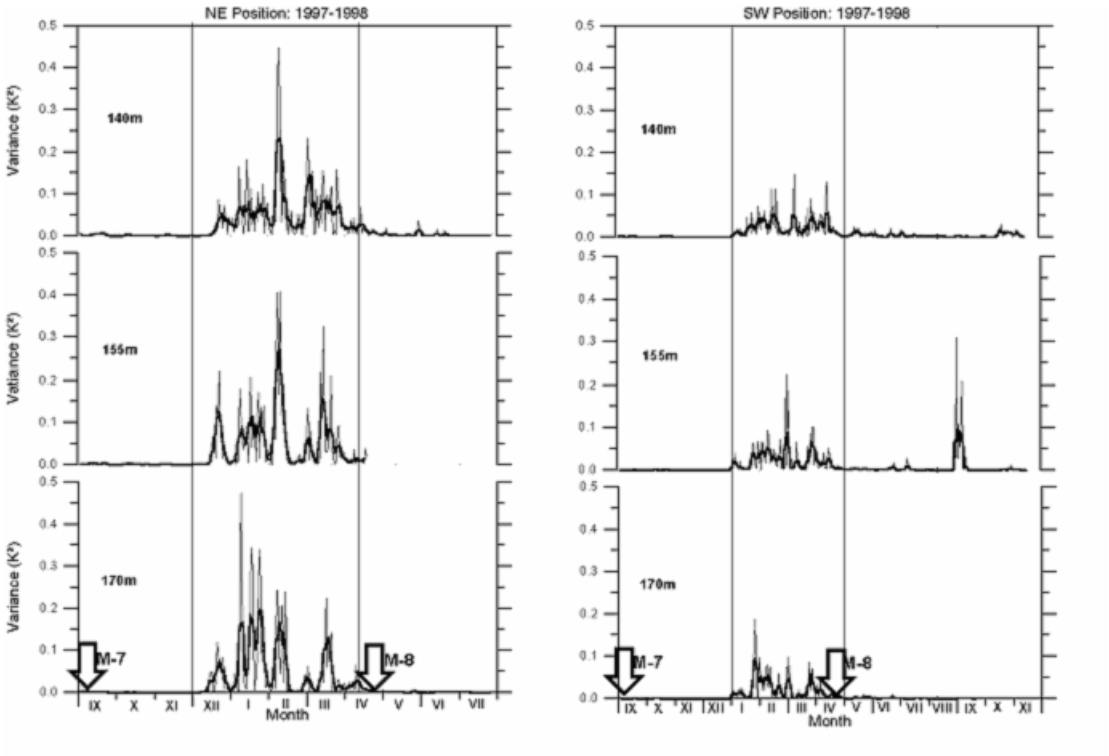

Fig. 18: Daily variances (in K², thin line) recorded with a sampling interval of 0.5 hours at 140 and 155 m and with the sampling interval of 1 hour at 170 m depth at both the NE position (57°25.38'N, 20°20.83'E) and the SW position (57°04.53'N, 19°45.12'E) according to Hagen and Feistel (2001). The bold line shows five daily running means for smoothing, vertical lines mark the inflow period lasting from 28 November 1997 until 6 May 1998 at the NE position and from 28 December 1997 until 26 May 1998 at the SW position, downward arrows indicate the two hydrographic field campaigns denoted M-7 and M-8, each of them followed the station grid shown in Fig. 17.

From the statistical point of view the *MKE* is based on the first (daily averages) and the *EKE* on the second moments (daily variances). Both estimates should be uncorrelated by definition. This means, however, that any statistical relationship between the *MKE* and the *EKE* points to a persistent energetic flux, either from the low frequent towards the high frequent spectral range of current fluctuations or vice versa. Because of the observed multi-day pulsations of deep inflows in the entrance area above the eastern topographic flank of the EGB, see Fig. 18, one may expect a somewhat stronger interaction between low frequent (*MKE*) and high frequent current fluctuations (*EKE*) at the NE than at the SW position, cf. Fig. 17. Therefore it may be also expected that the intensity of associated diapycnal mixing peaks in the vicinity of the NE position and relaxes along the pathway of the deep currents towards the SW position. This is confirmed by logarithmically scattered daily values of the *MKE* and the *EKE* in Fig. 19.

Regionally intensified vertical mixing over the basin's deep eastern flank generated a homogenization of thermohaline properties. Consequently, deep isopycnal surfaces climbed to shallower pressure levels, somewhat more intense over the eastern than over the western topographic flank of the EGB, see Fig. 20.

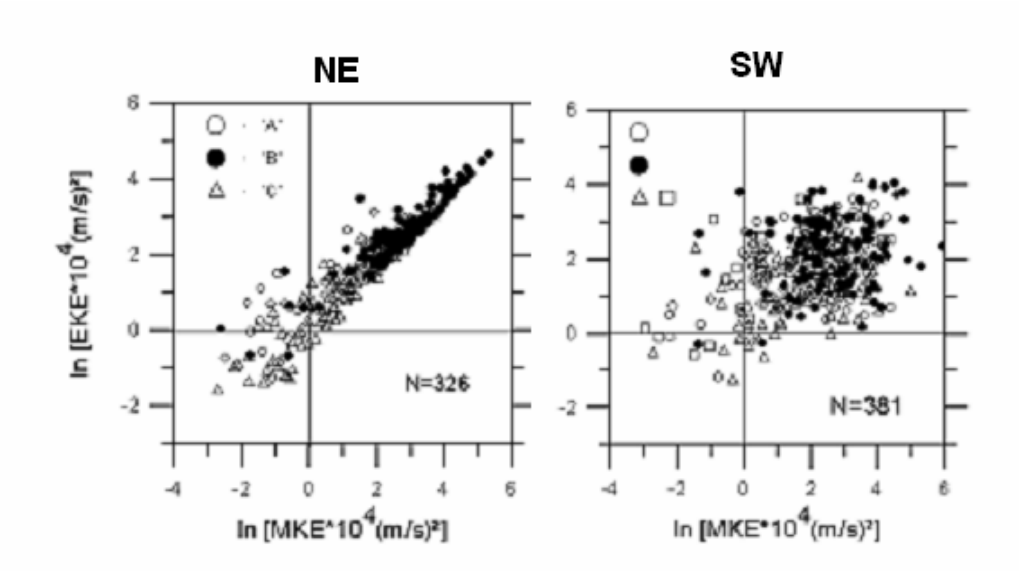

Fig. 19: Logarithmically scattered daily 'mean kinetic energy' $MKE = (u^2+v^2)/2$ versus corresponding 'eddy kinetic energy' $EKE = (\sigma^2_u + \sigma^2_v)/2$ in 170 m depth of the moored current meter strings NE and SW shown in Fig. 17. The recording length is N days and the pre-inflow is labelled by A (circles), the inflow by B (dots), and the post-inflow situation by C (triangles and squares). Note the strict relationship between the *MKE* and the *EKE* during the inflow period at the NE position.

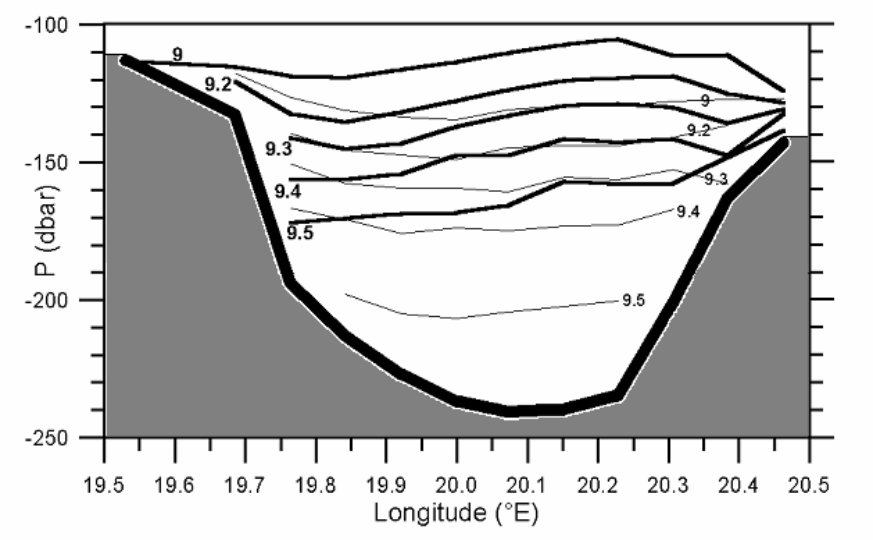

Fig. 20: Pressure levels (dbar) of deep potential isopycnal surfaces (9.5 = 1009.5 kg/m³) with the reference level at the sea surface along the zonal transect at 57.29°N, cf. Fig. 17, across the Eastern Gotland Basin before (thin lines, 1 September 1997) and after the inflow event (bold lines, 21-22 April 1998).

For the EGB Hagen and Feistel (2001) regressively estimated the deep volume $V(km^3) = 0.0141 \times h^2(m)$ with h= (242- water depth) m. For instance, it only occupies 7.5 km³ beneath the 219 m isobath, but 20.4 km³ beneath the 204 m isobath. The inflow of dense deep water produced an upward displacement of potential density surfaces between the pre-inflow and post-inflow situation, which are labelled M-7 and M-8 in Fig. 18. The associated overall vertical velocities <w> reached the magnitude of 10^{-6} m/s to decrease from near-bottom towards the intermediate layers by the factor of about four due to the corresponding changes in the deep water volume, see Fig. 21.

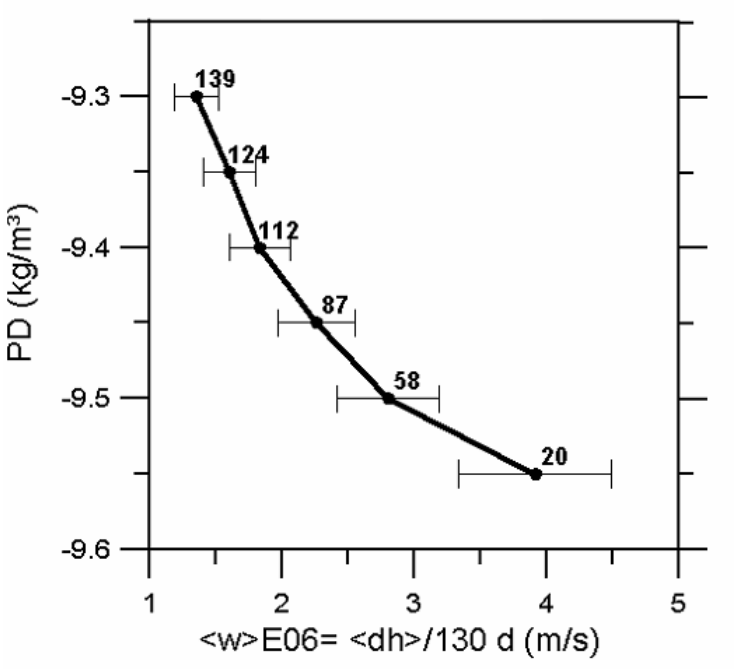

Fig. 21: Vertical profile of the deep overall vertical velocity <w> derived from spatially averaged upward displacements <dh> of six selected potential density surfaces (PD) during 130 days between pre- and post-inflow conditions labelled by M-7 and M-8 in Fig. 18. Error bars point to the 95% confidence level of the t-distribution on the base of given station numbers.

Three years lasting temperature records (31 August 1999 – 23 October 2002), which were carried out 20 m over the sea bed at the NE position and are described somewhat more in detail by Feistel et al. (2006a), confirm that such conditions are characteristic for all warm or cold deep water intrusions. During the early 2003 a relatively short inflow of warm deep water was immediately replaced by an effective cold inflow, which reached the EGB in April – May 2003. About three months later a strong warm water inflow changes the hydrographic conditions completely, see Fig. 22. For example, the mentioned cold inflow event peaked with a daily temperature minimum of 4.41°C at 219 m on 15 May, but with that of 5.1°C at 174 m depth on 20 May. This means that the temperature in the enclosed water column of δ=45 m was mixed intensively for about five days with the net upward velocity of about $\langle w \rangle = 9$ m/d or 1.04×10^{-4} m/s. This results in a diffusion coefficient $k_v = \delta \times \langle w \rangle = 4.7 \times 10^{-3} \sim 5 \times 10^{-3}$ m²/s. Because the estimated <w> varies by two magnitudes between the multi-day and the monthly scale, see Fig. 21, this example makes clear that discussions about the usability of constant values of k_v are, from the practical point of view, highly academic.

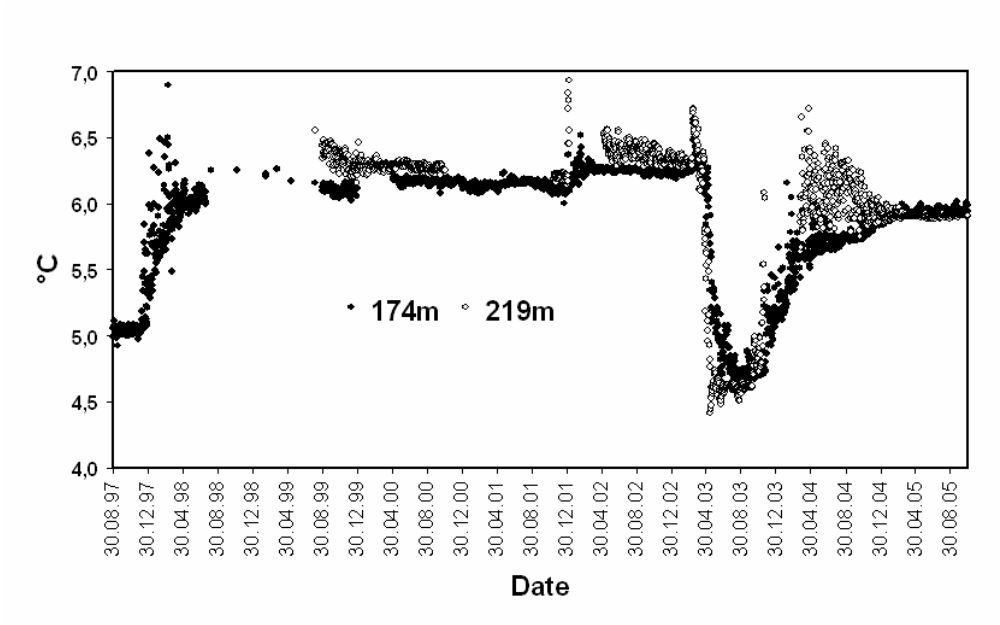

Fig. 22: Daily averaged temperature (°C) recorded in the horizons of 174 (dots) and 219 m (circles) with a sampling interval of one hour at the position NE (224 m water depth), see Fig. 17 for position.

Applying the above mentioned volume-depth regression, the estimated mean value of $\langle w \rangle = 1 \times 10^{-4}$ m/s suggests a mean thermal transformation rate of 0.24 km³/d. For instance, it results V (204 m) =20.4 km³ and V (219 m) =7.5 km³. Consequently, the total thermal homogenization of the deep water volume below the 219 m isobath requires about 31 days, but it needs 85 days to reach the 204 m horizon.

Concerning the trigger mechanisms of involved diapycnal mixing, all time records from the NE position clearly demonstrated the importance of the integral effect of short fluctuations in the vertical current shear occurring on the hourly scale. They mainly originate from local inertial oscillations with a period of about 14.4 hours. The power spectra of the zonal and meridional current components clearly showed a vertical dependence in the energetic levels of the inertial peak. Its value decreased with increasing water depth of the measuring horizons. However, it also became clear that the intensity of the local inertial period drastically increases during and after deep inflow events. Therefore all time series have been smoothed by 14 hours running averages to suppress associated signals in resulting averages, but also to elucidate associated fluctuations by corresponding standard deviations, see Fig. 23. It became evident that changes in the energetic level of deep inertial oscillations of the motion field control observed fluctuations in the thermal field, especially during and after deep inflow events. Associated dynamics also influenced the layer between 174 and 204 m depth during the whole ‘inflow year’ 2003, see Fig. 24. The tendency of increasing values of the daily *EKE* was accompanied by a similar tendency in the vertical shear S of horizontal currents.

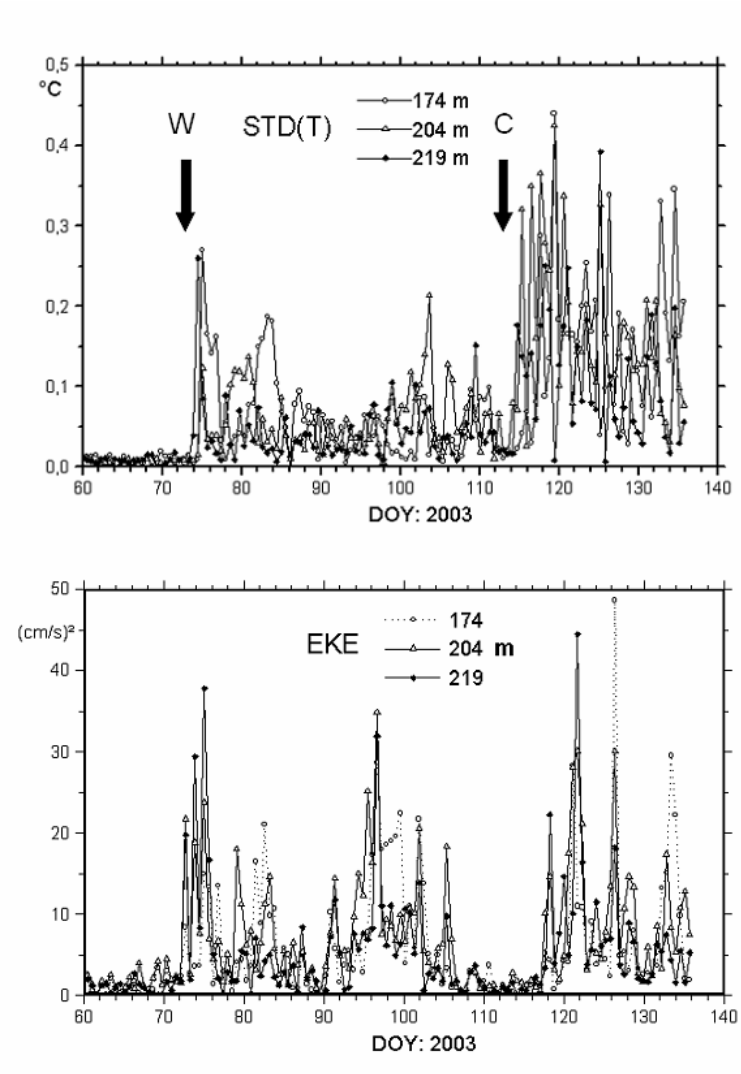

Fig. 23: 14 hours running standard deviations in temperature records, *STD* (T), and the corresponding 'eddy kinetic energy' per unit mass $EKE = (\sigma^2_u + \sigma^2_v)/2$ at three horizons of the NE position (224 m water depth) during 2003. The two effective intrusions of warm (W) and cold deep water (C) shown in Fig. 22 are marked in the upper panel by arrows at their starting day of the year (DOY).

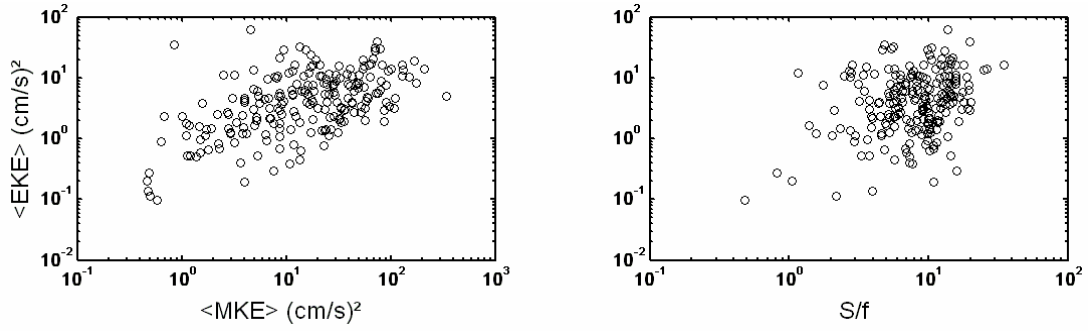

Fig. 24: Logarithmically scattered vertical means of the <*MKE*> versus corresponding values of the <*EKE*> (174 - 204 m layer) in analogy to Fig. 19 and corresponding scatters of the vertical current shear $S = [(du/dz)^2+(dv/dz)^2]^{1/2}$ normalised to the local inertial frequency $f = 1.25\times10^{-4}$ rad/s at the position NE during the 'inflow year' 2003.

Furthermore, it became clear that the time history (t) of daily anomalies in the vertical shear of along slope currents v, e.g. $\int (dv/dz)' \, dt \sim \sum (dv/dz)'$, reflects the major source for daily changes in the vertical temperature gradient dT/dz, see Fig. 25. After the deep inflow of warm water on the day of the year 73 (14 March 2003), the tendency of increasing vertical shear in the deep rim current was accompanied by increasing daily standard deviations of the vertical temperature gradient. However, the temperature signal was lagging the current shear tendency by four days. Thus the time scale of 4-5 days seems to be characteristic for the homogenization of thermal properties in the wake of inflows towards the deepest layers of the EGB.

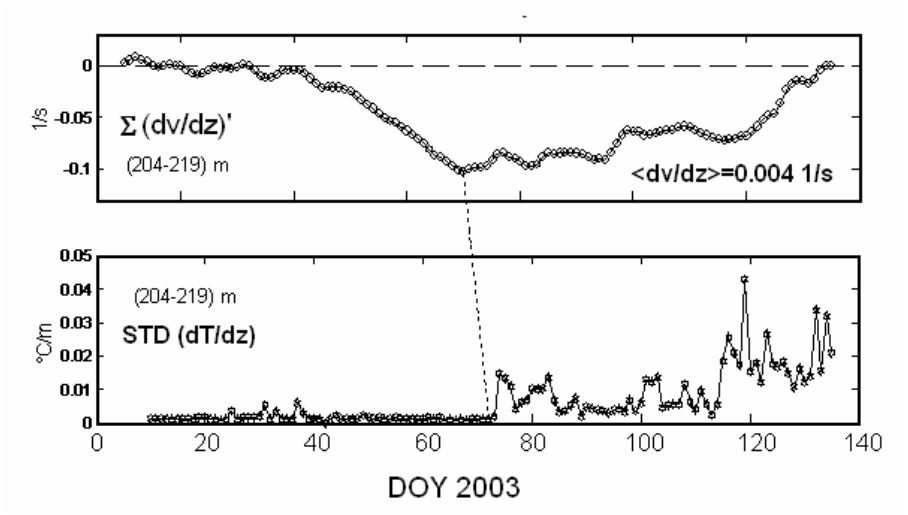

Fig. 25: Cumulative daily Reynolds's anomaly ($\Sigma (dv/dz)'$ = time history) of the vertical shear of the along-slope current component v ($\langle dv/dz \rangle$) estimated between 204 and 219 m depth at the position NE from 10 January until 15 May 2003 in comparison to the daily standard deviation (*STD*) of the corresponding temperature gradients (dT/dz). The dotted line indicates that the lower series lags the upper one by four days.

Finally, turning back to the question asked at the beginning of this subsection, we may conclude that there is some observational evidence from long-term temperature and current records in the context of the literature that multi-day changes in the vertical exchange of momentum accelerate, via intensified local inertial oscillations, the deep diapycnal mixing to transform thermohaline water properties in the wake of strong inflows on the monthly scale.

5.5. Boundary mixing due to coastal upwelling

Process of vertical mixing by upwelling

The most productive regions in the world oceans are feed with nutrients from the thermocline water by wind driven upwelling (Carr and Kearns 2003), originally described by Defant (1936) and Sverdrup (1937). Thus upwelling plays an important role for vertical transports in the oceans. Any divergence in the wind driven Ekman transport in the surface layer leads to a local sea level change, which forces a vertical displacement of the pycnoclines (Fennel and Seifert 1995), known as coastal upwelling in presence of a coast or Ekman pumping in the open ocean. An Ekman transport divergence can be caused by inhomogenious wind fields, the β-effect and the presence of a coast. In

case of the Baltic Sea it is hypothesized that upwelling induced vertical transports of salt and nutrients are mainly contributed by coastal upwelling. The Baltic Sea is a nearly enclosed sea with a highly structured coast line. Thus at any wind direction there exists a coast which favors upwelling. The coastal upwelling is confined to an offshore distance of the internal Rossby radius which is of about 4 to 8 km in the Baltic Sea (Fennel et al. 1990). The uplift of the pycnoclines itself will not result in a vertical mixing. A differential advection is required that establishes an instable stratification and convective mixing. Two different mechanisms are known, which can produce an instable stratification due to coastal upwelling.

Mixing in the surface layer: The Ekman offshore transport in the surface layer is compensated by an onshore flow (Ekman compensation flow) below the surface mixed layer. The dense water, originating from the deeper layers and upwelled near the coast, is advected offshore in the upper layer and is shifted over the lighter surface water, cf. Fig. 1. The onset of instable stratification forces vertical convection and an irreversible mixing. As result vertically oriented isopycnals are observed. The convection is limited to a layer bounded by the surface and the depth where the upwelled water originates.

Mixing in the bottom layer: In case of a bottom topography with a slope the uplift of the pycnoclines forces an onshore transport in the bottom layer. The bottom friction at the slope causes a differential advection in the near bottom layer, with decreasing onshore velocities towards the bottom as also mentioned and illustrated in Subsection 5.2. In presence of an density gradient along the bottom, which usually is found at the location where the halocline or thermocline hits the bottom, the vertical gradient in the current field leads to an unstable stratification and thus to a convective irreversible mixing by shear-induced convective mixing. An example is shown in Fig. 14.

Additionally, short wind pulses, which cause short term displacements of the isopycnals without mixing, can generate internal waves and contribute to the diapycnical mixing by the internal wave field, see Subsection 5.1.

In the Baltic Sea the impact of upwelling is restricted to the surface layer and the upper halocline. The vertical extent of the Ekman compensation flow below the Ekman layer, determines the depth from where the upwelled water originates. Whether the upwelling induced surface layer convection contributes to the diapycnical mixing depends on the actual stratification and on the depth of Ekman layer. During summer the seasonal thermocline traps the Ekman transport in the warm surface layer. The compensation flow covers the intermediate water above the halocline. Thus in summer conditions one can expect that the upwelling induced convection will not significantly contribute to diapycnical mixing through the halocline. However, it is of great importance for the transport of nutrients from intermediate winter water into the euphotic layer, cf. Section 6. During winter conditions without a shallow seasonal thermocline the compensation flow can cover the winter water and the upper halocline, depending on the depth of the mixed layer. Then the resulting shear induced mixing in the bottom layer near the coast contributes to the vertical transport through the halocline. The upwelling induced mixing in the surface layer enhances the deep winter convection due to cooling.

With respect to the global warming, in the future the upwelling process may become more important for the mixing of the upper layer. The expected change in atmospheric forcing will enhance the upwelling intensity during winter. If during warm winters the surface temperature of the Baltic Sea remains above the temperature of maximum density, the convective mixing due to seasonal cooling will be reduced. In that case upwelling and enhanced wind mixing can maintain the vertical transport of nutrients into the surface layer.

Observations and model results from the Baltic Sea

The first observations of local coastal upwelling in the Baltic Sea were published by Walin (1972a), who described an upwelling event in the Hanö Bay. Gidhagen (1984) gave an overview on the upwelling in the Baltic Sea based on remote sensing of SST. He found coastal upwelling cells thoughout the entire Swedish coast localised at several spots. In summer the temperature in active upwelling cells drops down typically by 4 to 5°C, although decreases of up to 10°C were also observed. The upwelling commonly persists for a week, but events with a month duration were observed, too. Gidhagen (1984) also found a strong interannual variation in the rate of upwelling events. He tried to compile statistics of the upwelling activity from remotely sensed SST, which however had to remain incomplete due to the fact that winter upwelling events have small SST signature only. Horstmann (1983) detected upwelling at the southern coasts of the Baltic Sea caused by easterly winds.

A systematization of the upwelling zones in the entire Baltic Sea was made by Bychkova and Victorov (1987), which was also based on satellite data of SST. Their main results are summariszed in Victorov (1996). 22 coastal upwelling zones were identified and described by means of their size, upwelling favorable wind directions, and observed upwelling frequency and intensity.

During the last two decades a number of publications described several local upwelling cells. A prominent one is the Hiddensee upwelling cell (Fennel and Sturm 1992, Lass et al. 1994, Lass et al. 1996). Fig. 26 illustrates the onset and decay of an upwelling event west of Hiddensee in Juli 1995. The event lasted for a week. The observed temperature differences between the core of the upwelling filament and the surrounding surface water exceeded 10°C.

However, besides some theoretical works (eg. Fennel 1992) about the upwelling dynamics most of the publications remained on a descriptive level and are focussed on summer events since they can be easily detected by SST observations. The role of upwelling for the vertical salt transport has hardly been discussed. Mainly upwelling induced vertical nutrient transport from the intermediate winter water into the surface layer were discussed, in terms of cyano bacterial bloomes (Janssen et al. 2004) and also its effect on the zooplankton (Kostrichkina and Yurkovskis 1986). Until today robust estimates of the contribution of coastal upwelling to the overall vertical transport do not exist.

Since direct measurements of upwelling events by remote sensing and/or in-situ observations are difficult and cannot overcome the undersampling problem, numerical models are increasingly used to analyse upwelling events in the Baltic Sea (eg. Jankowski 2002, Lehmann et al. 2002). Kowalewski and Ostrowski (2005) provide one of the most recent works about upwelling using a three-dimensional hydrodynamic model. On a basis of a seven year numerical simulation they could identify 12 upwelling zones in the southern Baltic Sea, where the vertical velocities for at least two adjacent wind sectors of 45° exceed $2 \cdot 10^{-4}$ m/s. For each of these zones a statistic of up- and downwelling was calculated. The percentage of upwelling frequency with vertical velocities above $2 \cdot 10^{-4}$ m/s range from 4.6 to 27.1 % in the specified regions.

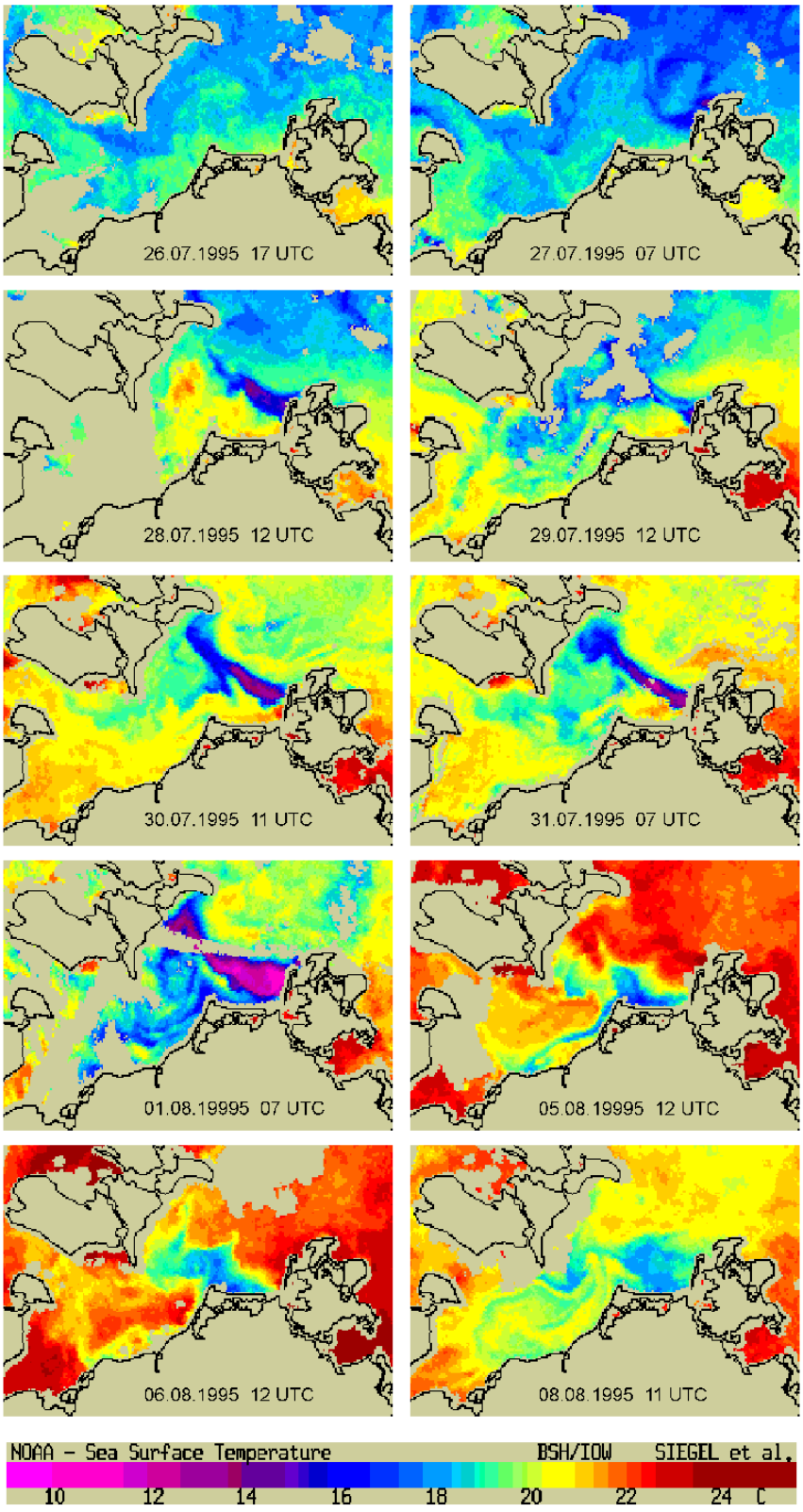

Fig. 26: Example for upwelling in the Baltic Sea. The series of SST images, compiled according to Lass et al. (1996), shows the development and decay of an upwelling filament, stretching from the west coast of Hiddensee island in north-westerly direction onto Møn island.

The total percentage of periods with vertical upward velocity was in nearly all regions around 50 % (41.6 % – 54.5 %), except for the east coast of Bornholm where upwelling is observed 72.8 % of the time. This is the region with the most intense upwelling in the model, showing the highest annual mean of vertical velocity of about $0.55 \cdot 10^{-4}$ m/s. A second zone of intense upwelling is the Hanö Bay with $0.24 \cdot 10^{-4}$ m/s annual mean vertical velocity. In contrast, Lehmann et al. (2002) found extreme values of the averaged vertical velocity $5 \cdot 10^{-6}$ m/s, resulting in a pycnocline uplift of 0.5 m/d, which is one order of magnitude less than reported by Kowalewski and Ostrowski (2005). Strongly enhanced vertical velocities were found for NAO+ phases as a result of the prevailing atmospheric conditions. Up to date estimates of the total vertical transport due to upwelling have not been made from numerical model simulations.

Quantification

Although the dynamics of upwelling are well investigated, a quantitative estimate of the contribution of coastal upwelling to the basin scale vertical mixing in the Baltic Sea is still missing and cannot be derived from in-situ measurements. Only hydrodynamic models will be able to supply the necessary data. However, to resolve the differential advection and convective mixing in the boundary layers high vertical and horizontal resolutions would be required which have not yet been reached in basin scale modelling of the Baltic Sea.

To estimate an upper limit of the upwelling driven vertical transport, the Baltic Sea is extremely simplified assuming a circular basin with a total surface area of 400000 km² (radius ~ 350 km). In this case upwelling is independent from the wind direction. Wind data, taken at the Darss Sill (1995 to 2004), were used to calculate a climatological wind field. The derived monthly means of windstress were applied to estimate the Ekman-transport E in Fig. 27, according to 9 (Csanady 1982).

$$E = \tau / f \qquad \text{with} \quad \tau = \frac{\rho_{air}}{\rho_{water}} \cdot W_{10} \cdot |W_{10}| \cdot c_d \qquad (9)$$

The drag coefficient c_d was assumed to be a constant of $1.6 \cdot 10^{-3}$, f is the inertial frequency at 57°N, and W_{10} is the windspeed 10 m above the sea surface. In case of an ocean with an infinite coast the Ekman-transport is equal to the vertical transport in the active upwelling zone at the coast. Therefore the derived Ekman-transport can be assumed as an upper limit of the vertical transport due to upwelling.

The corresponding depth of Ekman layer and horizontal velocities were approximately 20 m and 4 cm/s for typical summer conditions and 30 m and 5.5 cm/s for winter respectively. Using a mean baroclinic Rossby-radius of 6 km (Fennel et al. 1990) as measure for the extension of the upwelling zone at the coast, the vertical velocity ranges for this idealized experiment between $1.3 \cdot 10^{-4}$ m/s in summer and $2.6 \cdot 10^{-4}$ m/s in winter. The annual upwelled water volume amounts to 27100 km^3, which compares approximately to the total volume of the Baltic Sea. Seasonally it splits into 16600 km^3 in winter (Oct-Mar) and 10500 km^3 in summer (Apr-Sep). Related to the volume of the Baltic Sea surface layer (15000 km^3) upwelling has the potential to turn over the surface layer twice a year.

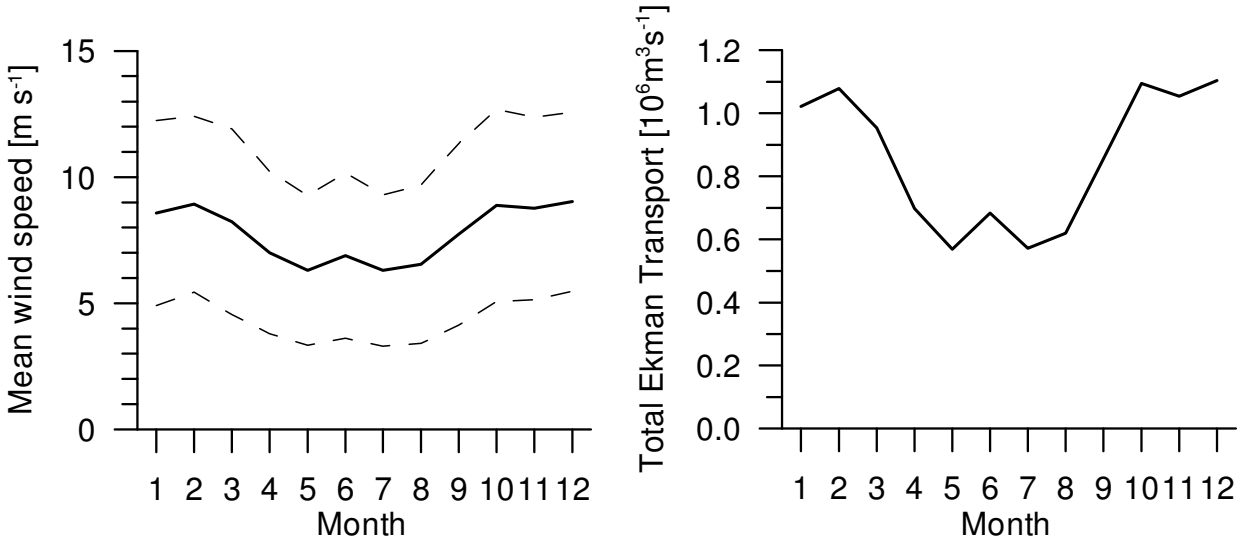

Fig. 27: Monthly climatological wind speed at the Darss Sill (1995-2004) and its first standard deviation (left panel) and the Ekman-transport (right panel) for a circular basin using the climatological wind as forcing.

However, in a real ocean with structured coastlines and spatial and temporal fluctuating wind fields, the situation is different from the simplified case. Eq. 9 describes the conditions after the adjustment of the current field to a constant wind forcing, which typically takes one inertial period (14.5 h in the Baltic Sea). Compared to the mean duration of wind events in the order of 2 to 4 days, the adjustment of current field will be a continuous ongoing process. Additionally, each inhomogenity in the wind field and the coastline generates Kelvin waves, traveling along the coast through the upwelling areas. After passing of the Kelvin wave the dynamic balance at the coast changed and the upwelling will be stopped (Fennel and Lass 1989). Also the upwelling can be exported by Kelvin-waves into regions without upwelling favorite wind forcing. Further, a significant number of forcing events are too short to generate a vertical mixing due to differential advection, since the tilted isopycnals are relaxing before an irreversible mixing has occured. With an Ekman-layer depth of 20 m and a vertical velocity of $1.3 \cdot 10^{-4}$ m/s the isopycnals need 1.5 days to reach the surface. It has to be concluded, that it is more or less impossible to give an robust estimate of the total vertical transport in the Baltic Sea caused by upwelling. Comparing the maximum annual mean vertical velocity from the model of Kowalewski and Ostrowski (2005) with the estimates from the circular basin, the true value of the total vertical transport can be an order of magnitude less than the upper limit given above.

6. Ecosystem perspective

The availability of nutrients in the euphotic zone determines to a large extent the intensity of primary production. Beside silicate which is essential for diatom growth only phosphate and inorganic nitrogen compounds (ammonium, nitrite and nitrate) have to be considered. In the central Baltic Sea the spring phytoplankton bloom is nitrogen limited due to the low N/P ratio of inorganic nutrients in the surface water in winter (Matthäus et al. 2001b). After the spring bloom phosphate remains at concentrations of about 0.10 µmol/l in May. These conditions are suitable for the development of diazotrophic cyanobacteria later the year. Intensive blooms are frequently observed in the Baltic Sea in summer. Processes and factors that control cyanobacteria growth and their mass development are manifold and by far not completely understood. Because of their ability to overcome the shortage of nitrogen by fixing atmospheric nitrogen, phosphorus plays a key role in the regulation process (Nausch et al. 2004).

The balance of phosphate in the mixed surface layer is determined through uptake processes by autotrophic organisms, mineralization of organic matter, and vertical transport in both directions. The downward vertical transport takes place mainly in particulate form as sedimentation whereas the upward transport is mainly passive and follows the hydrodynamic salt transport. Also upwelling processes can play a prominent role. In the last decades, especially during the 1960s and 1970s, the concentrations were strongly influenced by horizontal transport and advection due to the massive input of nutrients from the catchment area as a result of eutrophication (HELCOM 2003). Since the end of the 1970s winter concentrations fluctuate on a high level. This suggests that the downward and upward transport are in the same order of magnitude.

In this section the present knowledge is summarized about

a) the chemical reactions and variations of phosphate in the deep water
b) the upward transport of phosphate which is basically physically driven

Nutrient conditions in the deep basins of the Baltic Sea are strongly influenced by episodic inflows of larger volumes of highly saline, oxygen-rich water from the North Sea. Owing to their high density and their considerable oxygen content, these Major Baltic Inflows (MBI) are the only mechanism by which the deep water in the central basins can be replaced and significantly renewed. Until the mid 1970s such events occurred relatively frequently (Matthäus and Franck 1992, Matthäus and Nausch 2003), since then they have taken place only seldom. Within the last 30 years strong inflow events happened only in 1975/1976, 1983, 1993/1994, 1997 and 2003 (Feistel et al. 2003b, Matthäus 2006). Between these events long-lasting stagnation periods were observed.

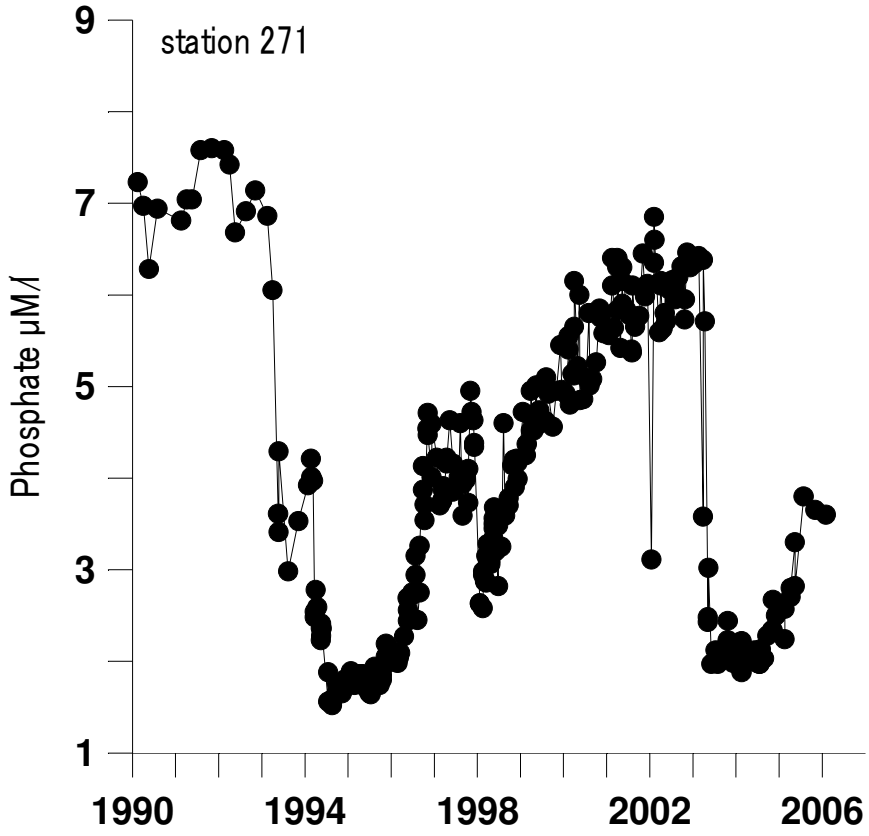

Fig. 28: Variations of phosphate concentrations (µmol/l) in the deep water (200 m) of the Gotland Deep between 1990 and 2006 - updated according to Matthäus et al. (2001a) and Nausch et al. (2003).

The nutrient conditions react strongly on the alternation between inflow and stagnation periods. In the presence of oxygen phosphate is partly bound in the sediment and onto sedimenting particles in the form of an iron-III-hydroxophophate complex. If the system turns to anoxic conditions, this complex is reduced by hydrogen sulphide and phosphate and iron(II)ions are liberated. This interplay is perfectly mirrored in Fig. 28. At the end of a long stagnation at the beginning of the 1990s phosphate concentrations of around 7 µmol/l were measured. The MBI in January 1993 supported by two smaller inflow events in December 1993 and April 1994 improved the oxygen concentrations considerably (Fig. 29) and dropped the phosphate down to values below 2 µmol/l (Fig. 28). With the restoration of anoxic conditions in the following years phosphate concentrations started to increase again. This increase was interrupted only shortly due to the effects of an exceptionally warm summer inflow in 1997 (Matthäus et al. 1998) and an inflow in autumn 2001 (Feistel et al. 2003a). A drastic decrease of the phosphate concentrations in the deep water took place after the MBI of January 2003 had reached the Gotland Basin in May 2003 (Nausch et al. 2003).

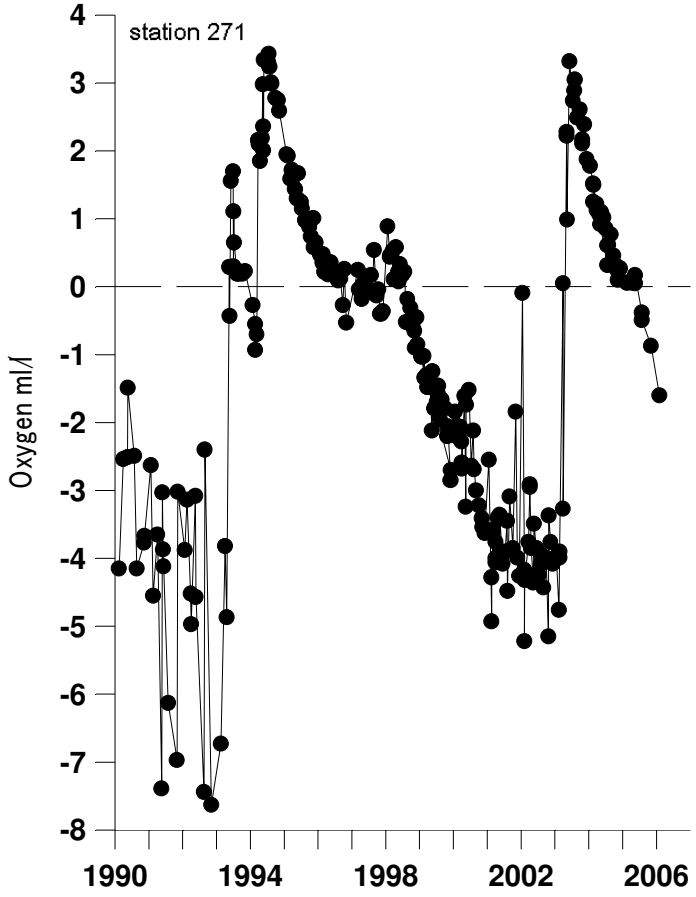

Fig. 29: Variations of oxygen/hydrogen sulphide concentrations (ml/l) in the deep water (200 m) of the Gotland Deep between 1990 and 2006, hydrogen sulphide is converted into negative oxygen equivalents - updated according to Matthäus et al. (2001a) and Nausch et al. (2003).

MBI's are assumed to mainly replace the deep water masses in central basins of the Baltic Sea and thus influencing the nutrient concentrations there. The question arises to which extent these changes can counterdraw to the surface layer. For comparison and nutrient trend analysis usually the surface layer in winter is used, because the biological activity is low and nutrient concentrations are high in winter (Nehring and Matthäus 1991). Furthermore, in such analysis the assumption is made that a

steady state between microbial mineralization, low biological productivity, and high vertical exchange and mixing has developed at this time. This steady state lasts 3 – 4 months and is most discernible in the Eastern and Western Gotland Basin, where values characteristic for the winter situation are sometimes measured as late as in early April.

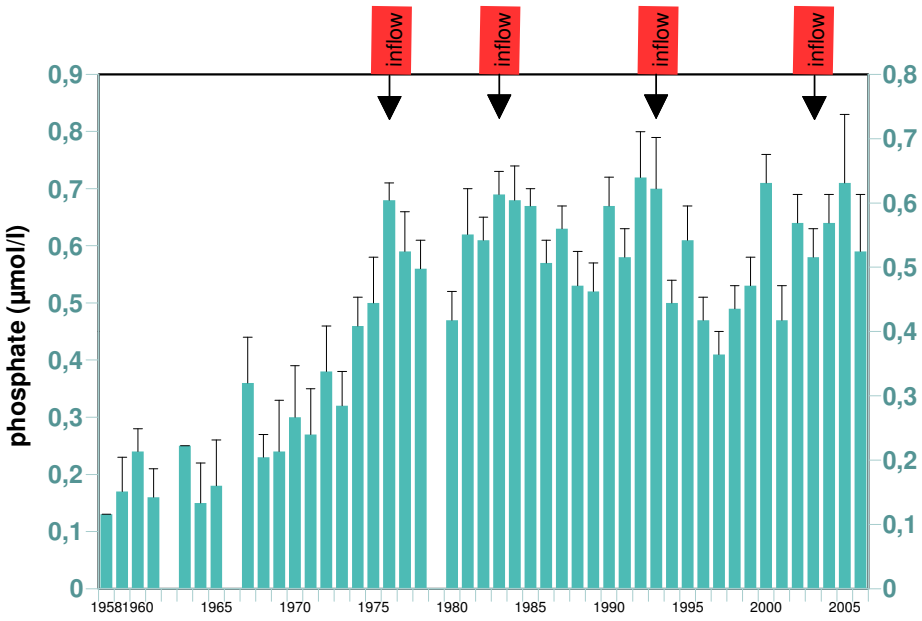

Fig. 30: Phosphate concentrations (µmol/l) in the mixed winter surface layer in the Eastern Gotland Basin from 1958 to date, with no data for 1962, 1966, and 1979.

Fig. 30 shows the averaged annual winter phosphate concentrations in the surface layer (0 m – 10 m) pooling 6 stations in the Eastern Gotland Basin. At the one side the steep increase in the 1960s and 1970s can be seen resulting from the intensive eutrophication during that period. Phosphate concentration of around 0.20 µmol/l as found in the late 1950s and early 1960 are assumed to be the natural background concentrations for the open Baltic Sea area. After the remarkable increase concentrations remain on a high level with strong fluctuations as a result of mainly internal processes. Among these the effects of MBIs have to be discussed. In Fig. 30 these events are marked. It is evident that after the inflows 1975/1976, 1983, and 1993 lower phosphate concentrations in the subsequent years were measured whereas a comparable decrease after the MBI of 2003 could not be observed.

To understand this different behaviour, the historicity of the inflow events has to be considered. During the inflow process salty, oxygen-rich water masses are penetrating into the near bottom layer, partly precipitate the dissolved phosphate, and lift up older, oxygen-poor water masses rich in phosphate. In case that the water layers below the halocline are relatively well supplied with oxygen, phosphate is precipitated again as iron-III-hydroxophophate complex and phosphate concentrations remain low. This can be assumed for the earlier inflow events. Consequently, relatively small amounts of phosphate can be transported into the surface during deep vertical mixing in winter.

Nausch et al. (2003) have tried to budget the amount of phosphate stored in a box in the Eastern Gotland Basin. The box area below 70 m is 12 300 km^2 with a volume 343 km^3. They described the phosphate content for three different depth regions: a) between the halocline and the bottom b) between the redoxcline and the bottom and c) between the halocline and the redoxcline. Here the most interesting is the latter one (Fig. 31). At the end of the stagnation period in 1992 the water body between 80 m and 125 m water depth was relatively well supplied with oxygen (Nehring et al. 1993). Therefore phosphate concentrations were comparatively low. Water renewal initially caused oxygen-poor water layers with high phosphate concentrations to be raised. Thus no further decrease between 1992 and 1995 could be observed. During the stagnation period from 1995 onwards the water layers below the halocline remained extremely poor in oxygen with the result that enormous amounts of phosphate had enriched in this layer leading to an increase of winter phosphate concentrations at the surface later on (Fig. 30).

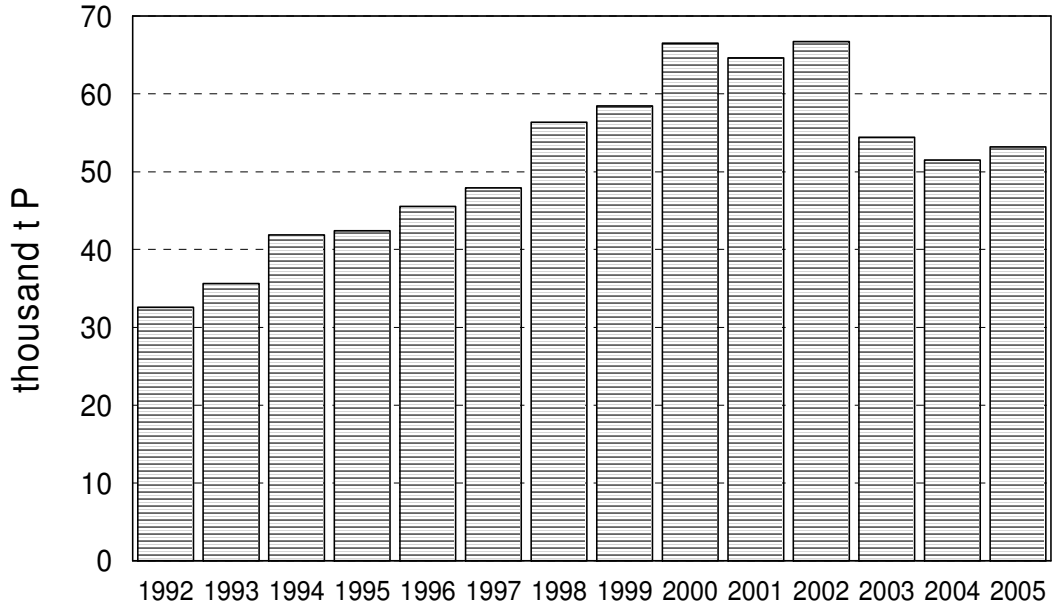

Fig. 31: Phosphate pool between the halocline (70 m) and the redoxcline (137 m) in the Eastern Gotland Basin, supplemented and updated according to Nausch et al. (2003).

Consequently, the lifting up of the "old" water masses after the MBI in January 2003 into the oxygen-poor water layer below the halocline resulted in an only moderate decrease of stored amount of phosphate. Thus 53 200 t P were stored in 2005 compared to 32 500 t P in 1992. Under these circumstances vertical mixing is able to transport much higher amounts of phosphate into the surface layer maintaining winter concentrations on a high level (Fig. 30). This behaviour can be described more in detail looking at the period January 2003 to December 2005 (Fig. 32). The oxygen-rich inflow near the bottom (green, beginning in April/May 2003) causes an elevation of the stagnant water (yellow) below the pycnocline from 100 m to 70 m depth, i.e. by almost 30 m. By comparing the development in the oxygen distribution with the measured phosphate concentrations substantial similarities are evident (Fig. 33). During the whole observation period high phosphate concentrations, partly higher than 4 µmol/l, were found directly below the halocline allowing for considerable vertical nutrient transport, if the appropriate physical forcing is given.

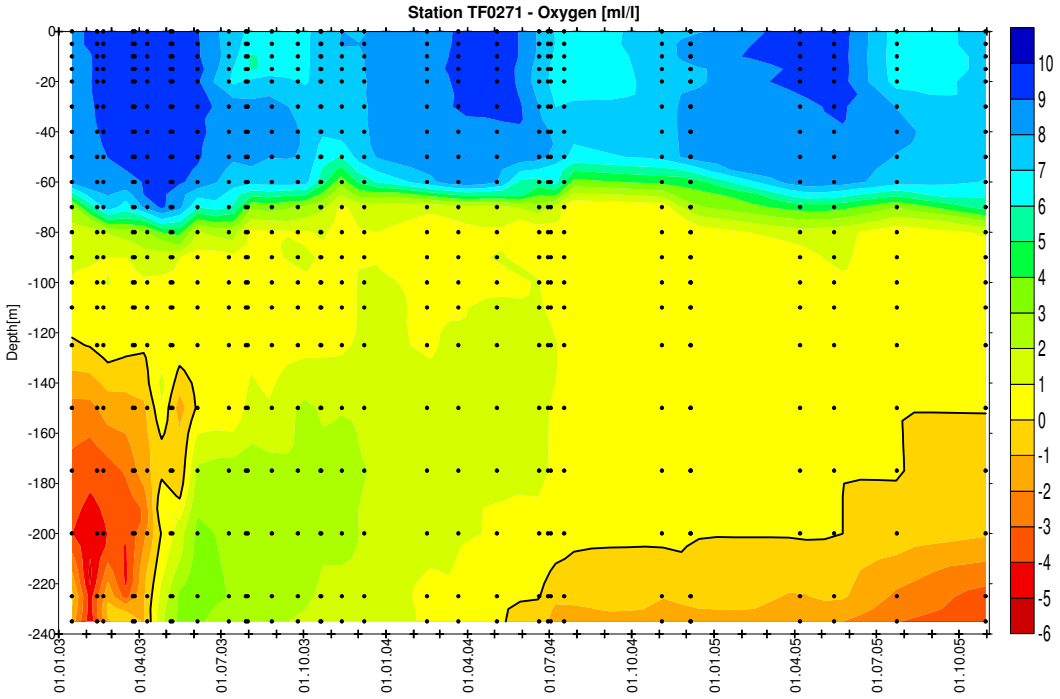

Fig. 32: Oxygen and hydrogen sulphide (shown as negative oxygen equivalent) at the Gotland Deep between 2003 and 2005 from Feistel et al. (2006b).

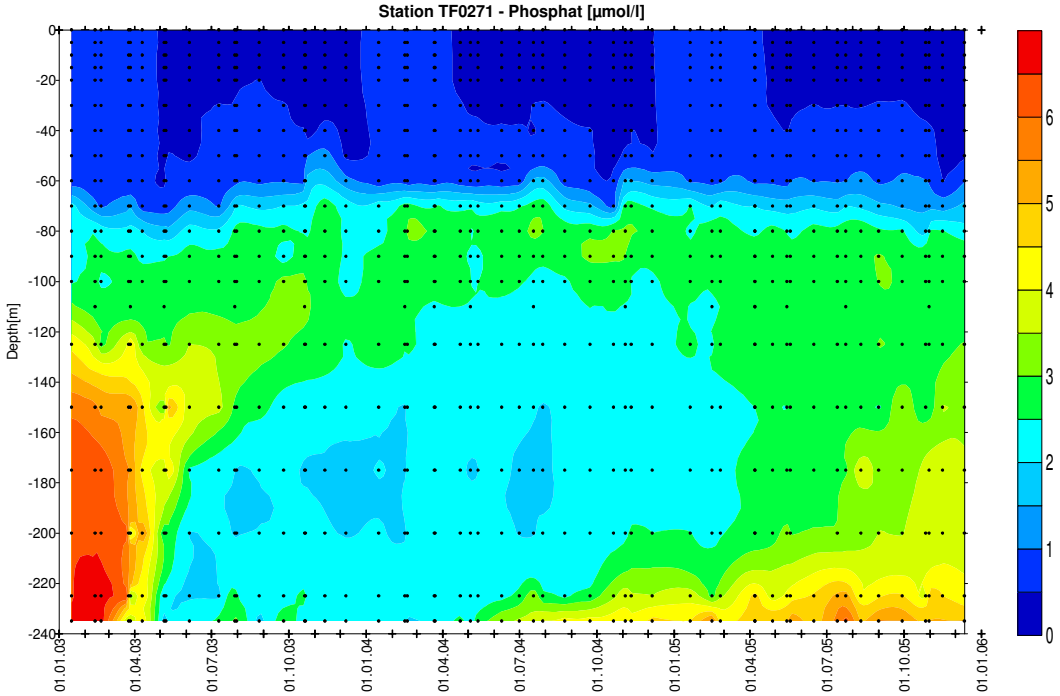

Fig. 33: Phosphate concentrations at the Gotland Deep between 2003 and 2005.

Table 2: Mean annual phosphate concentrations at 80 m water depth at the central station in the Eastern Gotland Basin

Year	Phosphate (µmol/l)	Year	Phosphate (µmol/l)
1992	0,79 ± 0,14	1999	2,99 ± 0,07
1993	1,04 ± 0,26	2000	2,55 ± 0,50
1994	1,33 ± 0,43	2001	2,82 ± 0,31
1995	1,55 ± 0,23	2002	2,96 ± 0,22
1996	1,67 ±0,30	2003	2,33 ± 0,36
1997	1,99 ± 0,39	2004	2,87 ± 0,29
1998	2,72 ±0,23	2005	2,64 ± 0,16

Finally looking at the mean annual phosphate concentrations in 80 m water depth at the central station in the Eastern Gotland Basin between 1992 and 2005 (Table 2), the described differences become much more visible. Despite a long lasting stagnation period which ended in 1993 the horizon below the permanent halocline contains only low phosphate concentrations due to the relative good ventilation of this water layer by intermediate inflow processes. A quite different situation was observed at the end of the following stagnation period in 2002. Nearly 3 µmol/l phosphate were measured as a result of a quite poor supply with oxygen. And the situation did not significantly improve after the MBI of 2003, cf. Fig. 33.

Using the transport rate of around 30 kg/(m^{2}a) estimated in Subsection 3.1 for the vertical salt transport across the pycnocline into the surface layer of about 60 m thickness resulting from the erosion of a layer with salinity of around S = 10 psu in combination with the measured phosphate concentrations P_{80} as given in Table 2 in the 80 m depth level, a phosphate increase in the mixed layer of about (d/dt) P_{mix} = 0.040 µmol/(l a) (1992) and (d/dt) P_{mix} = 0.15 µmol/(l a) (1999) hypothetically would result from the balance formula

$$\frac{\mathrm{d}}{\mathrm{d}t}P_{\mathrm{mix}} = 30\frac{\mathrm{kg}}{\mathrm{m}^2\,\mathrm{a}} \times \frac{1}{60\,\mathrm{m}} \times \frac{P_{80}}{10\,\mathrm{g/kg}} \times \frac{1}{1000\,\mathrm{kg/m}^3} = \frac{P_{80}}{20\,\mathrm{a}},$$

assuming a fixed S:P ratio during this process.

This result does not necessarily mean the transport is evenly distributed over the year. Most of the transport is realized during the deep vertical mixing in winter. Looking at their interplay, disagreements are evident between the estimated nutrient transport rates and the measured winter concentrations in Fig. 30. However, one has to keep in mind, that the water layer between the thermocline and the halocline is not completely exhausted from phosphate during the whole vegetation period. Also in the summer phosphate concentrations huge interannual differences can be observed depending on the preceding winter concentrations. For example, in summer 1997, which was a year with extremely low winter concentrations (Fig. 30), a phosphate content of around 0.20 µmol/l was measured at 30 m depth. In 2005 at the same water depth around 0.55 µmol/l phosphate could be detected.

In conclusion, looking at an ecosystem perspective, the vertical nutrient transport through the permanent halocline as well as the possible phosphate transport through the temporary thermocline is quantitatively not sufficiently well understood yet.

7. Discussion

The Baltic Sea has to be roughly divided into at least two parts with respect to the dominant vertical mixing processes – the entrance area and the deeper basins east of Bornholm. In the shallow Belt Sea, gale-force winds are capable of mixing the entire water column down to the sea floor. In the deeper western parts the direct interaction between the inflowing saline water from the North Sea and the outflowing brackish water governs the vertical transport. The associated entrainment processes have strong regional hot spots as discussed in Section 4. However, the impact of the resulting vertical transport on the water and salt budget of the Baltic Sea is hard to quantify, because the upward mixing of saline bottom water into the outflowing surface water and the downward mixing of brackish surface water joining the inflowing bottom water allow for complicated recirculation. Moreover, in certain regions this two-layer system can turn into a one-layer system of both brackish surface water and saline bottom water, see Section 2. This even complicates the challenging task to determine the impact of the vertical mixing in this part of the Baltic Sea to its water and salt budget. Nevertheless, these entrainment and recirculation processes determine the properties and amount of the inflowing dense water entering the other part of the Baltic Sea, where temporal changes and the associated transports are dominated by horizontal advection of saline water in the bottom layers below the permanent halocline and turbulent vertical transport through the halocline in the surface layers above the halocline, cf. Subsection 3.1. This part basically consists of the central Baltic Sea including primarily the Eastern Gotland Basin. The dominating transport processes in this part of the Baltic Sea allow for robust bulk estimations of the vertical salt transport, which are the focus of Section 3. The estimated vertical salt transports can be assumed to be almost uniform in space for those regions in the central Baltic Sea which are covered by the permanent halocline. Depending on the method the estimated vertical net transport of salt varies around values slightly above 30 kg/(m² a).

General picture of vertical mixing in the central Baltic Sea

The vertical transport through the halocline into the entire surface mixed layer in the central Baltic Sea can be described consistently. The general dynamics of the surface mixed layer are presented in Subsection 2.2. The vertical transport into the entire surface mixed layer is basically maintained by the weakening of the halocline in summer and its erosion in winter when the surface mixed layer reaches down to the halocline because of the absence of the thermocline.

The weakening of the halocline in summer is accomplished by turbulent mixing which can be largely associated with breaking internal waves. In Subsection 5.1 the corresponding observed diffusivity in the range of the halocline is estimated to be sufficient to maintain a turbulent vertical salt transport, which is of the order of magnitude required from the bulk estimates of the net upward transport of salt given in Section 3. However, this turbulent vertical transport is of short range in the order of magnitude of about 1 m at maximum, see Subsection 2.2. The turbulent salt transport J_S is calculated according to

$$J_S = -k_\nu \frac{\mathrm{d}S}{\mathrm{d}z} \qquad (10)$$

with the turbulent diffusivity k_ν, the salinity S, and the vertical coordinate z. Consequently, the turbulent transport vanishes right above the halocline where the vertical salinity gradient disappears in the mixed layer above the halocline, even though somewhat larger diffusivities are observed

outside the halocline, cf. Fig. 11. This can be explicitly seen from the parametrisations of k_v given in Eqs. 7 and 8. Assuming that the variations of the potential density ρ_{pot} in the definition of the Brunt-Väisälä frequency N, namely

$$N^2 = -\frac{g}{\rho_{pot}} \frac{\mathrm{d}\rho_{pot}}{\mathrm{d}z} \qquad (11)$$

with the acceleration g due to gravity and the vertical upward coordinate z, are mainly due to variations of the salinity S, i.e.

$$\frac{\mathrm{d}\rho_{pot}}{\mathrm{d}z} \approx \frac{\partial \rho_{pot}}{\partial S} \frac{\mathrm{d}S}{\mathrm{d}z}, \qquad (12)$$

Eq. 10 results in turbulent vertical salt transports $J_S \propto \sqrt{\frac{\mathrm{d}S}{\mathrm{d}z}}$ and $J_S \propto \varepsilon$ for Eqs. 7 and 8, respectively. Note that the rate ε of dissipation of turbulent kinetic energy itself is proportional to N according to Eq. 6 or to powers of N up to 2 depending on its parametrisation, cf. Subsection 5.1, and $N \propto \sqrt{\frac{\mathrm{d}S}{\mathrm{d}z}}$ with the approximation made in Eq. 12. Hence, the vertical turbulent salt transport J_S vanishes as expected for all parametrisations discussed here as the vertical salinity gradient disappears provided that the approximation made in Eq. 12 is valid. Therefore the halocline is slowly extended upward and weakened by the turbulent transport as a result of its short range. During summer the spreading of the halocline can be clearly seen in observations, cf. Table 1, and can be satisfactorily reproduced in simulations, see Fig. 3. In winter this effect is not visible because there is no thermocline protecting the halocline from surface mixing. Accordingly, the surface mixed layer reaches down to the halocline, and erosion due to wind mixing and convection acts effectively in sharpening the salinity gradients in the halocline region. Consequently, the salt transported through the halocline by turbulent diffusion is instantaneously mixed to the entire surface mixed layer in winter. In summer surface mixing by wind and by nightly convection only reaches down to the thermocline, which protects the halocline from erosion. As a consequence the weakening of the halocline due to turbulent diffusion is undisturbed and the corresponding salt transport can be observed in terms of the slow upward expansion of the halocline during summer.

The amount of salt, which is eroded from the halocline by surface mixing in winter, is determined by the maximum depth, to which the surface mixing reaches. This depth in turn depends on the meteorological conditions in winter and the vertical density gradient at the top of the halocline resulting from the weakening and expansion of the halocline due to the turbulent upward salt transport during summer. The eroded salt is mixed homogeneously into the entire surface mixed layer. In Subsection 3.2 the corresponding increase of the bulk sea surface salinity was used to estimate the amount of eroded salt to be slightly above 30 kg/(m² a) in the long-term mean. On the one hand, this is in good agreement with the other bulk estimates of the vertical salt transport through the halocline for the central Baltic Sea made in Section 3. On the other hand, it completes the consistent description of this transport with respect to the vertical transport within the halocline due to turbulent diffusion as discussed above and estimated in Subsection 5.1.

The outlined consistent description of the vertical salt transport in the central Baltic Sea is based on estimates of the turbulent salt transport within the halocline and the transport of salt into the entire surface mixed layer by erosion of the halocline. In spite of the excellent agreement of these estimates their uncertainty, which can be a factor 2 for such estimates, would still allow for additional relevant vertical transport mechanisms as suggested in Section 5.

Specific characteristics during stagnation periods

In general, the salt loss below the halocline resulting from vertical upward transport is compensated by inflows of saline water from the North Sea at the bottom, see Subsection 2.1. These inflows not only sustain the salinity below the halocline at its long-term mean, but also reset the halocline depth to its climatological level by a corresponding vertical uplift, cf. Subsection 3.3.

During stagnation periods without such inflows the halocline is slowly lowered due to the alternating weakening and erosion of the halocline as discussed above. In addition, the salinity continuously decreases both below and above the halocline, see Fig. 4.

Below the halocline this decrease obviously results from the continuing vertical upward salt transport. Above the halocline the decrease in salinity is about a factor 2 slower than below it. This decrease of the bulk sea surface salinity may be attributed to the increase of the surface mixed layer volume resulting from the lowering of the halocline, because the salt transported through the halocline is consequently mixed into increasing volumes of brackish water. Presuming that the environmental parameters such as freshwater surplus are almost the same during stagnation periods, this would obviously produce decreasing bulk sea surface salinities. However, the volume changes due to the lowering of the halocline can be assumed to be small relative to the total volume of the surface mixed layer. Consequently, this volume effect is expected to be of minor importance. Alternatively, the decrease of the bulk sea surface salinity may be a result of a reduced vertical salt transport through the halocline during stagnation periods. Such a reduced vertical salt transport is indicated by the about five times longer deepwater residence time during stagnation periods derived in Subsection 3.4. Therefore it is the more probable cause of the bulk sea surface salinity decrease compared to the volume effect. Additionally, decadal fluctuations in river discharge and in the precipitation/evaporation balance influence the surface salinity.

In Subsection 3.4 the shorter deepwater residence time during periods with small or major inflows of saline water at the bottom is associated with the corresponding uplift of the deepwater and the halocline. However, the nature of the cause for the shorter deepwater residence time during periods with such uplifts cannot be inferred solely from their occurrence at the same time. The shorter residence time and the corresponding intensified vertical mixing may be a direct effect of the vertical uplift as suggested in Subsection 3.4, but an indirect correlation of these phenomena seems to be somewhat more likely, because the inflows also import mechanical energy on various scales.

This energy import and some of its consequences are illustrated in Subsection 5.4. The imported energy has the potential to drive or intensify nearly all mechanisms of vertical mixing discussed in Section 5. Only the vertical mixing by upwelling discussed in Subsection 5.5, the surface wave mixing, and the winter convection are likely to be almost independent from the energy fluctuations imported by the inflows. The vertical mixing due to the internal wave field (Subsections 5.1 and 5.2) and the eddy activity (Subsection 5.3) is intensified during inflow events as well as the near-bottom currents (Subsection 5.4). Therefore the overall diffusivity directly or indirectly resulting from these phenomena most likely is increased by inflows and the corresponding energy fluctuations such as pulsating currents or the irregular uplift of the deepwater. In contrast, the diffusivities would drop to a lower level during stagnation periods. Consequently, the resulting deepwater residence time would be longer compared to periods with inflows.

Unfortunately, the actual quantification of the involved effects does not allow for a decision, whether these effects are sufficient to account for the difference of the deepwater residence times derived from observations in Subsection 3.4. Note that if they were, the vertical mixing induced by

upwelling would have to adjust the two different deepwater residence times to their absolute values, because this is the only transport mechanism through the halocline, which can be presumed to be almost independent from inflows.

8. Acknowledgment

The authors are grateful to the Swedish Baltic Sea 2020 Foundation who motivated and financially supported the compilation of this state-of-the-art review. The German part of the Baltic Monitoring Programme (COMBINE) and the operation of the measuring stations of the German Marine Monitoring Network (MARNET) in the Baltic Sea are conducted by the Baltic Sea Research Institute Warnemünde (IOW) on behalf of the Bundesamt für Seeschifffahrt and Hydrographie (BSH), financed by the Bundesministerium für Verkehr, Bau- und Wohnungswesen (BMVBW). Parts of the presented work were carried out in the framework of the international QuantAS Consortium (Quantification of water mass transformation processes in the Arkona Sea), which is partially supported by the QuantAS-Off project (QuantAS – Impact of Offshore Wind Farms, funded by the German Federal Ministry of Environment, Nature Conservation and Nuclear Safety) and the QuantAS-Nat project (QuantAS – Natural processes, funded by the German Research Foundation). Furthermore, this work was supported by the project 'Rim Currents in the Eastern Gotland Basin (RAGO)' financed by the Deutsche Forschungsgemeinschaft, contract HA 1900/3-2. The contribution of Volker Mohrholz was partly granted by the Deutsche Forschungsgemeinschaft in the context of the ShIC project. The authors thank Jan Szaron, Oceanographic Laboratory of Swedish Meteorological and Hydrological Institute (SMHI), Gothenburg, for providing additional hydrographic-hydrochemical observations from the Swedish Ocean Archive SHARK, obtained within the framework of the Swedish monitoring programme and used here in Section 6. Jan Donath, IOW, is appreciated for the preparation of Fig. 1 and Hannes Rennau, IOW, for the creation of Figs. 6 and 9.

References

Axell, L. B. (1998): On the variability Baltic of Baltic Sea deepwater mixing, J. Geophys. Res., 103(C10), 21667-21682.

Axell, L. B. (2002): Wind-driven internal waves and Langmuir circulations in a numerical ocean model of the southern Baltic Sea, J. Geophys. Res., 107(C11), 3204, doi:10.1029/2001JC000922.

Aitsam, A. and Elken, J. (1982): Synoptic scale variability of hydrophysical fields in the Baltic Proper on the basis of CTD measurements, in: Nihoul, J. C. J. (Ed.), Hydrodynamics of Semi-Enclosed Seas, Elsevier Oceanography Series, Vol. 34, Elsevier, Amsterdam, 433-467.

Aitsam, A., Hansen, H.-P., Elken, J., Kahru, M., Laanemets, J., Pajuste, M., Pavelson, J., and Talpsepp, L. (1984): Physical and chemical variability of the Baltic Sea: a joint experiment in the Gotland Basin, Continental Shelf Research, 3(3), 291-310.

Arneborg, L., Fiekas, V., Umlauf, L., and Burchard, H. (2007): Gravity current dynamics and entrainment - a process study based on observations in the Arkona Basin, J. Phys. Oceanogr., in print.

Arneborg, L. and Liljebladh, B. (2001a): The Internal Seiches in Gullmar Fjord. Part I: Dynamics, J. Phys. Oceanogr., 31(9), 2549-2566.

Arneborg, L. and Liljebladh, B. (2001b): The Internal Seiches in Gullmar Fjord. Part II: Contribution to Basin Water Mixing, J. Phys. Oceanogr., 31(9), 2567-2574.

Baines, P. G. (2001): Mixing in flows down gentle slopes into stratified environments, J. Fluid Mech., 443, 237-270.

Brogmus, W. (1952): Eine Revision des Wasserhaushaltes der Ostsee, Kieler Meeresforschungen, 9(1), 15-42.

Burchard, H. and Bolding, K. (2001): Comparative Analysis of Four Second-Moment Turbulence Closure Models for the Oceanic Mixed Layer, J. Phys. Oceanogr., 31(8), 1943-1968.

Burchard, H. and Bolding, K. (2002): GETM, a general estuarine transport model. Scientific Documentation, European Commission, Report EUR 20253, 157 pp.

Burchard, H., Bolding, K., Rippeth, T. P., Stips, A., Simpson, J. H., and Sündermann, J. (2002): Microstructure of turbulence in the Northern North Sea: A comparative study of observations and model simulations, J. Sea Res., 47, 223-238.

Burchard, H., Bolding, K., Kühn, W., Meister, A., Neumann, T., and Umlauf, L. (2006): Description of a flexible and extendable physical-biogeochemical model system for the water column, J. Mar. Syst., 61,180-211.

Burchard, H., Janssen, F., Bolding, K., and Rennau, H. (2007): Model simulations of a medium-intensity inflow into the Baltic Sea, Cont. Shelf. Res, submitted.

Burchard, H., Lass, H. U., Mohrholz, V., Umlauf, L., Sellschopp, J., Fiekas, V., Bolding, K., and Arneborg, L. (2005): Dynamics of medium-intensity dense water plumes in the Arkona Basin, Western Baltic Sea, Ocean Dynamics, 55, 391-402.

Bychkova, I. A. and Victorov, S. V. (1987): Elucidation and systematisation of upwelling zones in the Baltic Sea based on satellite data (in Russian), Oceanology, 27(2), 218-223.

Carr, M.-E. and Kearns, E. J. (2003): Production regimes in four Eastern Boundary Current systems, Deep-Sea Res. II, 50, 3199-3221.

Cenedese, C, Whitehead, J. A., Ascarelli, T. A., and Ohiwa, M. (2004): A Dense Current Flowing down a Sloping Bottom in a Rotating Fluid, J. Phys. Oceanogr., 34(1), 188-203.

Cheng, Y., Canuto, V. M., and Howard, A. M. (2002): An improved model for the turbulent PBL, J. Atmos. Sci., 59, 1550-1565.

Craig, P. D. (1996): Velocity profiles and surface roughness under breaking waves, J. Geophys. Res., 101, 1265-1277.

Csanady, G. T. (1982): Circulation in the Coastal Ocean, D. Reidel Publishing Company, Dordrecht, 279 pp.

Defant, A. (1936): Das Kaltwasserauftriebsgebiet vor der Küste Südwestafrikas, in: Festschrift W. Krebs, Länderkundliche Studien, Stuttgart, 52-66.

Elken, J. (1996): Deep Water Overflow, Circulation and Vertical Exchange in the Baltic Proper, Report Series, No. 6, Estonian Marine Institute, Tallinn, 91 pp.

Elken, J., Pajuste, M., and Kõuts, T. (1988): On intrusive lenses and their role in mixing the Baltic deep layers, Proceedings of the Conference of the Baltic Oceanographers, Vol. 1, Kiel, 367-376.

Feistel, S. (2006): Baltic Atlas of Long-Term Inventory and Climatology (BALTIC), Status Report September 2006. http://www.io-warnemuende.de/projects/baltic/index.html

Feistel, R. and Feistel, S. (2006): Die Ostsee als thermodynamisches System, in: Schimansky-Geier, L., Malchow, H., and Pöschel, T. (Eds.), Irreversible Prozesse und Selbstorganisation, Logos-Verlag Berlin, 247-264.

Feistel, R., Feistel, S., Nausch, G., Lysiak-Pastszak, E., Szaron, J., and Aertebjerg, G. (2008): BALTIC: Monthly time series 1952 – 2005, in: Feistel, R., Nausch, G., and Wasmund, N., State and Evolution of the Baltic Sea 1952 – 2005, Wiley, in preparation.

Feistel, R., Nausch, G., and Hagen, E. (2003a): The Baltic inflow of autumn 2001, Meereswissenschaftliche Berichte, 54, 55-68. http://www.io-warnemuende.de/research/mebe.html

Feistel, R., Nausch, G., and Hagen, E. (2006a): Unusual Baltic inflow activity in 2002-2003 and varying deep-water properties, Oceanologia, 48(S), 21-35. http://www.iopan.gda.pl/oceanologia/48_S.html#A2

Feistel, R., Nausch, G., and Hagen, E. (2006b): Response of Baltic Water Properties to the Unusual Inflow Sequence since 2002, ICES CM 2006/C:09, ICES Annual Science Conference 2006, Maastricht, the Netherlands, 19–23 September 2006.

Feistel, R., Nausch, G., Matthäus, W., and Hagen, E. (2003b): Temporal and Spatial Evolution of the Baltic Deep Water Renewal in Spring 2003, Oceanologia 45(4), 623-642. http://www.iopan.gda.pl/oceanologia/454feis2.pdf

Feistel, R., Nausch, G., Matthäus, W., Łysiak-Pastuszak, E., Seifert, T., Sehested Hansen, I., Mohrholz, V., Krüger, S., Buch, E., and Hagen, E. (2004): Background data to the exceptionally warm inflow into the Baltic Sea in late summer of 2002, Meereswissenschaftliche Berichte, 58, 1-58. http://www.io-warnemuende.de/documents/mebe58_2004_paper.pdf

Feistel, R., Nausch, G., Mohrholz, V., Lysiak-Pastuszak, E., Seifert, T., Matthäus, W., Krüger, S., and Sehested Hansen, I. (2003c): Warm waters of summer 2002 in the deep Baltic Proper, Oceanologia, 45(4), 571-592. http://www.iopan.gda.pl/oceanologia/454feis1.pdf

Fennel, W. (1992): Responses of a coastal ocean, Trends in Phys. Oceanogr., 1, 163-179.

Fennel, W. and Lass, H. U. (1989): Analytical Theory of Forced Oceanic Waves, Akademie-Verlag, Berlin, 311 pp.

Fennel, W. and Seifert, T. (1995): Kelvin wave controlled upwelling in the western Baltic, J. Mar. Sys., 6, 289-300.

Fennel, W., Seifert, T., and Kayser, B. (1990): Rossby radii and phase speeds in the Baltic Sea. Cont. Shelf Res., 11(1), 23-36.

Fennel, W. and Sturm, M. (1992): Dynamics of the western Baltic, J. Mar. Sys., 3(1–2), 183-205.

Fischer, H. and Matthäus, W. (1996): The importance of the Drogden Sill in the Sound for major Baltic inflows, J. Mar. Sys., 9(3-4), 137-157.

Fonselius, S. (1962): Hydrography of the Baltic Deep Basins, Fish. Bd. Sweden. Ser. Hydrography, Rep. 13.

Fonselius, S. and Valderrama, J., (2003): One hundred years of hydrographic measurements in the Baltic Sea, J. Sea Res., 49 (4), 229-241.

Franck, H., Matthäus, W., and Sammler, R. (1987): Major inflows of saline water into the Baltic Sea during the present century, Gerlands Beitr. Geophys., 96, 517-531.

Gargett, A. E. and Holloway, G. (1984): Dissipation and diffusion by internal wave breaking, J. Mar. Res., 42(1), 15-27.

Garrett, C. (1991): Marginal mixing theories, Atmosphere-Ocean, 29, 313-339.

Garrett, C. (2003): Internal tides and ocean mixing, Science, 301, 1858-1859.

Garrett, C., MacCready, P., and Rhines, P. (1993): Boundary mixing and arrested Ekman layers: rotating stratified flow near a sloping boundary, Ann. Rev. Fluid. Mech., 25, 291-323.

Garrett, C. J. R. and Munk, W. H. (1975): Space-time scales of internal waves: A progress report, J. Geophys. Res., 80, 281-297.

Gemmrich, J. R. and Farmer, D. M. (2004): Near-Surface Turbulence in the Presence of Breaking Waves, J. Phys. Oceanogr., 34(5), 1067-1086.

Gidhagen, L. (1984): Coastal upwelling in the Baltic Sea, SMHI rep. Hydrol. and Oceanogr., 37, Norrköping, 35 pp.

Gill, A. E. (1982): Atmosphere-Ocean Dynamics, Academic Press, London, 662 pp.

Gloor, M., Wüest, A., and Imboden, D. (2000): Dynamics of mixed bottom boundary layers and its implications for diapycnal transport in a stratified, natural water basin, J. Geophys. Res., 105, 8629-8646.

Goudsmit, G.-H., Peeters, F., Gloor, M., and Wüest, A. (1997): Boundary versus diapycnal mixing in stratified natural waters, J. Geophys. Res., 102, 27903-27914.

Gregg, M. C. (1987): Diapycnal mixing in the thermocline: A review, J. Geophys. Res., 92(C5), 5249-5286.

Gregg, M. C. (1989): Scaling turbulent dissipation in the thermocline, J. Geophys. Res., 94(C7), 9686-9698.

Gustafsson, T. and Kullenberg, B. (1936): Untersuchungen von Trägheitsströmungen in der Ostsee, Sven. Hydrogr. - Biol. Komm. Skr. , Hydrogr. No. 13.

Hagen, E. (2004): Beobachtungen fluktuierender Randströme im Östlichen Gotlandbecken der Ostsee, Meeresumwelt-Symposium 2004, Hamburg, Bundesamt für Seeschifffahrt und Hydrographie, 127-138.

Hagen, E. and Feistel, R. (2001): Spreading of Baltic Deep Water: A Case Study for the Winter 1997–1998, Meereswissenschaftliche Berichte, 45, 99-133. http://www.io-warnemuende.de/research/mebe45_inhalt.html

Hagen, E. and Feistel, R. (2004): Observations of low-frequency current fluctuations in deep water of the Eastern Gotland Basin/Baltic Sea, J. Geophys. Res., 109, C03044, doi:10.1029/2003JC002017. http://www.agu.org/pubs/crossref/2004/2003JC002017.shtml

Hagen, E. and Feistel, R. (2008): Baltic Climate Change, in: Feistel, R., Nausch, G., and Wasmund, N., State and Evolution of the Baltic Sea 1952 – 2005, Wiley, in preparation.

Hansen, N.-E. O. and Møller, J. S. (1990): Zero blocking solution for the Great Belt Link, in: Pratt, L.J. (Ed.), The physical oceanography of sea straits, Kluwer Academic Publishers, 153-169.

Hela, I. (1944): Über die Schwankungen des Wasserstandes in der Ostsee mit besonderer Berücksichtigung des Wasseraustausches durch die dänischen Gewässer, Ann. Acad. Sci. Fenn., 28, 1-108.

HELCOM (1993): First Assessment of the State of the Coastal Waters of the Baltic Sea, Baltic Sea Environment Proceedings, 54, Helsinki, Baltic Marine Environment Protection Commission.

HELCOM (2003): Environment of the Baltic Sea, 1994 – 1998, Background Document, Balt. Sea Environ. Proc., 82B, 1-215.

Henyey, F. S., Wright, J., and Flatte, S. M. (1986): Energy and action through the internal wave field: an eikonal approach, J. Geophys. Res., 91, 8487-8495.

Hondzo, M. and Haider, Z. (2004): Boundary mixing in a small stratified lake, Water Resour. Res., 40, doi:10.1029/2002WR001851.

Horstmann, U. (1983): Distribution patterns of temperature and water colour in the Baltic Sea as recorded in satellite images. Indicators for phytoplankton growth, Ber. Inst. Meeresk., 106(1), 147 pp.

Huisman, J., van Oostveen, P., and Weissing, F. J. (1999): Critical depth and critical turbulence: two different mechanisms for the development of phytoplankton blooms, Limnol. Oceanogr., 44, 1781-1787.

Imberger, J. and Ivey, G. N. (1993): Boundary mixing in stratified reservoirs, J. Fluid Mech., 248, 477-491.

Jackett, D. R., McDougall, T. J., Feistel, R., Wright, D. G., and Griffies, S. M. (2006): Algorithms for Density, Potential Temperature, Conservative Temperature, and the Freezing Temperature of Seawater, J. Atm. Ocean Technol., 23(12), 1709-1728.

Jacobsen, T. S. (1980): Sea water exchange of the Baltic – measurements and methods, The Belt Project, National Agency of Environmental Protection, Denmark.

Jankowski, A. (2002): Variability of coastal water hydrodynamics in the southern Baltic – hindcast modelling of an upwelling event along the Polish coast, Oceanologia, 44(4), 395-418.

Janssen, F., Neumann, T., and Schmidt, M. (2004): Inter-annual variability in cyanobacteria blooms in the Baltic Sea controlled by wintertime hydrographic conditions, Mar. Ecol. Prog. Ser., 275, 59-68.

Kato, H. and Phillips, O. M. (1969): On the penetration of a turbulent layer into stratified fluid, J. Fluid Mech., 37, 643-655.

Kielmann, J. , Krauss, W., and Keunicke, K. H. (1973): Currents and stratification in the Belts Sea and in the Arkona Basin during 1992 – 1968, Kieler Meeresforsch., 29, 90-111.

Knudsen, M. (1900): Ein hydrographischer Lehrsatz, Ann. Hydrogr. Mar. Meteorol., 28(7), 316-320.

Kostrichkina, E. M. and Yurkovskis, A. K. (1986): On the role of the coastal upwelling in the formation of zooplankton productivity in the Baltic Sea, ICES CM, J(11), 12 pp.

Kõuts, T. and Omstedt, A. (1993): Deep water exchange in the Baltic Proper, Tellus, 45A, 311-324.

Kowalewski, M. and Ostrowski, M. (2005): Coastal up- and downwelling in the southern Baltic, Ocanologia, 47(4), 453-475.

Krauss, W. (1963): Zum System der internen Seiches der Ostsee, Kieler Meresforsch., 19, 119-132.

Kullenberg, G. E. B. (1977): Observations of the mixing in the Baltic thermo- and halocline layers, Tellus, 29, 572-587.

Large, W. G., McWilliams, J. C., and Doney, S. C. (1994): Oceanic vertical mixing: a review and a model with a nonlocal boundary layer parameterization, Rev. Geophys., 32, 363-403.

Lass, H. U. and Mohrholz, V. (2003): On dynamics and mixing of inflowing saltwater in the Arkona Sea, J. Geophys. Res., 108(C2), 3042, doi: 10.1029/2002JC001465.

Lass, H. U., Mohrholz, V., Knoll, M., and Prandke, H. (2006): On the impact of a pile on a moving stratified flow, Cont. Shelf Res., submitted.

Lass, H. U., Mohrholz, V., and Seifert, T. (2005): On pathways and residence time of saltwater plumes in the Arkona Sea, J. Geophys. Res., 110, C11019, doi:10.1029/2004JC002848.

Lass, H. U., Prandke, H. , and Liljebladh, B. (2003): Dissipation in the Baltic proper during winter stratification, J. Geophys. Res., 108(C6), 3187, doi:10.1029/2002JC001401.

Lass, H.-U., Schmidt, T., and Seifert, T. (1994): On the dynamics of upwelling observed at the Darss Sill, Proc. 19th Conf. Baltic Oceanogr., Gdańsk, 247-260.

Lass, H.-U., Schmidt, T., and Seifert, T. (1996): Hiddensee upwelling field measurements and modelling results, ICES Coop. Res. Rep., 257, 204-208.

Ledwell, J. R. and Bratkovich, A. (1995): A tracer study of mixing in the Santa Cruz Basin, J. Geophys. Res., 100, 20681-20704.

Ledwell, J. R. and Hickey, B. M. (1995): Evidence for enhanced boundary mixing in the Santa Monica Basin, J. Geophys. Res., 100, 20665-20679.

Ledwell, J. R., Montgomery, E. T., Polzin, K. L., St-Laurent, L. C., Schmitt, R. W., and Toole, J. M. (2000): Evidence for enhanced mixing over rough topography in the abyssal ocean, Nature, 403, 179-182.

Ledwell, J. R., Watson, A. J., and Law, C. S. (1998): Mixing of a tracer in the pycnocline, J. Geophys. Res., 103(C10), 21499-21529.

Lee, M.-M., Nurser, A. J. G., and Coward, A. C. (2002): Spurious diapycnal mixing of the deep waters in an eddy-resolving global ocean model, J. Phys. Oceanogr., 32, 1522-1535.

Lehmann, A. and Hinrichsen, H.-H. (2000): On the wind driven and thermohaline circulation of the Baltic Sea, Physics and Chemistry of the Earth (B), 25(2), 183-189.

Lehmann, A., Krauss, W., and Hinrichsen, H.-H. (2002): Effects of remote and local atmospheric forcing on circulation and upwelling in the Baltic Sea, Tellus, 54(A), 299-316.

Lemckert, C., Antenucci, J. P., Saggio, A., and Imberger, J. (2004): Physical properties of turbulent benthic boundary layers generated by internal waves, J. Hydraul. Eng., 130, 58-69.

Liljebladt, B. and Stigebrandt, A. (1996): Observations of the deepwater flow into the Baltic Sea, J. Geophys. Res., 101, 8895-8911.

Lilly, D. K., Waco, D. E., and Adelfang, S.I. (1974): Stratospheric mixing estimated from high-altitude turbulence measurements, Journal of Applied Meteorology, 13, 488-493.

Lorke, A., Umlauf, L., Jonas, T., and Wüest, A. (2002): Dynamics of turbulence in low-speed oscillating bottom-boundary layers of stratified basins, Environmental Fluid Mechanics, 2, 291-313.

Lorke, A. and Wüest, A. (2005): Application of coherent ADCP for turbulence measurements in the bottom boundary layer, J. Atmos. Oceanic Technol., 22, 1821-1828.

Lorke, A., Wüest, A., and Peeters, F. (2005): Shear-induced convective mixing in bottom boundary layers on slopes, Limnol. Oceanogr., 50, 1612-1619.

MacIntyre, S., Flynn, K. M., Jellison, R., and Romero, J. R. (1999): Boundary mixing and nutrient fluxes in Mono Lake, California, Limnol. Oceanogr., 44, 512-529.

MacKinnon, J. A. and Gregg, M. C. (2003): Shear and Baroclinic Energy Flux on the Summer New England Shelf, J. Phys. Oceanogr., 33(7), 1462-1475.

MacKinnon, J. A. and Gregg, M. C. (2005): Spring Mixing: Turbulence and Internal Waves during Restratification on the New England Shelf, J. Phys. Oceanogr., 35(12), 2425-2443.

Matthäus, W. (1978): Zur mittleren jahreszeitlichen Veränderlichkeit des Oberflächensalzgehaltes in der Ostsee, Gerlands Beitr. Geophysik, 87, 369-378.

Matthäus, W. (1984): Climatic and seasonal variability of oceanological parameters in the Baltic Sea, Beiträge zur Meereskunde, 51, 29-49.

Matthäus, W. (1990): Mixing across the primary Baltic halocline, Beiträge zur Meereskunde, 61, 21-31.

Matthäus, W. (2006): The history of investigation of salt water inflows into the Baltic Sea – from the early beginning to recent results, Meereswissenschaftliche Berichte, 65, 1-73.

Matthäus, W., Feistel, R., Lass, H.-U., Nausch, G., Nehring, D., and Mohrholz, V. (2008): The inflow of highly saline water into the Baltic Sea, in: Feistel, R., Nausch, G., and Wasmund, N., State and Evolution of the Baltic Sea 1952 – 2005, Wiley, in preparation.

Matthäus, W. and Franck, H. (1992): Characteristics of major Baltic inflows – a statistical analysis, Cont. Shelf Res., 12(12), 1375-1400.

Matthäus, W., Lass, H. U., Francke, E., and Schwabe, R. (1983): Zur Veränderlichkeit des Volumen- und Salztransports über die Darsser Schwelle, Gerlands Beitr. Geophys., 92, 407-420.

Matthäus, W. and Nausch, G. (2003): Hydrographic-hydrochemical variability in the Baltic Sea during the 1990s in relation to changes during the 20th century, ICES Mar. Sci. Symp., 219, 132-143.

Matthäus, W., Nausch, G., Lass, H. U., Nagel, K., and Siegel, H. (1998): The Baltic Sea in 1997 – impacts of the extremely warm summer and of the exceptional Oder flood, Dt. Hydrogr. Z., 50(1), 47-69.

Matthäus, W., Nausch, G., Lass, H. U., Nagel, K., and Siegel, H. (2001a): The Baltic Sea in 1999 – stabilization of nutrient concentrations in the surface water and increasing extent of oxygen deficiency in the central Baltic deep water, Meereswissenschaftliche Berichte, 45, 3-25.

Matthäus, W., Nausch, G., Lass, H. U., Nagel, K., and Siegel, H. (2001b): Hydrographisch-chemische Zustandseinschätzung der Ostsee 2000, Meereswissenschaftliche Berichte, 45, 27-88.

Matthäus, W. and Schinke, H. (1999): The influence of river runoff on deep water conditions of the Baltic Sea, Hydrobiologia, 393 (1), 1-10.

McWilliams, J. C., Sullivan, P. P., and Moeng, C.-H. (1997): Langmuir turbulence in the ocean, J. Fluid Mech., 334, 1-30.

Meier, H. E. M. (2001): On the parameterization of mixing in three-dimensional Baltic Sea models, J. Geophys. Res., 106(C12), 30997-31016.

Meier, H. E. M., Feistel, R., Piechura, J., Arneborg, L., Burchard, H., Fiekas, V., Golenko, N., Kuzmina, N., Mohrholz, V., Nohr, C., Paka, V.T., Sellschopp, J., Stips, A., and Zhurbas, V. (2006): Ventilation of the Baltic Sea deep water: A brief review of present knowledge from observations and models, Oceanologia, 48(S), 133-164. http://www.iopan.gda.pl/oceanologia/48_S.html#A8

Meier, H. E. M. and Kauker, F. (2003): Sensitivity of the Baltic Sea salinity to the freshwater supply, Climate Res., 24 (3), 231-242.

Mohrholz, V., Dutz, J., and Kraus, G. (2006): The impacts of exceptionally warm summer inflow events on the environmental conditions in the Bornholm Basin, J. Mar. Sys., 60 , 285-301.

Møller, J. S, Hansen, N.-E.O., and Jakobsen, F. (1997): Mixing in stratified flow caused by obstacles, Coastal Engineering, 4, 97-111.

Moum, J.N. and Osborn, T.R. (1986): Mixing in the Main Thermocline, J. Phys. Oceanogr., 16, 1250-1259.

Moum, J. N., Perlin, A., Klymak, J. M., Levine, M. D., Boyd, T., and Kosro, P. M. (2004): Convectively-driven mixing in the bottom boundary layer, J. Phys. Oceanogr., 34, 2189-2202.

Müller, P. and Garrett, C. (2004): Near-boundary processes and their parameterization, Oceanography, 17, 107-116.

Munk, W. and Anderson, E. R. (1948): Notes on a theory of the thermocline, J. Mar. Res., 7, 276-295.

Munk, W. H. (1966): Abyssal recipes, Deep-Sea Research, 13, 707-730.

Nausch, G., Feistel, R., Lass, H.-U., Nagel, K., and Siegel, H. (2006): Hydrographisch-chemische Zustandseinschätzung der Ostsee 2005, Meereswissenschaftliche Berichte, 66, 3-82. http://www.io-warnemuende.de/documents/mebe66_2005-zustand-hc-und-schwermetalle.pdf

Nausch, G., Matthäus, W., and Feistel, R. (2003): Hydrographic and hydrochemical conditions in the Gotland Deep area between 1992 and 2003, Oceanologia, 45(4), 557-569.

Nausch, M., Nausch, G., and Wasamund, N. (2004): Phosphorus dynamics during the transition from nitrogen to phosphate limitation in the central Baltic Sea, Mar. Ecol. Progr. Ser., 266, 15-25.

Nehring, D. and Matthäus, W. (1991): Current trends in hydrographic and chemical parameters and eutrophication in the Baltic Sea, Int. Revue ges. Hydrobiol., 76, 297-316.

Nehring, D., Matthäus, W., and Lass, H. U. (1993): Die hydrographisch-chemischen Bedingungen in der westlichen und zentralen Ostsee im Jahre 1992, Dt. Hydrogr. Z., 45, 281-312.

Omstedt, A. and Axell, L. B. (1998): Modeling the seasonal, interannual and long-term variations of salinity and termperature in the Baltic Proper, Tellus, 50A, 637-652.

Osborn, T. R. (1980): Estimates of the local rate of vertical diffusion from dissipation measurements, J. Phys. Oceanogr., 10(1), 83-89.

Ozmidov, R. V. (1983): Small-scale turbulence and fine structure of hydrophyiscal fields in the ocean, Oceanology, 23(4), 533-537.

Ozmidov, R. V. (1994a): Vertical water exchange in deep basins of the Baltic Sea, Oceanology, 34, 141-144.

Ozmidov, R. V. (1994b): The role of boundary effects in the deepwater exchange in the Baltic Sea. Oceanology (English Translation), 34(4), 440-444.

Pacanowski, R. C. and Griffies, S. M. (1999): MOM 3.0 manual, technical report, 688 pp., Geophys. Fluid Dyn. Lab., Princeton, N.J.

Paka, V. T., Golenko, N., and Korzh, A. (2006): Distinctive features of water exchange across the Slupsk Sill (a full scale experiment), Oceanologica, 48, 37-54.

Paka, V. T., Zhurbas, V. M., Golenko, N. N., and Stefantzev, L. A. (1998): Effect of the Ekman transport on the overflow of saline waters through the Slupsk Furrow in the Baltic Sea, Izv. Atmos. Ocean. Phys., 34, 641-648. Translated from Izvestiya AN. Fizika Atmosfery i Okeana, vol. 34, No. 5, 1998, 713-720.

Phillips, O. M. (1970): On flows induced by diffusion in a stably stratified fluid, Deep-Sea Res., 17, 435-443.

Phillips, O. M., Shyu, J., and Schmitt, R. W. (1986): An experiment on boundary mixing: mean circulation and transport rates, J. Fluid Mech., 173, 473-499.

Piechura, J. and Beszczynska-Möller, A. (2004): Inflow waters in the deep regions of the southern Baltic Sea – transport and transformations (corrected version), Oceanologia, 46(1), 113-141.

Pizarro, O. and Shaffer, G. (1998): Wind-Driven, Coastal-Trapped Waves off the Island of Gotland, Baltic Sea, J. Phys. Oceanogr., 28(11), 2117-2129.

Polzin, K. L., Toole, J. M., Ledwell, J. R., and Schmitt, R. W. (1997): Spatial variability of turbulent mixing in the abyssal ocean, Science, 276, 93-96.

Polzin, K. L., Toole, J. M., and Schmitt, R. W. (1995): Finescale Parameterizations of Turbulent Dissipation, J. Phys. Oceanogr., 25(3), 306-328.

Reissmann, J. H. (1999): Bathymetry of four Deep Baltic Basins, Dt. Hydrogr. Z., 51(4), 489-497.

Reißmann, J. H. (2002): Integrale Eigenschaften von mesoskaligen Wirbelstrukturen in den tiefen Becken der Ostsee, Meereswissenschaftliche Berichte, 52, 149 pp. http://www.io-warnemuende.de/documents/mebe52_reissmann.pdf

Reißmann, J. H. (2005): An algorithm to detect isolated anomalies in three-dimensional stratified data fields with an application to density fields from four deep basins of the Baltic Sea, J. Geophys. Res., 110, C12018, doi:10.1029/2005JC002885.

Reissmann, J. H. (2006): On the representation of regional characteristics by hydrographic measurements at central stations in four deep basins of the Baltic Sea, Ocean Science, 2, 71-86. http://www.ocean-sci.net/2/71/2006/os-2-71-2006.html

Rippeth, T. P., Fisher, N. R., and Simpson, J. H. (2001): The Cycle of Turbulent Dissipation in the Presence of Tidal Straining, J. Phys. Oceanogr., 31(8), 2458-2471.

Robinson, A. R. (Ed.) (1983): Eddies in Marine Science, Springer, New York.

Rodhe, J. and Winsor, P. (2002): On the influence of the freshwater supply on the Baltic Sea mean salinity, Tellus A, 54(2), 175-186.

Rudnick, D. L., Boyd, T. J., Brainard, R. E., Carter, G. S., Egbert, G. D., Gregg, M. C., Holloway, P. E., Klymak, J. M., Kunze, E., Lee, C. M., Levine, M. D., Luther, D. S., Martin, J. P., Merrifield, M. A., Moum, J. N., Nash, J. D., Pinkel, R., Rainville, L., and Sanford, T. B. (2003): From tides to mixing along the Hawaiian Ridge, Science, 301, 355-357.

Sellschopp, J., Arneborg, L., Knoll, M., Fiekas, V., Gerdes, F., Burchard, H., Lass, H. U., Mohrholz, V., and Umlauf, L. (2006): Direct observations of a medium-intensity inflow into the Baltic Sea, Cont. Shelf Res., 26, 2393-2414.

Shaffer, G. (1979): Conservation calculations in natural coordinates (with an example from the Baltic), J. Phys. Oceanogr., 9(4), 847-855.

Sharples, J., Moore, C. M., Rippeth, T. P., Holligan, P. M., Hydes, D. J., Fisher, N. R., and Simpson, J. H. (2001): Phytoplankton distribution and survival in the thermocline, Limnol. Oceanogr., 46, 486-496.

Stigebrandt, A. (1979): Observational Evidence for Vertical Diffusion Driven by Internal Waves of Tidal Origin in the Oslofjord, J. Phys. Oceanogr., 9(2), 435-441.

Stigebrandt, A. (1987a): A Model for the Vertical Circulation of the Baltic Deep Water, J. Phys. Oceanogr., 17(10), 1772-1785.

Stigebrandt, A. (1987b): Computations of the flow of dense water into the Baltic Sea from hydrographical measurements in the Arkona Basin, Tellus, 39A, 170-177.

Stigebrandt, A. (1992): Bridge-induced flow reduction in sea straits with reference to effects of a planned bridge across Öresund, Ambio, 21, 130-134.

Stigebrandt, A. (2003): Regulation of vertical stratification, length of stagnation periods and oxygen conditions in the deeper deepwater of the Baltic proper, in: Fennel, W. and Hentzsch, B. (Eds.), Festschrift zum 65. Geburtstag von Wolfgang Matthäus, Meereswissenschaftliche Berichte, 54, 69-80.

Stigebrandt, A. and Aure, J. (1989): Vertical mixing in basin waters of fjords, J. Phys. Oceanogr., 19, 917-926.

Stigebrandt, A. and Gustafsson, B. G. (2003): Response of the Baltic Sea to climate change – theory and observations, J. Sea Res., 49, 243-256.

Stigebrandt, A., Lass, H.-U., Liljebladh, B., Alenius, P., Piechura, J., Hietala, R., and Beszczyńska, A. (2002): DIAMIX – an experimental study of diapycnal deepwater mixing in the virtually tideless Baltic Sea, Boreal Environment Research, 7(4), 363-369.

Stips, A., Burchard, H., Bolding, K., Prandke, H., and Wüest, A. (2005): Measurement and simulation of viscous dissipation rates in the wave affected surface layer, Deep Sea Res. II, 52, 1133-1155.

Stips, A., Prandke, H. and Neumann, T. (1998): The structure and dynamics of the Bottom Boundary Layer in shallow sea areas without tidal influence: an experimental approach, Progr. in Oceanogr., 41(4), 383-453.

Sturm, M., Helm, R. and Fennel, W. (1988): Mesoscale eddies in the western Baltic Sea, Beiträge zur Meereskunde, 58, 73-75.

Sverdrup, H. U. (1937): On The Process Of Upwelling, J. Mar. Res., 8, 155-164.

Sverdrup, H. (1953): On conditions for the vernal blooming of phytoplankton, J. Cons. Perm. Int. Explor. Mer, 18, 287-295.

Talipova, T. G., Pelinovskii, E. N., and Kõuts, T. (1998): Kinematic Characteristics of an Internal Wave Field in the Gotland Deep in the Baltic Sea, Oceanology, 38(1), 33-42.

Terray, E. A., Donelan, M. A., Agrawal, Y. C., Drennan, W. M., Kahma, K. K., Williams, A. J., Hwang, P. A., and Kitaigorodskii, S. A. (1996): Estimates of Kinetic Energy Dissipation under Breaking Waves, J. Phys. Oceanogr., 26(5), 792-807.

Thiel, G. (1938): Strombeobachtungen in der westlichen Ostsee im Juli 1936, Arch. Dtsch. Seewarte Marineobs., 58, 1-28.

Thorpe, S. A. (1987): Current and temperature variability on the continental slope, Philos. Trans. R.Soc. Lond. B Biol. Sci., A323, 471-517.

Thorpe, S. A. (1997): On the Interaction of Internal Waves Reflecting from Slopes, J. Phys. Oceanogr., 27(9), 2072-2078.

Thorpe, S. A., Osborn, T. R., Farmer, D. M., and Vagle, S. (2003): Bubble Clouds and Langmuir Circulation: Observations and Models, J. Phys. Oceanogr., 33(9), 2013-2031.

Thorpe, S.A. and Umlauf, L. (2002): Internal gravity wave frequencies and wavenumbers from single point measurements over a slope, J. Mar. Res., 60, 699-723.

Toole, J. M., Polzin, K. L., and Schmitt, R. W. (1994): New estimates of diapycnal mixing in the abyssal ocean, Science, 264, 1120-1123.

Trowbridge, J. H. and Lentz, S. J. (1991): Asymmetric Behavior of an Oceanic Boundary Layer above a Sloping Bottom, J. Phys. Oceanogr., 21(8), 1171-1185.

Turner, J.S. (1986): Turbulent entrainment: the development of the entrainment assumption, and its application to geophysical flows, J. Fluid Mech., 173, 431-471.

Umlauf, L. et al. (2006): Turbulence structure in a dense gravity current, Geophys. Res. Lett., submitted.

Umlauf, L., Bolding, K., and Burchard, H. (2005): GOTM – scientific documentation: version 3.2, Meereswissenschaftliche Berichte, 63, 231 pp.
http://www.gotm.net/pages/documentation/manual/pdf/a4.pdf

Umlauf, L. and Burchard, H. (2005): Second-order turbulence closure models for geophysical boundary layers. A review of recent work, Cont. Shelf Res., 25, 795-827.

Umlauf, L. and Lemmin, U. (2005): Inter-basin exchange and mixing in a large lake. The role of long internal waves, Limnol. Oceanogr., 50, 1601-1611.

van Aken, H. M. (1986): The onset of stratification in shelf seas due to differential advection in the presence of a salinity gradient, Cont. Shelf Res., 5, 475-485.

Victorov, S. V. (1996): Regional Satellite Oceanography, Taylor and Francis, London, 306 pp.

Vlasenko, V. and Alpers, W. (2005): Generation of secondary internal waves by the interaction of an internal solitary wave with an underwater bank, J. Geophys. Res., 110, C02019, doi:10.1029/2004JC002467.

Vlasenko, V. and Hutter, K. (2002a): Numerical Experiments on the Breaking of Solitary Internal Waves over a Slope–Shelf Topography, J. Phys. Oceanogr., 32(6), 1779-1793.

Vlasenko, V. and Hutter, K. (2002b): Transformation and disintegration of strongly nonlinear internal waves by topography in stratified lakes, Annales Geophysicae, 20, 2087-2103.

Walin, G. (1972a): On the hydrographic response to transient meteorological disturbances, Tellus, 24, 169-186.

Walin, G. (1972b): Some observations of temperature fluctuations in the coastal region of the Baltic, Tellus, 24, 187-198.

Walin, G. (1981): On the deep water flow into the Baltic, Geophysica, 17, 75-93.

Welander, P. (1974): Two–layer Exchange in an Estuary Basin, with Special Reference to the Baltic Sea, J. Phys. Oceanogr., 4(4), 542-556.

Winsor, P., Rodhe, J., and Omstedt, A. (2001): Baltic Sea ocean climate: an analysis of 100 yr of hydrographic data with focus on the freshwater budget, Climate Research, 18, 5-15.

Wüest, A. and Lorke, A. (2003a): The effect of the bottom boundary on diapycnal mixing in enclosed basins, in: Müller, P. and Henderson, D. (Eds.), 13th 'Aha Huliko'a Hawaiian Winter Workshop on Near Boundary Processes and their Parameterization, SOEST Special Publication, 9-15.

Wüest, A. and Lorke, A. (2003b): Small-scale hydrodynamics in lakes, Ann. Rev. Fluid Mech., 35, 373-412.

Wüest, A., Piepke, G., and van Senden, D. C. (2000): Turbulent kinetic energy balance as a tool for estimating vertical diffusivity in wind-forced stratified waters, Limnol. Oceanogr., 45, 1388-1400.

Wunsch, C. (1970): On oceanic boundary mixing, Deep-Sea Res., 17, 293-301.

Wüst, G., Noodt, E., and Hagmeier, E. (1957): Ergebnisse eines hydrographisch–produktionsbiologischen Längsschnitts durch die Ostsee im Sommer 1956. I. Die Verteilung von Temperatur, Salzgehalt und Dichte, Kieler Meeresforsch., 13, 163-185.

Wyrtki, K. (1954): Der große Salzeinbruch in die Ostsee im November und Dezember 1951, Kieler Meeresforsch., 10, 19-25.

Zhurbas, V. M. and Paka, V. T. (1997): Mesoscale thermohaline variability in the Eastern Gotland Basin following the 1993 major Baltic inflow, J. Geophys. Res., 102(C9), 20917-20926.

Zhurbas, V. M. and Paka, V. T. (1999): What drives thermohaline intrusions in the Baltic Sea?, J. Mar. Syst., 21, 229-241.